Role of eIF4A proteins in miR-122 mediated Hepatitis C virus regulation

CHOUDHARY SHOAIB AHMED, BSc, MSc

Thesis is submitted to the University of Nottingham for the degree of Doctor of Philosophy

November 2016

Declaration

Except where acknowledged in the text, I declare that this dissertation in my own work and it is based on the research work that was undertaken by me in Gene Regulation & RNA Biology group, School of Pharmacy, Faculty of Science, The University of Nottingham, UK.

Abstract

An estimated 2-3% of the global population is living with Hepatitis C virus (HCV) infection and 60-90% of these infections become chronic, which could leads to cirrhosis and liver cancer. While new antiviral therapies are emerging, a better understanding of how HCV interacts with host cells is important. HCV is a hepatotropic positive sense RNA virus. The HCV 5' untranslated region (UTR) contains two binding sites for a highly abundant liver-specific microRNA, miR-122. In contrast to the canonical function for microRNAs in binding to 3'UTR sites, leading to mRNA degradation and translational repression, HCV uses miR-122 as an essential positive regulator of viral replication. The mechanism of this regulation remains uncertain, with viral translation, RNA stability and replication all implicated in different studies.

In order to understand the mechanism of HCV regulation by miR-122, it is important to identify the host protein factors involved in this regulation. This thesis investigates the role for eukaryotic initiation factor 4A (eIF)4AII, which preliminary studies implicated in HCV replication and which has also been shown to function in miRNA activity. eIF4AI and eIF4AII are ATP-dependent helicases, which linearize secondary structures present in the 5' UTR of an mRNA and help ribosome binding to the mRNA and scanning for initiation codon. Eukaryotic initiation factor (eIF)4AII has been described as a binding partner of HCV RNA polymerase enzyme (NS5B) by binding to NS5B's C-terminal residues and is also involved in miRNA regulation of translation at 3'UTR sites. eIF4AI and eIF4AII have more than 90% sequence similarity due

to which these proteins have long been functionally interchangeable. However, eIF4AII depletion had no effect on cellular growth while eIF4AI depletion was shown to be inhibitory to cellular growth. Unlike eIF4AII, eIF4AI role in miRNA regulation at 3'UTR sites is unknown.

In this thesis, depletion of eIF4AII is shown to lead to a reduction in HCV RNA level, while eIF4AI knockdown had variable effects on HCV RNA levels. These variabilities could be due to the subtle differences in the confluence levels of cells or due to the experimental variability. These findings also support the idea that eIF4AI and eIF4AII function differently. In order to study whether this reduction in HCV RNA levels in eIF4AII depleted cells is linked with miR-122 regulation of HCV, sequestration, and overexpression of miR-122 in eIF4AII depleted cells were performed. We have been able to show that the presence or absence of miR-122 did not change the HCV RNA levels in eIF4AII depleted cells, which suggests that eIF4AII contribution to HCV replication is linked with miR-122 regulation of HCV and functional eIF4AII is required for miR-122 mediated regulation of HCV. However, eIF4AII did not affect miR-122 regulation of luciferase reporters in which the HCV 5'UTR controls luciferase translation. By co-immunoprecipitation, eIF4AII is shown to interact with HCV RNA and miR-122 in a miR-122-dependent manner**.** eIF4AII also interacts with miR-21 and miR-26a, but this interaction is not dependent on miR-122, indicating that miR-122 is specifically required for the eIF4AII-HCV RNA interaction. DDX6 and eIF4AII have been proposed to be involved in miRNA mediated repression by Ccr4-Not complex via CNOT1. The involvement of eIF4AII in miRNA mediated repression was questioned

in a different study in which the interaction between eIF4AII and CNOT1 was not confirmed. siRNA based knockdown of CNOT1 reduces both HCV RNA and miR-122 co-immunoprecipitation with eIF4AII, which indicates that Ccr4-NOT complex component CNOT1 contributes to eIF4AII association with miR-122 and HCV and may be part of the same complex. Taken together, eIF4AII is identified a new host factor that is important for HCV replication, and that requires miR-122 to interact with HCV RNA, but it was not possible to demonstrate conclusively that eIF4AII regulates HCV by modulation of miR-122 activity.

Acknowledgements

Firstly, I would like to thank Almighty Allah for enabling me to achieve this milestone.

I would like to thank my supervisor Dr. Catherine L Jopling for her constant and enduring support throughout my whole Ph.D. Without your guidance, I could never have achieved this. You always inspire me with your energy and enthusiasm in the lab. I am very lucky to have you as my mentor.

I would also like to thank my second supervisor, Dr. Keith Spriggs, for his help and support during the absence of Dr. Catherine L Jopling. I'd like to thank Dr. Cornelia de Moor for her expert help throughout my Ph.D. as an internal assessor. I would like to thank Dr. Hilary Collins for her help in confocal microscopy training and experimentation. I am very thankful to Dr. Andrew Lewis for his help in the early days of my Ph.D. I am very also very thankful to Barbara Rampersad for maintaining the lab and providing all sort of supplies on time. Thanks to all the members of Gene Regulation & RNA Biology group for their help along the way, particularly Aimee Parsons, Dr. Hannah Parker and Daniel Smalley. I am also thankful to Dr Alexandra Hughes, Dr Graeme Thorn, Dr Richa Singhania, Dr Asma Khursheed, Dr Joel Fulton, Lin Jialiang, Hibah Al-Masmoum, Raj Gandhi, Mustafa Al-Siraj, Maryati Maryati, Dario Leonardo Balacco, Blessing Airhihen, Bismoy Mazumder, Lorenzo Pavanello, and Masar Radhi for making my time in the group an enjoyable and a life-long memory.

I am very thankful to my late mother for her encouragement during my early studies and for calling me ‘doctor’ which always gave me the energy to fulfill her dream. I would like to thank my father for quietly praying for my success throughout my life. I would also like to thank my paternal Aunt, for taking me out from the village and raising me like her own son and providing me an opportunity to study and live a better life. It was a kindness I could never repay. I also want to thank her children (Sisters Mussarat Shamsher, Shamim Akhter and Uzma Shaheen, Brothers Aftab Ahmed and Mehtab Ahmed and Brother in law Fahim Khan) who always consider me as their real brother and supported me in this whole journey.

Thanks to my ‘in-laws’ especially my parents-in-law for providing me a lot of encouragement and for supporting my family especially my sons’ early days.

Lastly, I am thankful to my lovely wife Saiqa Shoaib for her endless support throughout my Ph.D. I would not have started this without your encouragement and would not have finished it! You are absolutely loving and caring and I can’t thank you enough. I also want to thank my sons Abdul Ahad and Emad Ahmed and my lovely daughter Bareerah Noor Ahmed for playing with me and asking innocent questions which always relieved the pressure and stress.

October 2016, Choudhary Shoaib Ahmed

Table of contents

List of abbreviations

APS	Ammonium persulphate
ATP	Adenosine 5'- triphosphate
BSA	Bovine Serum Albumin
C	Core
cDNA	Complementary deoxyribonucleic acid
CDS	Coding sequence
CLDN1	Claudin-1
CM	Confocal microscopy
Co-IP	Co-immunoprecipitation
CTD	C-terminal domain
CTL	Cytotoxic T lymphocycte
CHX	Cycloheximide
dATP	Deoxyadenosine 5'-tripohosphate
dCTP	Deoxycytidine 5'-triphosphate
DMEM	Dulbecco's Modified Eagles Medium
DNA	Deoxyribonucleic acid
DNase	Deoxyribonuclease
dNTP	Deoxyribonucleotide 5-triphosphate
dsRNA	Double stranded RNA
DTT	Dithiothreitol
ECL	Enhanced Chemiluminescence
E.coli	*Escherichia coli*
EDTA	Ethylene Diamine Tetraacetic Acid
eIF	Eukaryotic initiation factor
EGFR	Eukaryotic growth factor receptor
EMCV	Encepahlomycarditis Virus
ER	Endoplasmic reticulum
GAG	Glycosaminoglycan
HAV	Hepatitis A virus
HBV	Hepatitis B virus
HCV	Hepatitis C virus
HDV	Hepatitis D virus
HDL	High density lipid
HEV	Hepatitis E virus
HBS	HEPES-buffered Saline
HeLa	Human cervical epithelial carcinoma cells
HRP	Horseradish peroxidase
HSV	Herpes simplex virus
IFN-γ	Interferon-γ
IPTG	Isopropyl-β-d-Thiogalactopyranoside
IREs	Iron response elements
IRES	Internal ribosomal entry site
Kb	Kilobase
kDa	Kilodalton
LB	Lysogeny Broth

LEL	Large extracellular loop
m^7G	7-methylguanosine
MAVs	mitochondrial antiviral signalling
miRNA	MicroRNA
mRNA	Messenger ribonucleic acid
mRNP	Messenger Ribonucleoprotein
NTD	N-terminal domain
NANBH	**N**on-A non-B hepatitis
NMD	Nonsense-mediated decay
NPC1L1	Neimann-Pick C1-like 1(NPC1L1)
NS2	Non-structural-2
NS3	Non-structural-3
NS4A	Non-structural 4A
NS4B	Non-structural 4B
NS5A	Non-structural 5A
NS5B	Non-structural 5B
NTP	Nucleoside triphosphate
OCLN	Occludin
OD	Optical density
ORF	Open reading frame
PABP	Poly-A Binding Protein
PAGE	Polyacrylamide gel electrophoresis
PB	Processing bodie
PBS	Phosphate buffered saline
RT-QPCR	Polymerase Chain Reaction
PDCD4	Programmed cell death 4
PDCs	Plasmacytoid dendritic cells
PI4KIIIα	phosphatidylinositol 4-kinase III alpha
PKR	sensor protein kinase R
PRRs	Pattern recognition-receptors
PTB	Polypyrimidine tract binding protein
PVDF	Polyvinylidene difluoride
RISC	RNA-induced silencing complex
RT	Room temperature
RNA	Ribonucleic acid
RNase	Ribonucleic acid hydrolase
rRNA	Ribosomal RNA
SDS	Sodium Dodecyl Sulphate
SEL	Small extracellular loop
SF	Superfamily
SG	Stress granule
siRNA	Silencing ribonucleic acid
SR-B1	Scavenger receptor B1
SSC	Saline sodium citrate
ssRNA	Single stranded RNA
TAE	Tris acetic acid EDTA buffer
TC	Ternary complex

Taq	Thermus aquaticus
TBE	Tris-borate EDTA buffer
TBS	Tris buffered saline
TBST	Tris Buffered Saline Tween
TE	Tris-EDTA
TEMED	Tetramethylethylenediamine
TGF-β	Transforming growth factor-β
TLR	Toll-like receptor
tRNA	Transfer RNA
uORF	Upstream open reading frame
UTR	Untranslated Region
UV	Ultraviolet
VR	Variable region
VLDL	Very low density lipid

List of tables

List of figures

1 Introduction

1.1 Hepatitis

The term hepatitis is derived from two Greek words, *hepar* meaning "liver" and *itis* meaning "inflammation". Hepatitis is multi-symptom liver inflammation which leads to yellow discoloration of eyes, skin and mucous membranes, fatigue and poor appetite. It can be divided into acute hepatitis (can be self-resolving) and chronic hepatitis (long term) (Bernal and Wendon 2013).

On the basis of causative agent, hepatitis can be divided into several types. These types include viral hepatitis, alcoholic or non-alcoholic hepatitis (Wree, Broderick et al. 2013), autoimmune hepatitis (Teufel, Galle et al. 2009), drug induced hepatitis (Lee 2003) and genetic hepatitis. Among all these, viral hepatitis is the most common cause of hepatitis related annual deaths globally.

1.1.1 Viral hepatitis

Several different viruses have been identified to cause viral hepatitis. Among them, the most common viruses are hepatitis A virus (HAV), hepatitis B virus (HBV), hepatitis C virus (HCV), hepatitis D virus (HDV) and hepatitis E virus (HEV). Another hepatotropic virus known as GB virus C has been identified from patients but there is no evidence of GB virus C infection (Alter 1996). This thesis focuses on HCV, but other hepatitis viruses are first discussed briefly below.

1.1.1.1 Hepatitis B virus

Hepatitis B virus is the first hepatitis virus discovered in the mid-1960s (Blumberg, Alter et al. 1965). It is a partially double stranded DNA virus belonging to the *Hepadnavaridea* family. The DNA is packaged into an icosahedral core surrounded by a lipid envelope. Like HCV it is a blood borne virus but also can be transmitted through damaged skin and mucous membranes and through sexual contact (Locarnini 2004, Fairley and Read 2012). Vaccination at an early age gives 95% protection while these levels drop with increase in age and this could be due to the fact that HBV infection at early age leads to the development of chronic HBV infection in more than 90% of the cases (Aspinall, Hawkins et al. 2011).

1.1.1.2 Hepatitis A virus

Hepatitis A virus was the second hepatotropic virus discovered after HBV (Feinstone, Kapikian et al. 1973). It is non-enveloped, a single stranded RNA virus which is transmitted through faecally contaminated food. HAV infections are usually self-resolving while vaccination provides protection for up to 25 years (Nothdurft 2008, Matheny and Kingery 2012).

1.1.1.3 Hepatitis D virus

Hepatitis D virus was first thought to be HBV, while later experiments showed that it is a separate virus which required hepatitis B virus to replicate. (Rizzetto, Canese et al. 1977). It is a single stranded RNA virus

which has a similar route of transmission to HBV. Due to the HDV dependency on HBV, HBV vaccination provided protection against HDV infections (Saldanha, Thomas et al. 1990).

1.1.1.4 Hepatitis E virus

Like HAV, Hepatitis E virus is a single-stranded RNA, non-enveloped virus with an icosahedral structure (Balayan, Andjaparidze et al. 1983). It also transmits through unhygienic food via the oral-faecal route while the infection is usually self-resolving (Zhou, de Man et al. 2013).

1.2 Hepatitis C virus

1.2.1 Origin of Hepatitis C virus

After the discovery and development of diagnostic tests for Hepatitis B (HBV) and Hepatitis A (HAV) viruses, the patient serum specimens non-reactive to anti-B and anti-A were termed as non-A non-B hepatitis (NANBH) (Purcell 1997). These sera contained 30-60nm particles which could transmit the disease in chimpanzees and these particles also contained lipid molecules (He, Alling et al. 1987). In 1989 the genome of the non-A non-B agent was isolated and screened with the plasma (containing NANBH antibodies) of NANBH patients. This screening resulted in the isolation of complementary genome and later on it (NANBH agent) was named as Hepatitis C virus and classified as a separate genus in *Flaviviridae* (Choo, Kuo et al. 1989).

1.2.2 Flaviviridae

The word *Flaviviridae* is derived from a *Latin* term *flavus* which means "yellow" and was given to the family containing yellow fever virus (Chambers, Hahn et al. 1990). The members of this family are positive sense, single stranded, enveloped viruses. There are about one hundred species in this family which are divided into four different genera on the basis of phylogenetic analysis of sequence divergence in helicase or RNA polymerase sequences. These are the genus *Flavivirus*, genus *Hepacivirus*, genus *Pestivirus* and genus *Pegivirus* (Suzuki, Ishii et al. 2007). HCV is an RNA virus which belong to the genus *Hepacivirus*.

1.2.3 Epidemiology

HCV is a globally prevalent infection and more than 180 million (2.8%) people are infected by this virus (Mohd Hanafiah, Groeger et al. 2013). HCV is the leading cause of liver transplantation and HCV related mortalities surpassed HIV related deaths in 2006 (Ortega-Prieto and Dorner 2016). Due to the increase in availability and advent of new drugs the incidence of HCV infections is decreasing but HCV related deaths will increase over the next two decades (Gower, Estes et al. 2014, Messina, Humphreys et al. 2015). During the course of infection, 10-40% of HCV infections are cleared by the immune system but the majority (60-90%) of these infections develop into chronic infection which could lead to end stage liver disease in 30% of cases (Thomas 2013).

1.2.4 HCV genotypes and their prevalence

HCV strains are classified into 7 different genotypes on the basis of 31-33% genetic variability at nucleotide level and these genotypes are further classified into 67 subtypes on the basis of 20-25% diversity at nucleotide level(Simmonds, Bukh et al. 2005, Ortega-Prieto and Dorner 2016). This high variability among the HCV strains could be attributed to the high mutation rate in HCV replication. HCV have 10^{-3} mutations/site/year in the whole genome, while the hypervariable regions have 10 times higher mutation rate (Simmonds 1995). The identification of genotypes is very important for not only predicting the course and prognosis of the treatment, but also tracing the route of infection and prediction of anti-viral treatment response (Simmonds 1995, Alexopoulou and Dourakis 2005).

HCV genotype 1 is the most prevalent genotype as it accounts for 46% of all HCV infections, while genotype 2, 3 and 4 are present in 13%, 22% and 13% of cases respectively (Gower, Estes et al. 2014). Different genotypes are prevalent in different geographical locations (Figure 1-1). In North America and Western Europe genotypes 1a, 1b, 2a, 2b and 3a are prevalent, while genotype 1 is most prevalent in Central Europe. Genotype 1b is present in South East Asian countries while genotype 3a has been detected in most of the cases reported form South Asia. Genotype 4 is the most prevalent genotype in Middle East and Central Asia (Alexopoulou and Dourakis 2005, Gower, Estes et al. 2014).

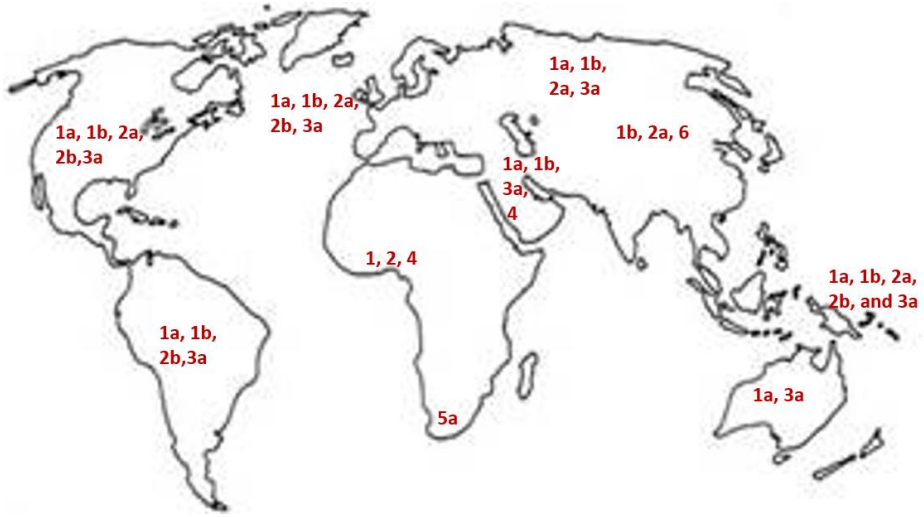

Figure 1-1 Geographic distribution of HCV genotypes and subgenotypes

The figure represents the geographic distribution of HCV genotypes (numbers) and subtypes (small letters).

1.2.5 HCV genome organization

Like other members of *Flaviviridae*, HCV is enveloped in a lipid bilayer which is derived from cellular lipid membranes and encompasses the icosahedral viral nucleocapsid (figure 1-2). The viral glycoproteins E1 and E2 are embedded in the lipid envelope. The nucleocapsid is made up of multiple copies of the core protein Inside the capsid the 9000 nucleotide (nt) long positive sense RNA resides (Penin, Dubuisson et al. 2004). This serves as the template for the production of the 3000 amino acid long polyprotein(Suzuki, Ishii et al. 2007). This polyprotein is then processed by host and viral protease enzymes into structural (Core, p7, E1, E2) and non-structural (NS) components (NS2, NS3, NS4A, NS4B, NS5A and NS5B) (Brass, Moradpour et al. 2006).

The protein coding region of the HCV genome is flanked by two highly conserved regions which are the 5' untranslated region (UTR) and the 3' UTR. Both of these regions are involved in HCV genome replication and translation (Romero-Lopez and Berzal-Herranz 2009). The 3' UTR is about 220 nt and comprises 3 different regions: the 3'X and poly (U) region are conserved compared to the variable region (VR). All regions have a role in HCV replication and infectivity (Friebe and Bartenschlager 2009). The HCV 5' UTR contain a specific secondary structure called the internal ribosome entry site (IRES), which is required for HCV translation.

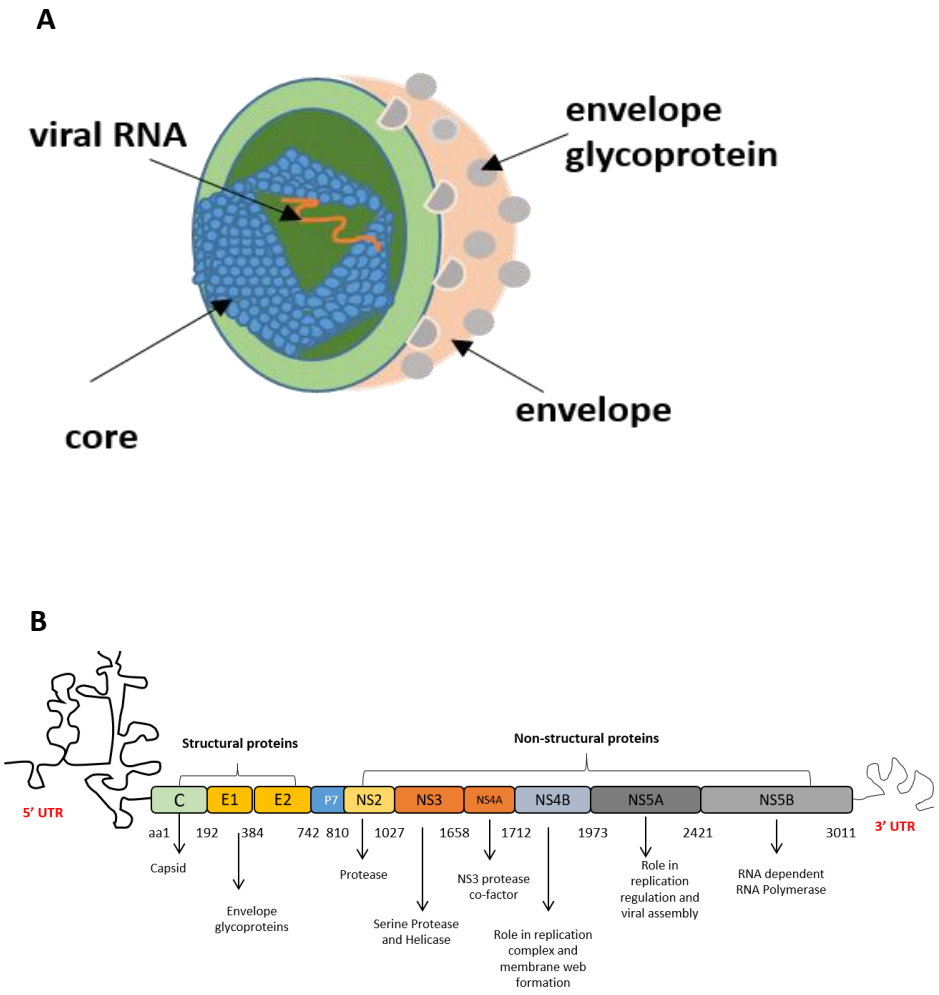

Figure 1-2 HCV viral particle and genome organization

A) HCV virus particles consist of the outer lipid envelope in which envelope proteins E1 and E2 are embedded. The icosahedral capsid structure, made of core protein subunits (blue circles), is present under the lipid envelope. The single stranded positive sense RNA genome is buried inside the core. B) HCV genome organization. The HCV polyprotein coding region is flanked by 5' and 3' untranslated regions (UTR). The polyprotein consists of three (Core, E1 E2) and seven non-structural proteins (NS2, NS3, NS4A, NS4B, NS5A and NS5B). The functions of proteins are indicated by arrows while the number of amino acids are represented as numbers.

1.2.6 HCV life cycle

The HCV life cycle consists of a series of stages which include i) attachment of the HCV particle to the hepatocyte surface ii) fusion and RNA release iii) viral protein translation and processing iv) viral RNA replication v) packaging and assembly vi) release of mature virus. All stages are described below.

1.2.6.1 Attachment of HCV virions to hepatocytes

The circulation of HCV virus particles in blood provides the direct contact necessary for HCV attachment to hepatocytes. The cellular surface lipoprotein Apo-E binds to the low density lipid receptors (LDLR) and Glycosaminoglycan GAG. These receptors provide initial attachment of HCV virions while several other receptors are implicated in viral entry. Scavenger receptor class B I (SR-BI) is one of the earliest identified receptors involved in HCV entry. This receptor is involved in transporting the high density lipid (HDL) in the cell and it is highly expressed on the hepatocyte surface (Scarselli, Ansuini et al. 2002). SR-BI enhances and facilitates HCV entry by its ability to modify the lipid composition of either HCV virions or the plasma membrane (Popescu, Riva et al. 2014).

After binding to SR-BI HCV is then transferred to another receptor known as CD-81. This receptor is a tetraspanin containing four hydrophobic transmembrane regions with two extracellular loops, small extracellular loop (SEL) and large extracellular loop (LEL). The LEL is reported to be sufficient for HCV entry while the SEL only optimizes the HCV LEL function

by a mechanism of increased expression of LEL on the hepatocyte surface (Masciopinto, Campagnoli et al. 2001), (Figure 1-3).

Two tight-junction proteins, Claudin-I (CLDN1) and Occludin (OCLN), are also reported to participate at early and late stages of HCV entry respectively (Evans, von Hahn et al. 2007, Ploss, Evans et al. 2009). Eukaryotic growth factor receptor (EGFR) induces CD-81 diffusion, which promotes the CD-81-CLDN1 co-receptor complex formation and results in subsequent HCV entry. This co-receptor complex is also suggested to define the HCV tissue tropism (Lindenbach and Rice 2013). Recently, a cholesterol transporter protein Neimann-Pick C1-like 1(NPC1L1) has been reported to be involved in HCV entry.

After sequential binding with several receptors, CD81-CLDN1 bound HCV virus enters the cell by clathrin mediated endocytosis (Popescu, Riva et al. 2014).

1.2.6.2 Fusion and RNA release

After the clathrin mediated internalization, the HCV particle is transported to actin fibres by early endosomes, where the fusion of HCV envelope and cell membrane occurs. The viral E1E2 complex has been suggested to promote viral and host membrane fusion at low pH levels (Lavillette, Pecheur et al. 2007). However, a recent study showed that the composition of HCV envelope and cell membrane, the HCV E2 protein and low pH

environment in the endosome are the main factors involved in the fusion process (Haid, Pietschmann et al. 2009).

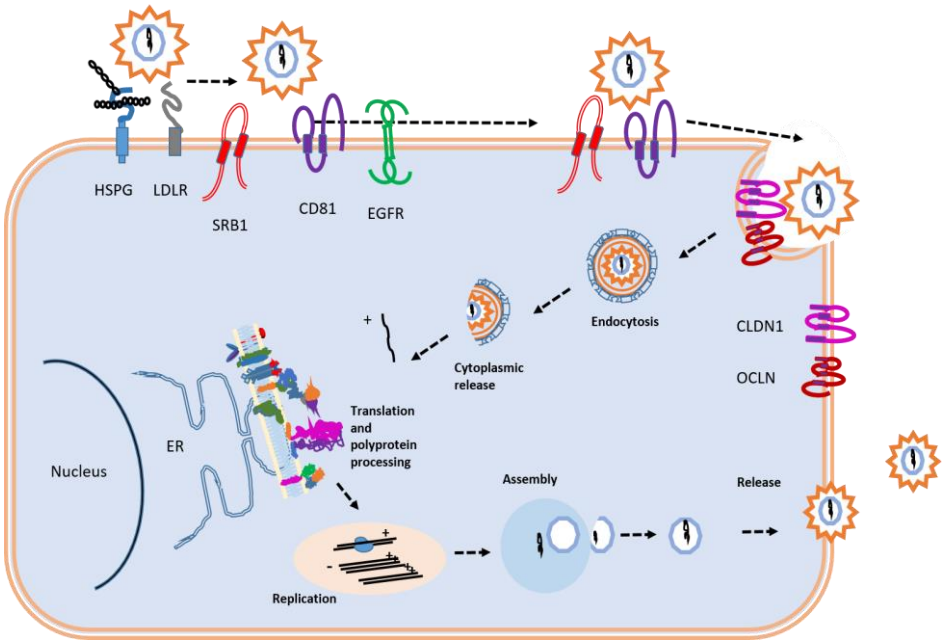

Figure 1-3 Hepatitis C virus life cycle

The life cycle of HCV virus is shown from entry into the host cell to the release of mature virus. The main steps are represented by doted arrows. HCV binds to different receptors like HSPG, LDLR, SRB1, CD81 OCLN and CLDN1 on the surface of the hepatocyte, and is then internalized in the cytoplasm by endocytosis. The low pH environment in the cytoplasm helps in the release of positive (+) sense RNA. This RNA is used for HCV polyprotein translation in ER followed by HCV RNA replication in membranous web structures. HCV RNA and proteins assemble into new virions which are released by the process of exocytosis.

1.2.6.3 Viral protein translation and processing

After un-coating, the HCV RNA serves as a template for protein translation. Usually mRNA is protected from exonucleases degradation at both 5' and 3' ends by a 7-methylguanosine (m^7G) cap and poly A tail, which are also necessary for translation. The HCV RNA bypasses the requirement of cap binding factors by using the internal ribosome entry site (IRES) element present in the 5'UTR which will be discussed later in section (1.3.3).

HCV proteins are translated as a single polyprotein and then processed into individual proteins by host and viral proteases. The signal peptide sequence between the C-terminal of core and the N-terminal of glycoprotein E1 is necessary for the cotranslational translocation of polyprotein into the endoplasmic reticulum. After the translocation of polyprotein to the endoplasmic reticulum (ER) membrane, the processing starts with HCV core protein cleavage by the host protease signal peptidase at the signal peptide sequence between core and E1, leaving the signal peptide at the C-terminal end of core embedded in the ER membrane (Figure 1-4). This is followed by release of mature core by the ER enzyme signal peptide peptidase by cutting off the signal sequence (Hijikata, Kato et al. 1991, McLauchlan, Lemberg et al. 2002). E1E2 is cleaved by signal peptidase which is followed by the reorientation of the C-terminal domains of both E1 and E2 in the ER membrane with the N-terminal oriented to the ER lumen (Penin, Dubuisson et al. 2004). The host signal peptidase then cleaves between p7 and NS2 in the ER lumen. This is followed by the auto-cleavage between NS2 and NS3 by NS2/3 protease, while the serine protease NS3 is responsible for the

separation of N3 and NS4. NS4A is a cofactor of this enzyme and is vital for NS3 activity (Hijikata, Mizushima et al. 1993). This virally encoded enzyme is also responsible for processing the remaining viral proteins by cutting at three positions present between NS4A/NS4B, NS4B/NS5A and NS5A/NS5B (Hijikata, Mizushima et al. 1993).

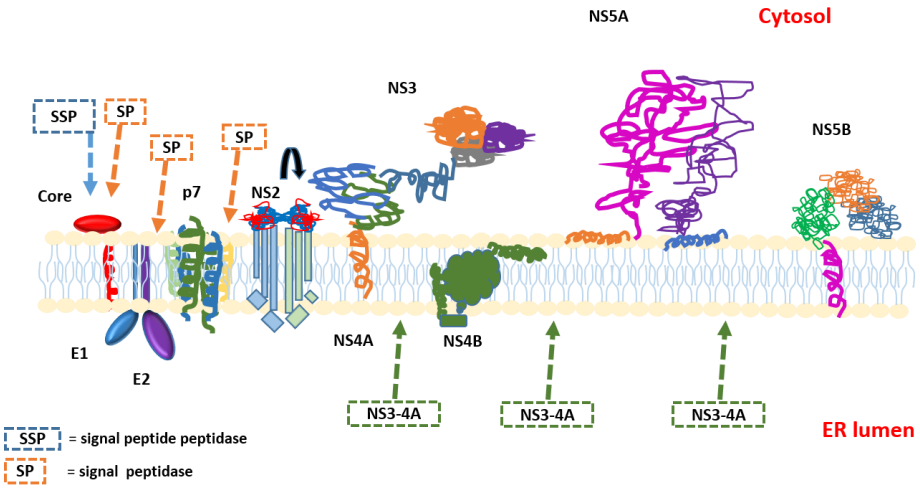

Figure 1-4 HCV polyprotein processing

HCV translation take place in cytoplasm of liver cells where HCV proteins are made as one polyprotein. The specific signals in polyprotein translocate it to ER membrane where this polyprotein is processed into individual mature proteins. The cellular (SSP and SP) and viral enzymes (NS3-4A) involve in processing are shown by blue, orange and green dashed arrows and boxes.

1.2.6.4 HCV replication

After polyprotein processing, the HCV positive sense RNA is used to generate the full-length negative RNA strand intermediate. This negative sense RNA serves as the template for synthesis of 10-100-fold excess positive sense progeny RNA molecules. HCV non-structural proteins NS3, NS4A, NS4B, NS5A and NS5B are involved in HCV replication by forming HCV replication complexes at the ER derived membranous web structures (Lohmann, Korner et al. 1999) which provide the site for HCV replication. The protease-nuclease- and detergent-resistant nature of these membranous vesicles indicates that viral replication is protected and that these vesicles are derived from ER (Aizaki, Lee et al. 2004, Targett-Adams, Boulant et al. 2008). NS4B induces the formation of membranous web vesicles (Egger, Wolk et al. 2002) where the RNA replication complex including the negative-sense RNA assembles (Paul, Madan et al. 2014). NS3 helicase function is necessary for the removal of secondary structures from the template RNA. The weak helicase activity of NS3 is enhanced by NS4A which anchors NS3 with the membrane structure (Lindenbach and Rice 2013). NS5A protein is involved in RNA binding and enhancement of NS5B RNA polymerase activity. NS5B is an RNA dependent RNA polymerase which is the main enzyme of HCV RNA replication. It binds to the 3’ end of the positive sense viral RNA with very low specificity and initially incorporates two nucleotides to use them as a primer (Ferrari, He et al. 2008). *In vitro* studies suggest replication initiation may require helicase activity to unwind the local structure for NS5B binding and initiation. The primer mode switches to progressive elongation mode by

the binding to GTP. The GTP binding induces a high degree of conformational changes in NS5B which not only moves the primer but also opens up the polymerase core for elongation. After the initial priming, NS5B incorporates 100-400 nucleotides per minute and replicates the whole RNA genome (Simister, Schmitt et al. 2009).

1.2.6.5 HCV assembly and release

The HCV assembly process is not fully understood. It involves different cellular and viral factors and complexes, including E1 and E2 complexes, host lipid droplets (LDs) and ER membrane. The E1E2 proteins are glycosylated in the ER (Silberstein and Gilmore 1996), where these glycoproteins work as ER retention factors and HCV receptors (Duvet, Cocquerel et al. 1998, Penin, Dubuisson et al. 2004). NS2 helps in virus assembly by bringing p7, E1E2 complexes and NS3-NS4A enzyme complex together in the ER membrane (Suzuki, Ishii et al. 2007). The mature core assembles into the HCV capsid at the cytoplasmic side of the ER (Blanchard, Hourioux et al. 2003), which is the virus assembly site, while nucleocapsid formation and budding are reported to take place in concert (Lindenbach and Rice 2013) followed by the transportation of viral particles through the Golgi apparatus where modifications like E1E2 glycan addition and acquisition of low density lipid occur before viral release (Paul, Madan et al. 2014) (Figure 1-3).

1.2.6.6 Host factors involved in the HCV life cycle

During the life cycle in hepatocytes, HCV interacts with and uses several host factors at different stages. On the bases of literature mining and analysis of protein-protein interactions, a recent study has shown 969 human proteins as the HCV interactome (Saik, Ivanisenko et al. 2016). HCV interacts with all these proteins to modulate and coordinate several cellular systems and mechanisms to successfully propagate in the hepatocytes. As described earlier in section 1.1.5.1, hepatocyte surface protein receptors like LDLR, CD81, SRB1 and others are host factors involved in tissue tropism, recognition and internalization of HCV (Scarselli, Ansuini et al. 2002, Popescu, Riva et al. 2014). After entry and release into the cytoplasm, HCV RNA is translocated to ER, where translation of HCV polyprotein takes place. The are many host factors involved in the translation which include the ribosomal subunits and eukaryotic translation initiation factors. Other factors involved in HCV translation include poly C binding protein 2 (PCBP2), poly-pyrimidine tract-binding protein (PTB), La protein, Gemin5 and LSm proteins. PCBP2 binds stem-loop I of the 5' UTR and increases HCV translation by its involvement in RNA circulation (Wang, Jeng et al. 2011), while the role of PTB in HCV translation enhancement in controversial and obscure (Anwar, Ali et al. 2000, Nishimura, Saito et al. 2008). Another host protein La is also reported to bind the AUG start site in the stem-loop IV and enhance HCV translation (Anwar, Ali et al. 2000). LSm1-7 and Gemin5 bind to stem-loop III of the HCV IRES and positively and negatively regulate the HCV translation, respectively (Pacheco, Lopez de Quinto et al. 2009).

In addition to the host factor involvement in HCV entry, translation and polyprotein processing, there are several other host factors involved in HCV replication, assembly and release. HCV replication takes place in membranous webs or membrane vesicles. The host lipid kinase phosphatidylinositol 4-kinase III alpha (PI4KIIIα) plays an important role in HCV replication by its involvement in NS5A phosphorylation and membrane vesicle morphology (Reiss, Rebhan et al. 2011). A liver specific microRNA, miR-122, binds to two sites in HCV 5' UTR and increases HCV RNA abundance (Jopling, Yi et al. 2005). The role of miR-122 in HCV regulation will be discussed later in section 1.5.5.

1.2.7 HCV pathogenesis and immune response

The innate immune system uses different pattern recognition-receptors (PRRs) like Toll-like receptors (TLRs), retinoic acid-inducible gene I-like receptor (RIG-1) and cytoplasmic dsDNA sensor protein kinase R (PKR) to detect molecular patterns associated with infection. PKR detects dsRNA formed during HCV replication and RIG-1 recognises HCV RNA (Arnaud, Dabo et al. 2011). Both pathways activate mitochondrial antiviral signalling (MAVs), leading to recruitment of tumour necrosis factor receptor-associated factor 3 (TRAF-3). TRAFs are involved in the regulation of apoptosis and stress responses (Arch, Gedrich et al. 1998). HCV pathogen-associated patterns recruit the signalling complexes and initiate the activation of type I and III and proinflammatory cytokines. IFN production further initiates the interferon stimulated genes (ISGs) (Horner and Gale 2009), which collectively initiate an innate immune response against the

invading virus. Type I IFN and IL-12 secretion by plasmacytoid dendritic cells (pDCs) increases the natural killer (NK) cell proliferation, their ability to produce IFN-γ and cytotoxicity and also inhibits viral replication (Vivier, Tomasello et al. 2008). As a part of the early innate immunity against viral infections, natural killer (NK) cells recognize the infected cells, destroy them and secrete IFN-γ.

On the other hand, HCV uses different strategies to overcome the innate immune response. HCV NS3-4A protease cleaves MAVS (also termed as IPS-I, Cardif and VISA) and TRIF and inhibits the IFN mediated signalling in infected cells (Li, Foy et al. 2005, Li, Sun et al. 2005). NS4B disrupts MAVS and blocks the production of IFN (Douam, Ding et al. 2016). Polymorphisms associated with IFN- γ mRNA are also reported to be associated with clinical outcome of HCV. This also provides evidence of the role of IFN-γ polymorphism with different innate immune responses. After the failure of the innate immune response to clear HCV infection, the adaptive immune response is induced to fight against HCV. This response system is comprised of HCV-specific T cells and HCV neutralizing antibodies (Douam, Ding et al. 2016). Several reports indicate the failure of the T-cell response against HCV which ultimately leads to persistence of HCV infection leading to development of chronic infection. During the chronic infection, HCV viral replication leads to continuous stimulation of cytotoxic T cells (CTLs) and inflammation, which leads to the dysfunctional CTL response. The T-cell response can be seriously impaired by repeated HCV infections. HCV also circumvents the T-cell response by development of viral variants or

quasispecies and impaired T-cell function or T-cell exhaustion (Lauer 2013). In HCV infection, HCV-specific CD8+ T cells have the ability to clear the virus at an early stage and help in establishment of HCV specific T cell memory. One third of CD8+ T cells in chronic hepatitis C virus were shown to have naive phenotype which indicate that they have not yet interacted with specific antigen, even when HCV is replicating in hepatocytes (Nitschke, Flecken et al. 2015).

As described in the above section (1.2.3), the majority of patients develop chronic infection. High genetic variability in the hyper variable region (HVR) of the E2 protein leads to escape of HCV virus from host immune system (Choo, So et al. 1995, Logvinoff, Major et al. 2004). As described above, other HCV proteins are also reported to be involved in inhibition of the immune response, which could lead to the persistence of the infection (Kato 2001). Other factors like co-infection with HBV or HIV and alcohol consumption are also reported to contribute to the development of HCV chronic infection (Zhang, Li et al. 2003). All these factors contribute to the persistence of HCV virus infection which leads to cirrhosis and hepatocellular carcinoma (HCC). On the basis of HCV genetic variants (genotypes) and the stage of the infection, different types of treatment plans and drugs have been suggested (Panel 2015). Current and new drugs and their advantages and problems will be discussed in later sections.

1.3 Translation

Translation is a process by which a messenger RNA (mRNA) is read and used as a template to make the corresponding protein. Usually translation starts from the binding of the eIF4F complex to the 7-methylguanosine (m^7G) cap at the 5' end of the mRNA. This type of translation is called cap-dependent translation. There is also another type of translation initiation, in which the initiation factors and ribosomal subunits are recruited directly to specific structures present in the 5'UTR called internal ribosome entry sites (IRES). Both type of translation initiation process and the factors involved are discussed below.

1.3.1 Cap-dependent translation

Protein translation can be divided into three main steps, initiation, elongation and termination. Each of these steps is highly complex and organized in a sequential manner. Translation initiation is the most complex and highly regulated phase (Marintchev and Wagner 2004, Aitken and Lorsch 2012) and spans all the events from the dissociation of ribosomes in termination to the assembly of these ribosomes on the mRNA start codon ready for elongation. The basic purpose of this phase is to assemble different initiation factors (IFs) on ribosomal subunits to bind and then scan mRNA in search of an initiation codon.

Translation initiation starts with the joining of eIF2-GTP and Met-tRNA to form the ternary complex (TC). eIFs 1, 1A, 3 and 5 then bind to the 40S

ribosomal subunit which brings a conformational change in 40S and provides open access to the binding of TC and results in the formation of the 43S pre initiation complex (PIC). eIF4F is an initiation complex consisting of eIF4A, eIF4E and eIF4G; these components give eIF4F diverse functions like RNA unwinding, Cap-binding and mRNA-ribosome binding (Gingras, Raught et al. 1999). eIF4E binds to the cap as part of the eIF4F complex. eIF4G is a scaffold protein which binds to eIF4E, poly A binding protein (PABP), eIF3 and eIF4A. eIF4G, eIF4E, PABP and eIF3 binding give mRNA a typical "closed loop" structure. eIF4A, eIF4H, eIF4B and eIF4G enhance unwinding of the 5'UTR to provide a single stranded region on mRNA, allowing 43S recruitment and subsequent base-by-base scanning of the 5'UTR until the recognition of an AUG start codon in the correct context (Figure 1-5). Codon-anticodon recognition by Met-tRNAi leads to eIF1 release and conversion of eIF2-GTP to eIF2-GDP state. Release of the phosphate group converts the PIC into a closed state of conformation and halts the scanning process (Hinnebusch 2011, Aitken and Lorsch 2012). 60S recruitment is then mediated by eIF5B and elongation commences.

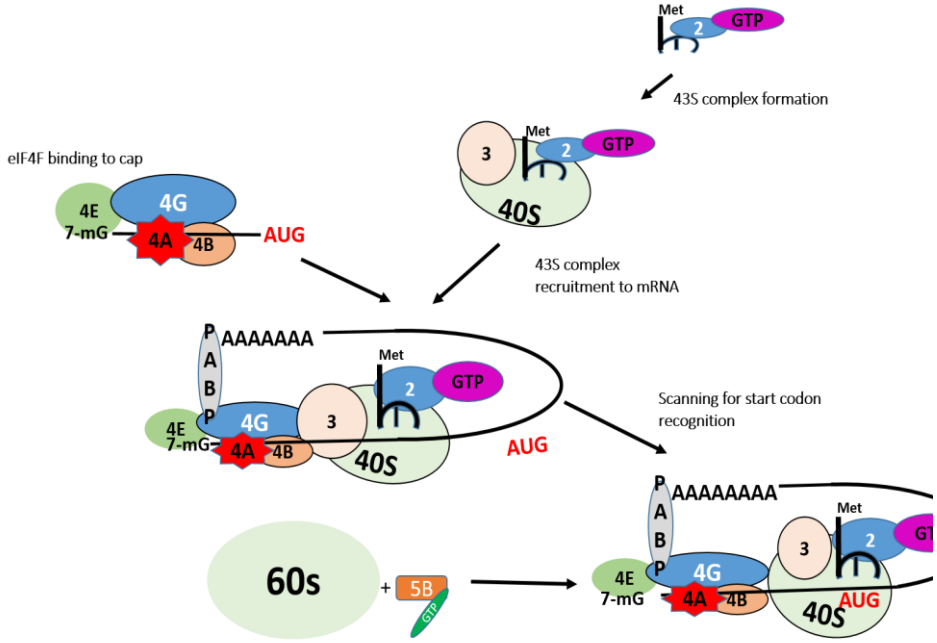

Figure 1-5 Cap-dependent translation initiation

Cap-dependent translation initiation starts with the binding of Met-tRNA to the eIF2-GTP complex, to form the ternary complex. The ternary complex binds to the 40S ribosomal subunit, which results in the formation of the 43S pre-initiation complex. eIF4E, a member of eIF4F complex, binds to the 5' cap structure of the mRNA and recruits the 43S pre-initiation complex to the mRNA. The eIF4A helicase unwinds the secondary structure and helps 43S scanning and subsequent start codon recognition, which is followed by 60S ribosomal subunit recruitment and a transition to elongation.

1.3.2 IRES-dependent translation

Although the majority of RNA transcripts are translated in a cap-dependent manner, certain viral and cellular mRNAs are translated via special RNA structures known as internal ribosome entry sites (IRES) present in the 5'UTR. These cis-acting elements help cellular mRNA to be translated in different stress conditions (e.g. starvation, hypoxia and apoptosis) and also involved in cancer (Thompson 2012), while enabling viruses to inhibit the cellular translation without affecting the viral translation (Belsham 2009).

On the basis of structure-based classification, viruses with closely related IRES elements were classified into four different classes with different initiation factor requirements. The HCV IRES belongs to class 3 and does not require the eIF4F complex (Pestova, Shatsky et al. 1998).

1.3.3 HCV IRES

The HCV 5' UTR is about 340 nt long (Friebe and Bartenschlager 2009) and is more structured than the 3' UTR. The 5' UTR comprises four domains (dI-dIV) while dIII is further divided into four stem loop structures and a highly structured component known as a pseudoknot (Wang, Le et al. 1995). Unlike host mRNA, HCV RNA doesn't have a 5' m7G cap structure. This lack of cap structure results in cap-independent translation in HCV. A specific structural motif in dII-IV of HCV IRES allows HCV RNA to directly recruit the translation initiation factor eIF3 and the 40S ribosomal subunit (Lukavsky, Otto et al. 2000) (Figure 1-6). Domain III loops abc contain the eukaryotic initiation factor 3 (eIF3) binding site while loops def harbour the 40S binding site and

also provide the correct orientation for the open reading frame (ORF) on the 40S subunit (Pineiro and Martinez-Salas 2012). HCV IRES directly recruits eIF3 and the 40S ribosomal subunit which results in the efficient 80S complex formation and translation initiation (Lukavsky 2009).

Although HCV IRES domain II is not required for 40S subunit binding, it is reported to stabilize the conformational changes in the ribosome and help in the mRNA binding at the right position and subsequently closes the mRNA binding cleft (Spahn, Kieft et al. 2001).

Apart from the 5'UTR domains, HCV 3' UTR loop structures are also reported to regulate HCV translation (Tuplin, Struthers et al. 2015). A three to five-fold difference has been shown in the efficiency of translation between the presence and absence of the 3'UTR X region (Ito, Tahara et al. 1998). 60S recruitment and elongation of translation proceed in a similar fashion to cap-dependent translation following 40S recruitment by the HCV IRES (Hellen 2009, Filbin, Vollmar et al. 2013).

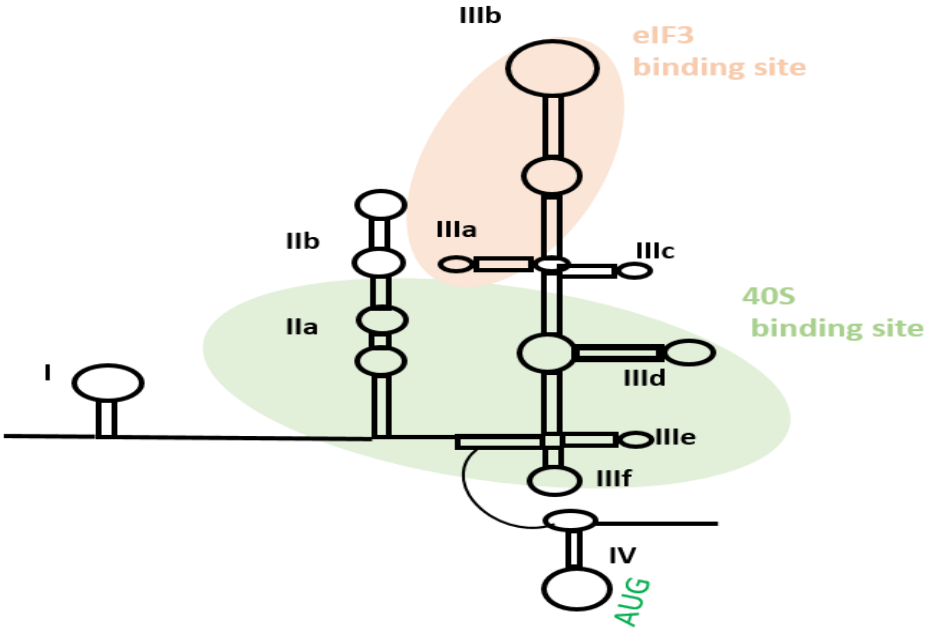

Figure 1-6 HCV 5'UTR

The figure represents a cartoon depiction of the 5'UTR of HCV. The 5'UTR contains four domains (I to IV) and many stem-loops. Domain II, III and IV comprise the IRES. These domains provide the 40S ribosomal subunit binding site (light green oval), while domain IIIa and IIIb form the binding site for eIF3 (light orange oval). The AUG start codon is shown in green.

1.3.4 HCV 3'UTR

Beside the RNA structures in HCV 5' UTR, there are secondary structures in NS5B and 3' UTR regions which contain cis signals involved in HCV translation and replication (Tuplin, Wood et al. 2002, Romero-Lopez and Berzal-Herranz 2009).

On the basis of computer modeling, six stem-loop structures have been predicted in the NS5B coding region of subgenomic replicons. Five structures have a significant functional role in HCV RNA replication while disrupting one of the theses stem-loop structures (5BSL3.2) blocked the HCV RNA replication.

HCV 3'UTR consist of three distinctive regions, which include a variable region, poly U/UC region and X region. The variable region is variable in length (from 27 to 70 it) and sequence among different HCV genotypes and contain two stem-loop structures (Kolykhalov, Feinstone et al. 1996). The Poly U/UC region consist a poly C(U) repeat region which is also called translational region and is unique to HCV and GBV-B viruses in flaviviruses (Simons, Pilot-Matias et al. 1995)(simons 1995). The X region contains three stem-loop structures (SL1-SL3) and proposed to have a hypothetical pseudoknot (Dutkiewicz and Ciesiolka 2005)(Dutkiewicz and ciesiolka 2005). Sequence-based analysis of the strains isolated from the patient sera indicates that the stem-loop structure of x-tail region provides a double-stranded stem to HCV genome. These stem-loop structures play an important role in HCV translation, replication, stabilization and packaging of HCV RNA genome. Mutations in terminal 3' UTR sequence fail to initiate the

infection in chimpanzees, which indicate the involvement of this region in HCV replication Kolykhalov et al., 2000; Yanagi et al.,1999b). The poly-U region on X region of HCV 3' UTR act as poly A region in mRNA and binds PTB proteins which result in circularization of HCV RNA and enhancement of HCV translation. A different study showed an increase translation of HCV RNA in the absence of polyU/UC region (Murakami et al., 2001). Additional studies are required to fully understand the 3'UTR involvement in HCV replication and translation.

1.4 Helicases

Helicase is a class of enzymes that function to unwind nucleic acid strands. Double-stranded DNA or RNA are bound by hydrogen bonds between the complementary bases. A helicase enzyme uses ATP hydrolysis to gain energy to break the hydrogen bonds and to separate the strands. These proteins are implicated in many processes which include DNA recombination, transcription, RNA splicing, translation, ribosome biogenesis and RNA editing (Patel and Donmez 2006). Helicases are part of a large group of enzymes know as translocases. Both DNA and RNA helicases are classified into six superfamilies (SF1-6) on the basis of conserved motifs (Gorbalenya and Koonin 1993). Most of the RNA helicases belong to SF2. Both SF1 and SF2 helicases consist of about nine motifs (Bleichert and Baserga 2007). DEAD-box helicases are the largest group in SF2 and are discussed below.

1.4.1 DEAD-box helicases

eIF4A belongs to the DEAD-box protein family which function as ATP-dependent RNA helicases. These proteins are present in both eukaryotes and prokaryotes and involved in all RNA related functions like transcription, splicing, translation, export, decay and ribosomal biogenesis (Rogers, Lima et al. 2001). The name DEAD-box is given due to the presence of an Asp-Ala-Glu-Asp sequence in Walker motif B. The nine conserved motifs in DEAD-box helicases are located in two different domains (figure 1-7). Motifs I (Walker A), Ia, Ib, II (Walker B) and III are in domain 1 and IV, V and VI are present in domain 2. All DEAD-box proteins have RNA binding and ATP hydrolysis activity but only a subset has unwinding activity. All these activities are shared by different motifs (figure 1-7). Motif I and II have Mg^{2+} binding activity, and with motifs Q and VI are also required for ATP binding. Helicase activity is present in motif III and is energy dependent which is provided by the breakdown of ATP. RNA binding is present in Ia, Ib, IV and V motifs. The DEAD-box helicase eIF4A is involved in translation initiation and is discussed below in detail.

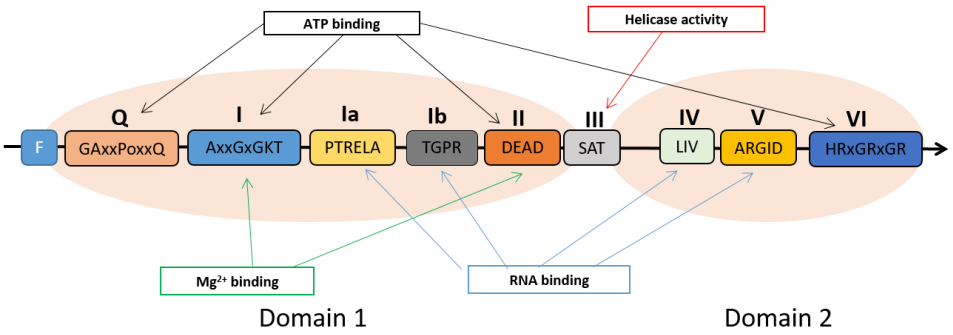

Figure 1-7 DEAD-box helicase structure and functions

The figure represents the typical motifs of a DEAD-box protein, and the important amino acids in the motifs. The two domains are represented by orange ovals. The activities are represented by rectangles while the arrows show the involvement of motifs in these activities.

1.4.1.1 eIF4A Helicase

1.4.1.1.1 General overview

eIF4A proteins are DEAD-box helicases and belong to the largest RNA helicase family SF2. eIF4A proteins have short N and C terminals and minimal conserved motifs necessary for basic DEAD box helicases, hence serve as a paradigm for the study of DEAD box proteins (Lorsch and Herschlag 1998, Lorsch and Herschlag 1998). eIF4A is considered as “godfather” of the DEAD box proteins because of its discovery as one of the first helicase proteins which provided the basis for the establishment of governing principles for DEAD box protein functions (Rogers, Komar et al. 2002).

1.4.1.1.2 eIF4A homologs and their functions

eIF4A has three isomers in mammals: eIF4AI, eIF4AII and eIF4AIII. eIF4AI and eIF4AII show more than 90% sequence similarity and have long been considered as functionally interchangeable, while eIF4AIII is considered as functionally distant as it has only 60% sequence similarity with eIF4AI and eIF4AII (Nielsen and Trachsel 1988, Owttrim, Hofmann et al. 1991). The motifs in eIF4A impart the ATP-dependent RNA helicase and RNA-dependent ATPase activities, while the helicase activity was only reported in eIF4AI and eIF4AII (Li, Imataka et al. 1999). Both eIF4AI and eIF4AII have been shown to interact with eIF4G and freely exchange in eIF4F complex (Yoder-Hill,

Pause et al. 1993). eIF4A is part of the eIF4F complex and helps ribosome binding and scanning function by unwinding the secondary structure present in the mRNA 5'UTR (Pestova, Kolupaeva et al. 2001).

eIF4AIII is expressed at much lower levels than eIF4AI and there is no evidence of eIF4AIII involvement in translation, indicating that eIF4AIII is functionally distinct from the other two eIF4A proteins (Li, Imataka et al. 1999). eIF4AIII is part of the exon junction complex that is deposited on transcripts during RNA splicing. In the nucleus, eIF4AIII binds to RNA in close conformation and helps in nuclear export (Le Hir, Gatfield et al. 2001). eIF4AIII is also involved in nonsense-mediated decay (NMD) of mRNA (Palacios, Gatfield et al. 2004). Interestingly, despite their close homology, recent studies show that both eIF4AI and eIF4AII proteins are also functionally distinct which is discussed below in section 1.4.1.1.3 (figure 1-8).

1.4.1.1.3 Differences between eIF4AI and eIF4AII

eIF4AI/II's basic role is to unwind the RNA secondary structures present in 5'UTR regions of mRNA transcripts which helps the ribosomal subunit in binding and downstream translocation and recognition of the start codon. Although both eIF4AI and eIF4AII were considered to be functionality interchangeable, differential expression has been reported previously (Nielsen and Trachsel 1988). Another study showed that eIF4AI is expressed in dividing cells, while eIF4AII is more strongly expressed in growth arrested

cells (Williams-Hill, Duncan et al. 1997). eIF4AII has also been shown to bind to the C-terminal region of HCV NS5B RdRp, and it was suggested that eIF4AII helps the HCV RNA polymerase function of replication by unwinding the secondary structures present in HCV genome (Kyono, Miyashiro et al. 2002). eIF4AI showed higher affinity than eIF4AII for the eIF4F complex and knockdown of eIF4AI resulted in the increase in both transcription and protein expression of eIF4AII. However, this increase in eIF4AII couldn't rescue the eIF4AI function related to cell viability (Galicia-Vazquez, Cencic et al. 2012). High expression of eIF4AII has also been associated with better treatment outcomes in cancer while eIF4AI has been reported to be upregulated in different malignancies (Shaoyan, Juanjuan et al. 2013, Modelska, Turro et al. 2015).

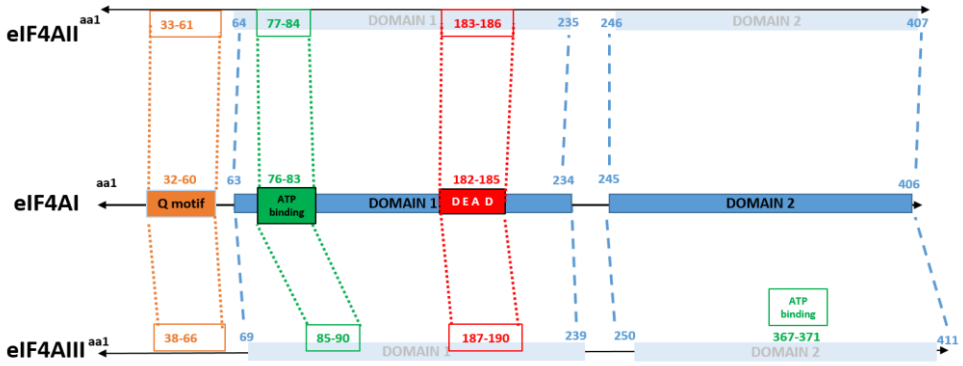

Figure 1-8 Domains and the relative length of eIf4A proteins

Motifs and domains of eIF4A homologs are compared and relative positions of Q motif (orange), ATP binding (green) and DEAD box motif (red) and domains (blue) are shown in numbers.

1.4.1.1.4 eIF4A and miRNAs

Recently, it has been shown that eIF4AII but not eIF4AI is critical for microRNA-mediated gene regulation (Meijer, Kong et al. 2013). Furthermore, it was shown that eIF4AII interacts with CCR4-NOT complex via CNOT1, and suggested that this results in clamping of eIF4II on the mRNA and a subsequent block of 43S scanning. This model was not proved by later studies as the interaction between CNOT1 and eIF4AII was not confirmed (Mathys, Basquin et al. 2014). Another study showed that the CRISPR-mediated knockout of eIF4AII does not inhibit miRNA mediated repression (Galicia-Vazquez, Chu et al. 2015). Recently it has been shown that miRNA and CCR4-NOT based repression is independent of 43S scanning (Kuzuoglu-Ozturk, Bhandari et al. 2016). In *Drosophila*, miRNAs Ago1-RISC induces dissociation of eIF4A from the target mRNA and blocks the formation of eIF4F complex in translation initiation (Fukaya, Iwakawa et al. 2014).

1.4.1.1.5 eIF4A specific regulation and effects

eIF4A proteins interact with several proteins to efficiently perform its role in translation. These proteins either activate, aid and enhance the eIF4A function or work as eIF4A inhibitors. There are four mammalian homologues of eIF4G and all bind to eIF4A protein via different domains and shown to act at different cellular mRNAs translation (Caron, Charon et al. 2004). Both eIF4GI/II bind to eIF4A in close configuration on mRNA which result in eIF4A based linearization of mRNA secondary structures. the third eIF4G protein DAP5/p7 is associate itself to polysomes in no-stressed cells and moves to

stress granules in stressed condition which indicates its role in translation of mRNAs in stressed condition (Nousch, Reed et al. 2007). The fourth eIF4G homologue Paip1 binds to eIF4A at different site then eIF4GI/II and has role in stabilization of close-loop in translation by bind PABP. While its role in eIF4A's function is still unknown.

Programmed cell death 4 (Pdcd4) protein binds to eIF4A via MA3 middle (MA3-m) and MA3 C-terminal (MA3-c) domains and prevent the closure of eIF4A RNA binding domains, hence block its helicase activity (Shibahara, Asano et al. 1995). Pdcd4 has been shown to play tumour suppressor activity as an anti-neoplastic factor (Jin, Kim et al. 2006). It is also involve in the development of resistance to inflammatory diseases in mice model via increase in the expression of anti-inflammatory cytokines especially of the cytokines which have more structured 5'UTR regions in mRNA (Hilliard, Hilliard et al. 2006).

Several natural anti proliferative compounds including hippuristanol, pateamine A and silvestrol have been identified as novel inhibitors of eIF4A.

Hippuristanol is isolated from the gorgonian *Isis hippuris* (Shen et al 2001), it binds to C-terminal domain of eIF4AI/II with equal affinity due to the similarities hippuristanol binding sites. It inhibits eIF4AI/II helicase, ATPase and RNA binding activities in dose dependent manner (Bordeleau, Mori et al. 2006).

There is an enough body of work growing that indicate the role of eIF4A in tumour formation, maintenance. Blocking eIF4A activity by either Pdcd4,

anti-sense RNAs and natural inhibitor like silvestrol delayed the tumour initiation and progression and in pre-clinical trials in cancer models. Although hippuristanol mechanism of action against eIF4A is different from silvestrol, it has the highest activity as eIF4A inhibitor against tumour cells in cell culture system.

1.5 MicroRNAs

MicroRNAs (miRNAs) are small non-coding RNA molecules which regulate protein expression in different organisms (Han, Lee et al. 2004). Mature miRNAs are 21-22 nucleotides long and these are the most abundant regulatory molecules in animals (Landgraf, Rusu et al. 2007). More than 60% of human genes have been reported to be target of miRNAs (Friedman, Farh et al. 2009) and almost every process in the cell is reported to be regulated by miRNAs (Fabian, Sonenberg et al. 2010).

1.5.1 miRNA biogenesis

Like mRNA transcription, microRNAs are synthesized by RNA Polymerase II in the nucleus in the form of primary (pri-) miRNAs. These pri-mRNAs are up to several thousand nucleotides (nt) long and are recognized by a nuclear processing enzyme called Drosha, which endo-nucleolytically cleaves the pri-mRNA to release an about 70nt long, hairpin molecule called precursor (pre)-miRNA, while another protein called DGCR8, a double stranded RNA binding protein, is necessary for Drosha cleavage of pri-mRNA (Han, Lee et al. 2004). Drosha cleavage leaves a 2nt 3' overhang on pre-miRNAs which helps exportin5 protein in binding and subsequently transporting pre-miRNA into

the cytoplasm (figure 1-9). In the cytoplasm, another enzyme, Dicer, binds to the pre-miRNA and further cuts it into a mature miRNA duplex of about 21-22nt length (Denli, Tops et al. 2004, Gregory, Yan et al. 2004).

1.5.2 miRNA-mediated target regulation

Mature miRNAs bind to the RNA induced silencing complex (RISC). One strand called the guide remains bound while the other complementary strand of the Dicer-processed duplex leaves the RISC and is degraded. The guide strand helps RISC in recognition of complementary targets, usually present in the 3' UTR of mRNAs. Partial or full complementarity of double stranded structure of RNA is then recognized by Argonaute1-4 (Ago1-4) proteins which either repress translation or cleave the target mRNA (Figure 1-9). Full complementarity between the miRNA and the target results in Ago2-mediated cleavage of target mRNA, but in animals most targets are imperfectly complementary and are therefore not cleaved, but are post-transcriptionally repressed (Schwarz, Hutvagner et al. 2003, Fabian and Sonenberg 2012). Perfect Watson-Crick complementarity between miRNAs nucleotides 2-8, known as the seed, and the target has been suggested to be most important for target recognition and subsequent repression (Lewis, Shih et al.). Although the exact mechanism of miRNA mediated repression is not completely known and is controversial, it seems that both inhibition of translation and deadenylation followed by mRNA decay are involved (Fabian, Sonenberg et al. 2010). It is estimated that about 65% of human mRNAs are regulated by miRNAs. This gene regulation has made miRNAs an

attractive and powerful tool for diagnostic and therapeutic application (Nana-Sinkam and Croce 2013). Accumulating evidence suggest that the dysregulation in expression of specific miRNA is linked with development of different diseases like cancer, cardiac diseases, neurodegenerative diseases and viral infections.

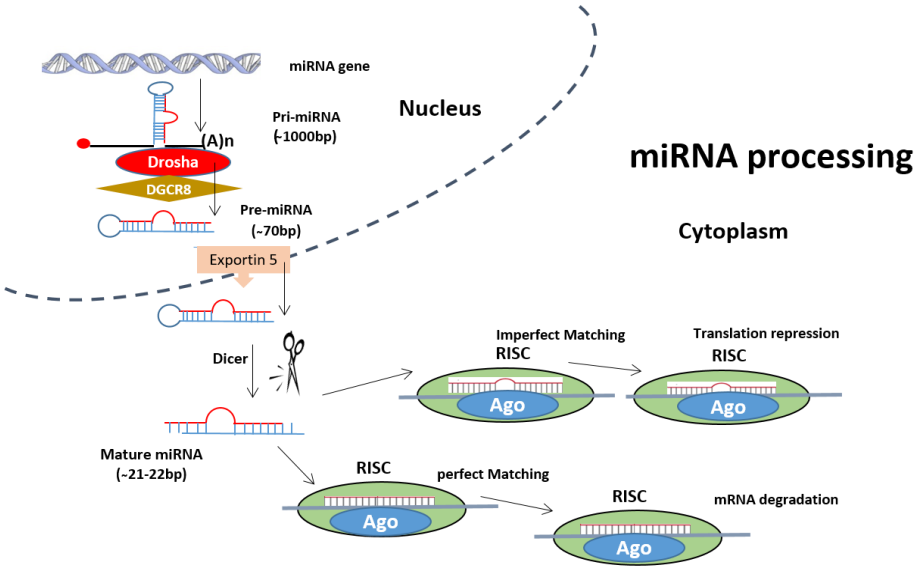

Figure 1-9 miRNA biogenesis and function

microRNA biogenesis starts with the transcription of pri-miRNA from the miRNA gene. The pri-miRNA is then processed to produce a ~70nt long pre-miRNA by the action of the nuclear RNAse III enzyme Drosha, which binds with its cofactor DGCR8. This pre-miRNA is exported to the cytoplasm by Exportin 5. Once in the cytoplasm, the pre-miRNA is further processed by Dicer into 21-22bp mature miRNA duplexes. The guide strand of the mature miRNA is loaded onto RNAi-induced silencing complex (RISC) and guides the RISC to mRNA targets. The miRNA binding to its target can result in translational repression and/or degradation of the message, depending on the degree of complementarity.

1.5.3 miRNAs and CCR4-NOT complex

In animals, usually miRNA targets are partially complementary to the miRNA and catalytically active Ago proteins do not cleave the target but recruit other proteins to mediate the repression. The best categorised Ago-binding protein is GW182 which is required for miRNA mediated silencing (Fabian and Sonenberg 2012, Braun, Huntzinger et al. 2013). The GW182 proteins use multiple GW (glycine and tryptophan) repeats to bind to the N-terminal of Ago protein. This binding further recruits the effector complexes like CCR4-NOT and deadenylase complexes like PAN1 and PAN2 to complete the miRNA mediated repression (Braun, Huntzinger et al. 2013) (figure 1-9).

The CCR4-NOT complex is a multiunit complex in which CNOT1 acts as a scaffold for the other subunits to dock. Different regions of CNOT1 interact with different subunits. The MIF4G like middle region of CNOT1 interacts with CCR4-NOT complex. CNOT1 also interacts with CNOT9 and DDX6 helicase (Chu and Rana 2006).

During the miRNA mediated repression, the binding of GW182 to PABP recruits the CCR4-NOT complex to the target mRNA for deadenylation (Zekri, Huntzinger et al. 2009, Inada and Makino 2014). While depletion of different CCR4-NOT subunits, like CNOT1 and Caf1 inhibited the miRNA mediated repression (Behm-Ansmant, Rehwinkel et al. 2006). This shows that CCR4-NOT complex is required for miRNA mediated repression by its action through deadeanylation.

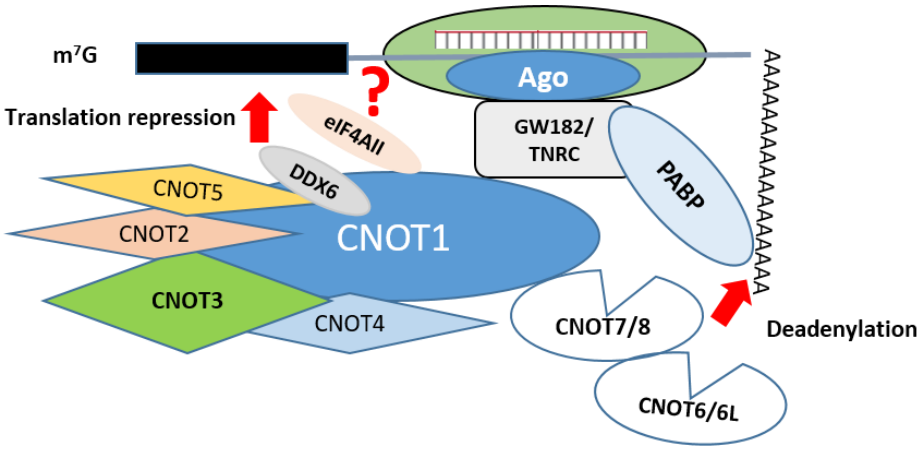

Figure 1-10 CCR-NOT complex function in miRNA mediated repression

Depiction of CCR4-NOT complex formation and its role in miRNA mediated repression of the protein translation. Ago interacting protein GW182 recruit CCR4-NOT complex via its interaction with CNOT1, which also works as a scaffold for the binding of other subunits which involve in translation repression and deadenylation.

1.5.4 miR-122

miR-122 is a liver specific miRNA and it is highly expressed in liver and comprises 70% of the total microRNA expressed in normal liver. High abundance of miR-122 in liver is linked with the maintenance of normal liver metabolism and phenotype. miR-122 works like a central controlling molecule for hundreds of liver genes involved in metabolism, proliferation, diseases and cancer related processes (Boutz, Collins et al. 2011). Although miR-122 has an established role as a tumour suppressor in the liver, recent studies also suggest its involvement in extra hepatic cancers and inflammatory disease (Wang, Wang et al. 2012, Chen, Wang et al. 2013).

The miR-122 gene *hcr* is present on chromosome 18 and its primary (pri-mir-122) transcript is ~5Kb and comprised of two exons (Dhir, Dhir et al. 2015). miR-122 liver specific expression is controlled by hepatocyte nuclear factor 4α (HNF4 α). This liver specific transcription factor binds directly to miR-122 promoter region which results in positive regulation of miR-122 synthesis (Li, Xi et al. 2011).

1.5.5 miR-122 regulation of HCV

miR-122 express in Huh7 and mouse liver cells but not in Hela and human liver derived HepG2 cells. Both miR-122 expressing cell lines are also permissive for Hepatitis C virus propagation.

Two miR-122 binding sites were identified in HCV 5'UTR region by computer based sequence analysis and blocking the miR-122 binding to HCV RNA by addition of anti-miR-122 oligomers results in reduction of HCV in Huh7 cells. Furthermore, the mutation of miR-122 binding sites result in decrease on

HCV abundance in Huh7 N/Neo C-5B cells while addition of miR-122 containing corresponding compensatory mutations restored the HCV RNA abundance, which showed that miR-122 modulate the abundance of HCV in Huh7 cells by directly binding to two binding sites in 5' UTR region of HCV RNA (Jopling, Yi et al. 2005, Jopling, Norman et al. 2006). While miR-122 binding to site 1 in HCV is required for HCV infection (Jangra, Yi et al. 2010). It is also shown that miR-122 simultaneously binds to two sites present in the HCV 5' UTR to execute its action of positively regulate the HCV (Figure 1-11). miR-122 regulation of HCV is the only known example of a miRNA interacting with a 5'UTR being required for positive regulation of viral replication. Different possible mechanisms for the role of miR-122 in HCV regulation have been proposed, but the definite mechanism is still elusive and needs to be determined. It has been shown that two molecules of mir-122 bind simultaneously to HCV which may provide a unique hetero-trimeric structure which stabilizes HCV RNA. One such potential mechanism could be that miR-122 binding provides a dsRNA structure which provides protection to HCV RNA against the 5' to 3' exonuclease activity of cytoplasmic enzymes like Xrn1 and Xrn2 (Machlin, Sarnow et al. 2011, Li, Masaki et al. 2013). However, this is unlikely to fully explain the mechanism of regulation, as mutant miR-122 provided similar protection against exonucleases but could not regulate HCV replication (Li, Masaki et al. 2013).

Recent studies have also shown that Ago proteins are required for miR-122 regulation of HCV, indicating that miR-122 is acting as part of the RISC (Wilson, Zhang et al. 2011). HCV translation is stimulated by miR-122 (Henke,

Goergen et al. 2008, Roberts, Lewis et al. 2011) but it was also shown that this stimulation is not sufficient for full regulation (Jangra, Yi et al. 2010).

In the present study, the miR-122 regulation of HCV is investigated by studying the involvement of eIF4A protein in this regulation.

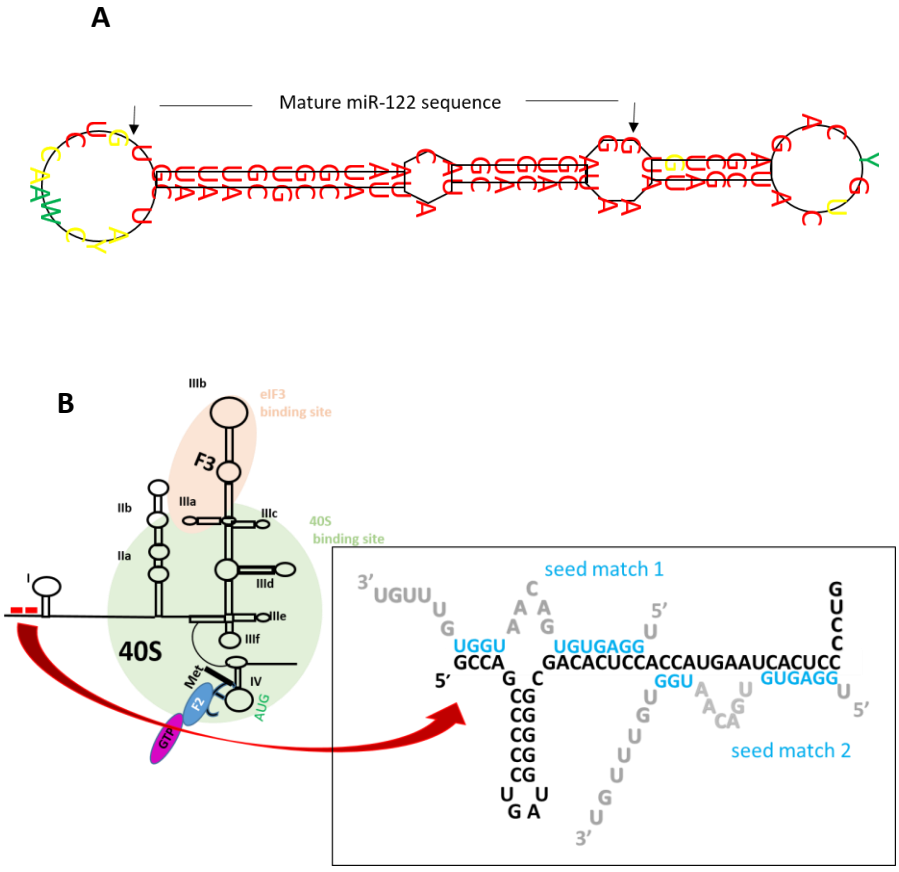

Figure 1-11 miR-122 interaction with HCV

A) Structure of the pre-miR-122 hairpin in which the mature miR-122 sequence is indicated by black arrows. The colour of the nucleotide bases shows the scale of conservation, with red being most conserved and green being the least conserved. B) Interaction between two miR-122 molecules (red rectangles) and their target sites in the HCV 5'UTR. The green circle indicates the 40S binding site and the orange oval show eIF3 binding to stem loops IIIa and IIIb step loops region on IRES. The big black rectangle shows the miR-122 nucleotides level binding to two sites on HCV IRES. The black nicleotides represent HCV sequence while blue nucleotide shows miR-122's HCV interacting nucleotides.

1.6 Tools used in HCV research

1.6.1 Animal Models

Chimpanzee has been used to study the transmission, duration and chronic nature of Non-A, Non-B hepatitis virus even before the identification of HCV (Alter, Purcell et al. 1978) and later on HCV virus genome was also isolated using the chimpanzee model (Bradley, Krawczynski et al. 1991). This same model was also used to in the establishment of HCV infectious clones and proving HCV as a causative agent of the disease (Kolykhalov, Agapov et al. 1997). This system provides many advantages like its similarity with the human which provide the closest possible aspect of HCV infection in human. It also provides a wide range to sample selection including tissues, which are otherwise not easily obtainable in humans especially due to the asymptomatic nature of the HCV infection. This model also allows to rechallenge the animal to study the immune system response.

Number of transgenic mouse models are used to study the pathogenic effects of HCV proteins. Although these models played a great role in the HCV related research, the results are contradictory between the studies. These conflicting results could be due to the use of different mouse strains in these studies or due to the use to different promoters to express the transgenes proteins (Kawamura, Furusaka et al. 1997, Moriya, Nakagawa et al. 2001). This model system provides advantages over the chimpanzee due to the availability and ease in raring and monitoring. The disadvantage includes the its ability to tolerate the human transgenic proteins which elicit

milder immune response compared to normal human liver cell infection. This limitation was overcome by the activation of human transgene by expressing other proteins using adenoviral vector (Wakita, Taya et al. 1998). Although this activation cause the hepatitis but it was not clear whether it was resulted due to the HCV proteins or adenovirus (Yang, Jooss et al. 1996, Wakita, Katsume et al. 2000).

The limitations of transgenic mouse model and chimpanzee system were overcome by the development of xenograft mouse model system. The first models were optimised by combining the properties of SCID mice which allow human liver engraft (Heckel, Sandgren et al. 1990, Mercer, Schiller et al. 2001). the xenograft mice models and chimeric models have been used to study several aspects of HCV biology including development of HCV replication and development of infectious viral particles, evaluation of novel therapies, including gene therapy and interferon based anti-HCV therapies (Pause, Kukolj et al. 2003).

1.6.2 HCV replicons

Although HCV genome organization, structure and role of HCV proteins have been studied in great deal, the studies related to viral life cycle and development of anti-HCV therapies have been limited by the lack of HCV cell culture systems until the development of first subgenomic replicon system.

This system was derived from the cDNA of HCV genotype 1b infected patient. This system was developed and modified by addition of HCV 5' UTR including first 12 codons of capsid protein with neomycin

phosphotransferase (Neo) to confer resistance to G418 cytotoxic drug followed by addition of EMCV IRES element to direct the translation of HCV no-structural proteins and HCV 3' UTR (Lohmann, Korner et al. 1999). although this system successfully replicate within the selected cell clones, the G-418 resistance allowed low frequency of HCV transfected cells. Sequence analysis of this subgenomic replicon showed adaptive mutations in non-structural proteins coding region, with majority of clustering in NS4B, NS5A and NS5B (Blight, Kolykhalov et al. 2000). These mutations were incorporated into the replicon and reinfection of Huh7 cells enhanced the RNA replication and Con1b (consensus 1b) was developed. Although these mutations increased the replication fitness of this system in Huh7 cells, it also lead to the failure of replication in vivo.

After successful development of Con1b subgenomic replicon system, other HCV genotypes were also used to develop similar type of subgenomic replicon system including HCV-N isolate of genotype 1b without the requirement of adaptive mutations (Guo, Bichko et al. 2001, Ikeda, Yi et al. 2002). Similarly replicon consisted of genotype 1a stain H77 1a strain successfully replicate in highly permissive Huh7 subtype cells known as Huh7.5 and later in Huh7 cells (Grobler, Markel et al. 2003, Liang, Rieder et al. 2005). Another subgenomic replicon consisted of genotype 2a was also developed by using the JFH-1 (genotype 2a) sequence isolated form patient of fulminant hepatitis. This replicon was efficiently replicating in Huh7 cells without adaptive mutation with 60-fold higher efficiency (Kato, Date et al.

2003). This subgenomic replicon is the most efficient system and it also provide the evidence that adaptive mutation are not necessary for efficient replication of HCV in cells.

1.6.3 Reporter genes and full length HCV replicons

To overcome the limitation of assays for colony formation and to facilitate the rapid and direct detection of relative replication efficiencies reporters such as luciferase and B-lactamase have been used (Ikeda, Abe et al. 2005).These systems not only helped in the efficient determination of replication abilities in subgenomic systems but also helped in the development of high-throughput screening of anti-HCV drugs and inhibitors (Zuck, Murray et al. 2004).

A number of the HCV full-length replicon system have been developed from HCV-O, H77, and HCV-N. these replicons replicate in Huh7 and Huh7.5 cells (Blight, McKeating et al. 2002, Ikeda, Yi et al. 2002, Ikeda, Abe et al. 2005). These full-length HCV replicons allow the study of full viral life cycle including the mechanisms of viral entry, assembly, and release.

In the present study full-length bicistronic N/Neo C-5B system was used which is further explained in the next chapter (Ikeda, Yi et al. 2002).

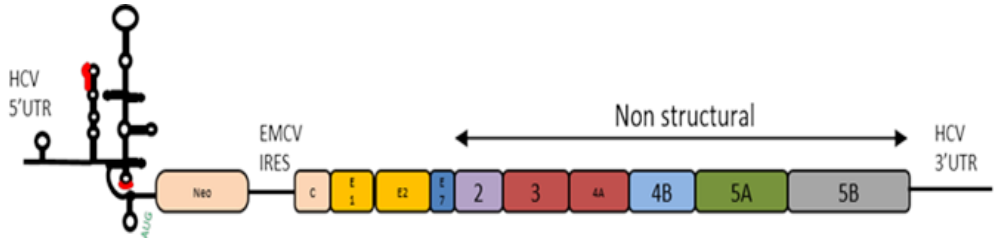

Figure 1-12 Schematic diagram of N/Neo C-5B Huh7 cell

The figure represents the schematic diagram of Huh7 N/Neo C-5B cell used in the study. These are Huh7 cell harbouring stable HCV full length genome. It's a bi cistronic replicon system in which the neomycin gene is under the control of HCV 5'UTR whereas the rest of HCV coding region and 3' UTR region are under the control of EMCV IRES. The red marks show the primer binding sites used in the qRT-QPCR based detection of HCV RNA while start codon is shown in green letters.

1.7 Aim and Objectives

eIF4II's role in miRNA mediated repression at 3'UTR sites is still illusive and need further studies. In the yeast two hybrid system, It interacts with NS5B and so could contribute to HCV replication. miR-122 binds to the 5'UTR of HCV and positively regulates viral replication. The preliminary data in our lab indicated that eIF4AII positively regulate HCV. These observations lead us to hypothesise that eIF4AII modulates HCV by contributing to mir-122 regulation.

The aim of this project is to study the role of eIF4AII in regulation of HCV replication and its relationship to miR-122 regulation.

The objectives are:

- To identify the stage at which eIF4AII regulates HCV replication/translation.
- To determine whether eIF4AI performs a similar role
- To establish whether this regulation involves miR-122
- To determine whether eIF4AII interacts with HCV RNA and whether any interaction involves miR-122.

2 Materials and Methods

2.1 General reagents

2.1.1 Reagent and equipment suppliers

EMD Millipore Headquarters, 290 Concord Road, Billerica, Massachusetts 01821, USA

Bio-Rad Laboratories, Inc. 2000 Alfred Nobel Drive, Hercules, California 94547 USA

Invitrogen Ltd. 3 Fountain Drive, Inchinnan Business Park, Paisley, UK. PA4 9RF

Fisher-Scientific. Bishop Meadow Road, Loughborough, Leicestershire. LE11 5RG

GE Healthcare (Amersham). GE Healthcare Life Sciences, Amersham Place, Little Chalfont, Buckinghamshire. HP7 9NA

Techno Plastic Products (TPP) AG. Zollstrasse 7, 8219 Trasadingen, Switzerland

New England Biolabs (NEB). 75-77 Knowl Piece, Wilbury Way, Hitchin, Herts. SG4 0TY

Roche Products Limited. 6 Falcon Way, Shire Park, Welwyn Garden City. AL7 1TW

Sigma-Aldrich Company Ltd. The Old Brickyard, New Road, Gillingham, Dorset. SP8 4XT

Agilent Technologies, INC. 5301 Stevens Creek Blvd, Santa Clara, CA 95051,

USA

2.2 Specific reagents

Table 2-1 Plasmids used in the study

Plasmids	Description	Source/References
pFLAGeIF4AI	Origene (NM 001416) containing eIF4A1 ORF with N-terminal FLAG coding sequence.	A gift from Martin Bushell, University of Leicester, UK (Meijer, Kong et al. 2013)
pFLAGeIF4AII	Origene (NM 001416) containing eIF4AII ORF and N-terminal FLAG coding sequence.	
eIF4AI-SR	Origene (NM 001416) containing siRNA-resistant eIF4AI ORF and FLAG coding sequence.	
eIF4AII-SR	Origene (NM 001416) containing siRNA-resistant eIF4AII ORF and FLAG coding sequence.	
pLUC122x2	pGL3-MCS backbone (Promega pGL3con with MCS inserted in 3'UTR) containing two copies of the miR-122 binding region from strain H77 (1-60nt), ie four miR-122 binding sites, inserted between SpeI and EcoRI sites in the 3'UTR of firefly luciferase.	(Jopling, Schutz et al. 2008)
pLUC122x2m4	As pLUC122x2 with both the miR-122 binding sites mutated at positions 3 and 4 (nt U26C to A26G and U41C and A41G of H77) of the seed match	As Above
pJFH1-NS5B-Bi	Bicistronic translation reporter plasmid containing HCV sequences from JFH1 with firefly luciferase gene under HCV 5'UTR control and NS5B under EMCV IRES with HCV3'UTR	Gift form David Evans, University of Warwick, UK.
pCon1b-NS5B-Bi	As pJFH1-NS5B-Bi but with HCV sequences derived from Con1b strain	As above
p5'LUC3'	pGL3 plasmid backbone (Promega) containing full HCV 5'UTR and 3' UTR regions from strain H77 flanking the firefly luciferase coding region.	(Roberts, Lewis et al. 2011)

Table 2-2. Antibodies used

Antibody	Description	Supplier
Rabbit anti-eIF4AI	ab31217 anti-eIF4AI	Abcam
Rabbit anti-eIF4AII	ab31218 anti-eIF4AII	Abcam
Rabbit anti-β-Tubulin	ab6046 anti- β-Tubulin	Abcam
Rabbit anti-FLAG	ab1162	Abcam
Rabbit anti-CNOT1	14276-1-AP	Proteintech
Secondary antibody	Goat anti-rabbit HRP	Sigma
Alexa Flour 488nm	a21441 anti-rabbit	Thermo Scientific
DRAQ5	62254	Thermo Scientific

Table 2-3. 2'O-methylated and RNA oligonucleotides used in study. m indicates 2'O-methylated RNA nucleotide

Name	Sequence
miR-122 2'Ome	mAmCmAmAmAmCmAmCmCmAmUmUmGmUmCmAmCmAmCmUmCmC
miR-21 2'Ome	mUmCmAmAmCmAmUmCmAmGmUmCmUmGmAmUmAmAmGmCmUmA
Random 2'Ome	mGmUmGmUmAmAmCmAmCmGmUmCmUmAmUmAmCmGmCmCmCmAmA
Pre- miR-122	UGGAGUGUGACAAUGGUGUUUGUGUCUAAACUAUCAAACGCCAUUAUCACACUAAAUA
Pre-miR122 p3+4	UGCUGUGUGACAAUGGUGUUUGUGUCUAAACUAUCAAACGCCAUUAUCACACAAAAUA

Table 2-4 siRNA sequences

Name	Sequence	supplier	position
Control si	proprietary	Dharmacon D-001810-03	
Control si A	proprietary	Ambion ID AM9611.	
Control si B	proprietary	Ambion ID AM4613	
eIF4AI si	ACAUCAACGUGGAACGAGA.TT	Ambion ID s4567	nt893 in eIF4AI CDS
eIF4AI si A	ACAUCAACGUGGAACGAGA.TT	Dharmacon	nt885-903 in eIF4AI CDS
eIF4AII si A	GGAGAGUGUUUGAUAUGUU.TT	Ambion ID s4572	nt529 in eIF4AII CDS
eIF4AII si A2	GGAGAGUGUUUGAUAUGUU.TT	Dharmacon	nt 521-542 in eIF4AII CDS
eIF4AII si B	proprietary	Ambion ID s4571	
eIF4AII si C	proprietary	Ambion ID s4570	
eIF4AII si C2	GAGACUUUCUACAAUACUA.TT	Dharmacon	nt1212 in eIF4AII CDS
eIF4AII si ASM	GGAGAGUGAAAGAUAUGUU.TT	Dharmacon	nt 521-542 in eIF4AII CDS
CNOT-1 si	proprietary	Ambion ID s22844	

2.3 Tissue culture techniques

2.3.1 Tissue culture reagents

Phosphate buffered saline (PBS): 4.3 mM Na_2HPO_4, 1.5 mM KH_2PO_4, 137 mM NaCl, 2.7 mM KCl, pH 7.4. (OXOID)

Dulbecco's Modified Eagles Medium (DMEM) (Sigma-Aldrich)

Foetal calf serum heat-inactivated (PAA)

Non-essential amino acids (NEAA) (Gibco)

Trypsin (PAA)

G418 antibiotic

Table 2-5 Cell lines

Cell Lines	Origin	Description
NNeo/C-5B Huh7	Huh7 stably expressing full length HCV replicon (Ikeda, Yi et al. 2002)	Adherent cells maintained in DMEM with 10% FBS, 1% NEAA and 1mg/ml G-418 antibiotic, 5% CO_2 at 37°C Gift from Peter Sarnow Lab, Stanford University, USA
Huh7	Human hepatocellular carcinoma	Adherent cells maintained in DMEM with 10% FBS and 1% NEAA, Gift from Peter Sarnow Lab, Stanford University, USA
HeLa	Human cervical epithelial carcinoma	Adherent cell line maintained in DMEM with 10% FBS, 5% CO_2 at 37°C Gift from Kirsti Hill Lab, University of Cambridge, UK
Huh7.5	Huh7 cells with RIG-I mutation which support strong HCV replication (Blight, McKeating et al. 2002)	Adherent cells maintained in DMEM with 10% FBS and 1% NEAA, 5% CO_2 at 37°C Gift from Alex Tarr Lab, University of Nottingham, UK.

2.3.2 Cell maintenance

All cells were grown in the appropriate medium as described in table 2.5, in the presence of 5% humidified atmospheric CO_2 at 37°C. For routine passage cells were grown in a T75 flask to full confluence, washed 2 times with 1X phosphate buffer saline (PBS) and then to disassociate the cells from the flask 2ml 1X trypsin was added and cells were incubated for 5-10 minutes at 37°C. Fresh DMEM medium was added to neutralise the trypsin and to adjust the seeding confluence to 20-40%. Cells were usually maintained for up to 40-45 passages. For specific seeding confluence, a haemocytometer was used to count the cells.

2.3.3 Cell transfection

2.3.3.1 siRNA transfection

For RNA transfection 300 µl Optimem medium (Invitrogen) + 1.5µl Lipofectamine RNAiMAX (Invitrogen) + 1µl (20µM) respective siRNAs (20 nM final concentration) in 700 µl of fresh DMEM was used per well of a 6 wells plate. The transfection mixes were prepared as; Mix 1, Optimem and lipofectamine RNAiMAX; Mix 2, Optimem and siRNA. The mixes were combined and incubated for 20 minutes at RT. Medium was removed and then 700 µl of fresh DMEM added. 300 µl siRNA transfection mixes were added and gently swirled to mix. Cells were incubated at 37^{o}C in 5% CO_2 incubator and after 4-6 hours the media was changed. Cells were harvested by lysing in TRI reagent (2.5.1) after 72hours. siRNA transfection procedure was optimized by Catherine Jopling.

2.3.3.2 RNA/DNA transfection using lipofectamine 2000

For lipofectamine 2000 transfection, 0.2µg plasmid DNA or luciferase reporter RNA, 0.05µg pSV40-*Renilla* control plasmid or 0.01µg *Renilla* luciferase control RNA, 2.5 µl of lipofectamine 2000 and 1ml of Optimem medium were used per well of a 6 wells plate. Where included, siRNAs were used at 20nM final concentration. DNA and lipofectamine 2000 mixes in 500 µl of optimum medium were made separately and after 5 minutes both mixes were combined and incubated for 15 minutes at room temperature (RT). Medium was removed from the cells and 1ml of transfection mix added. The transfection mix was replaced with fresh DMEM medium after

4-6 hours. The volume of DNA transfection mix was increased proportionally for larger cell cultures; for example, for 6cm plates 2X volume of one well of 6 wells plate were used.

2.3.3.3 Electroporation

Apart from lipofectamine-based transfection, H77 RNA and oligonucleotides, were also transfected to NNeo/C-5B and Huh7 cells by using Neon transfection system (Invitrogen) following the manufacturer's instructions. Before the electroporation, cells were grown up to 60-70% confluence. Cells were trypsinized, re-suspended in the DMEM media and counted using the haemocytometer and 400,000 cells per electroporation were taken. Cells were pelleted by centrifugation at 1100rpm for 5 min and washed with Ca^{2+}, Mg^{2+} free PBS (Invitrogen) and again pelleted by centrifugation. Washed cells were re-suspended into 10µl of buffer R (Invitrogen) and 1µg of the RNA per electroporation was added and mix with gentle pipetting. By using special Neon pipette, 10 µl of the mix was taken up by Neon gold platted tip (Invitrogen). Electroporation was performed by using program 8, which uses a single pulse at 1300 V for 30 sec. The same procedure was repeated two to three times to get enough cells for 6 cm and 10 cm plates respectively and cells were plated in fresh media. Cells were harvested for RNA or subjected to IP after required time.

2.3.3.4 DNA transfection with Fugene

For Co-immunoprecipitation (Co-IP) of HCV and miR-122 RNAs with FLAG eIF4AI/AII, 15cm plates were used for pFLAGeIF4AI/AII DNA transfection with Fugene (Promega). 15µl Fugene was mixed with 1ml of Optimem medium and incubated for 5 minutes are room temperature. 5µg of FLAG tagged plasmid DNA was then added, mixed and incubated for another 15 minutes at RT and then dripped onto the cell plates and gently swirled to mix. Transfected cells were incubated for 24 hours at 37^{o}C in a 5% CO_2 incubator.

2.4 Bacterial methods

2.4.1 Reagents and solutions

Lysogeny Broth (LB) medium (1L): 10g tryptone; 5g yeast extract; 5g NaCl; pH adjusted to 7.5 with NaOH then autoclaved.

LB agar was made as above with addition of 15g of agar before autoclaving the medium at 121^{o}C for 45 min at 15 psi. 100mg/ml of Ampicillin or 50mg/ml kanamycin was added to the LB agar after cooling before pouring plates.

2.4.2 Bacterial strains used

DH5α (Promega) - *F'ϕ80dlacZΔM15 Δ(lacZYA-argF) U169 deoR recA1 endA1 hsdR17 phoA supE44* λ- *thi--1 gyrA96 reA1.* Prepared as described in the Promega handbook.

2.4.3 Preparation of *E. coli* competent cells

E. coli were prepared by Barbara Ramparsad, Gene Regulation and RNA biology group, School of Pharmacy, University of Nottingham, as described in the Promega handbook.

2.4.4 Plasmid transformation and purification

10ng plasmid was mixed with 50µl of *E.*coli competent cells (DH5α) on ice and incubated for 5-10 minutes. Cells were then incubated at 42^{o}C for 60-90 sec for heat-shock and 150µl of Luria broth (LB) was added and incubated at 37^{o}C for 1 hour with shaking. 100µl of transformed culture was spread on a pre-warmed antibiotic (kanamycin/ampicillin) agar plate and incubated at 37^{o}C overnight. The next day, the plates were observed for isolated colonies. A single colony was picked and inoculated in 5ml of LB broth in the presence of antibiotic and incubated for 6-8 hours at 37^{o}C with shaking. 100µl of this seed culture was inoculated into 100ml of LB suspension culture in the presence of antibiotic and grown at 37^{o}C overnight with shaking. The next morning, cells were pelleted by centrifugation at high speed for 15 minutes at 4°C. Plasmid DNA was extracted by maxi-prep (Sigma) according to as per manufacturer's protocol.

2.5 Molecular biology techniques

2.5.1 Plasmid linearization

Plasmid DNA was linearized by restriction digestion using enzymes from Promega or New England Biolabs according to the manufacturer's instructions. 10μg of plasmid was digested in the presence of the appropriate buffer and BSA (1ug/ml) with 5-10 units of enzyme in a total volume of 30μl, for 2-3 hours at 37°C and then another 0.5μl of enzyme was added and further incubated at 37°C for 1 hour.

2.5.2 Agarose gel electrophoresis

To check that the plasmid was completely digested, nucleic acids were separated according to molecular weight by agarose gel electrophoresis. 1μl of linearized or uncut plasmid DNA with 9μl of water and 2μl of DNA loading dye (30% (v/v) glycerol, 0.25% (w/v) bromophenol blue, 0.25% (w/v) xylene cyanol FF) was run on a 1% (w/v) agarose gel in the presence of DNA size marker (Norgen). SYBR-Safe gel staining dye (Invitrogen) was used to stain the gel. Bands of DNA were visualized with a UV transilluminator.

2.5.3 *In vitro* transcription

The remaining plasmid digest was heat inactivated at 65°C for 10 minutes and the DNA was purified by phenol: chloroform extraction and ethanol precipitated as described in section 2.5.5. Purified DNA was used for in-vitro transcription by T7 Megascript kit (Ambion) according to as per manufacturer's instructions.

2.5.4 RNA extraction using TRI reagent

Transfected cells were washed two times with chilled PBS. 1ml of TRI reagent (Sigma) was added to each well and incubated for 10 minutes at RT, or frozen at -20^{o}C for subsequent extraction. The Tri reagent lysate was removed by scraping with a pipette tip and was transferred to microcentrifuge tubes. 200µl chloroform was then added and the tubes were vigorously shaken for 15 seconds, incubated at RT for 2-15 minutes and centrifuged at 13,000 rpm for 15 minutes at 4^{o}C. The supernatant was transferred into a new 1.5ml tube without disturbing the interface and 500µl of isopropanol and 1µl of glycogen were added, mixed briefly and incubated at -20^{o}C for 10 minutes. The tubes were then centrifuged at 13,000 rpm for 10-15 minutes at 4^{o}C and the supernatant was carefully discarded. 1ml of 75% ethanol was added to the pellet and mixed by inverting the tube and again centrifuged at 13,000 rpm for 10-15 minutes at 4^{o}C. The supernatant was discarded carefully and the remaining ethanol was removed with a pipette after brief centrifugation. RNA pellets were re-suspended in 20-50µl of nuclease free water and quantified by Nanodrop. RNA was aliquoted in separate tubes and stored at -20^{o}C for cDNA synthesis and northern blot analysis.

2.5.5 Phenol: Chloroform Extraction

To purify the plasmid DNA, water was added to 200µl total, then 100 µl of phenol and 100 µl of chloroform:isoamyl alcohol (24:1) were added and vigorously shaken. The mix was centrifuged at high speed for 3 minutes and the supernatant was transferred to another tube. 200 µl of chloroform was added, mixed and centrifuged. The supernatant was transferred into a new

tube and 20 µl of 3M sodium acetate pH5.2 + 3X volume of ethanol were added and stored at -20 °C for 10 minutes or overnight. Next day the mix was centrifuged at high speed and 1ml of 70% ethanol was added, centrifuged, removed, and the pellet resuspended in water.

2.5.6 Determination of nucleic acid concentration

The concentration of DNA and RNA were determined by using Nanodrop (Nanodrop ND-1000, Thermo Fisher Scientific) spectrophotometer by measuring the absorbance at 260nm.

2.5.7 cDNA synthesis

For quantitative RT-RT-QPCR (qRT-QPCR) to detect HCV RNA and actin mRNA, cDNA was synthesised using Superscript III (Invitrogen). 0.1µg RNA was combined with 1µl of random primers (150ng/µl, Invitrogen), 1µl dNTP mix (100mM, Invitrogen) and nuclease-free water to a final volume of 13.45µl. This mix was heated at 65°C for 5 minutes, placed on ice for 5 minutes, and then 4µl of 5X first strand buffer (Invitrogen), 1µl of 0.1M DTT (Invitrogen), 0.05µl of RNAse inhibitor (Promega) and 0.5µl of Super script III reverse transcriptase enzyme were added. The reaction mix was incubated at 25°C for 5 minutes, transferred into a water bath at 50°C for 60 minutes and then heat inactivated at 70°C for 15 minutes.

2.5.8 mRNA qRT-QPCR

For qRT-QPCR, 1µl of cDNA, 10µl of 2 X GoTaq SYBR Green mastermix (Promega), 0.1µl of each 100µM primer (HCV qRT-QPCRF and HCV qRT-QPCRR for HCV; Actin QF and Actin QR for the actin control; see Table 2-6

for primer sequences) and 9µl of water in a total of 20µl were used. A mastermix combining all components except the cDNA was assembled and aliquoted into a 96-wells qRT-QPCR plate before addition of the cDNA to wells in triplicate. The Stratagene Mx3005P qRT-QPCR machine was used with cycle parameters of 95^{o}C for 10 min, then 95^{o}C for 10sec, 51^{o}C for 15sec, and 70oC for 30sec for 40 cycles, then 95^{o}C for 1min, 51^{o}C for 30sec and 95^{o}C for 30sec.

Normally, the fluorescent labelled primers (also called probe) the fluorescence is not emitted due the presence of fluorophore and quencher molecules in very proximity to each other. During the RT-QPCR, the probe binds to complementary sequences present in the target gene, the Taq polymerase hydrolyse the probe during the extension process which result in the increase in fluorescence signals. These signals are recorded by the machine. During the repeat cycles of RT-QPCR more and more fluorescence is released and when the intensity of fluorescence increase above an arbitrary line the instrument record the cycle (CT) number.

The delta-delta CT (ddCT) method was used to analyse the qRT-QPCR data while statistical significance was determined by student t test. This ddCT method is convenient method to acquire the relative expression of genes. It relies on the assumption that the selected housekeeping gene to be uniformly and constantly expressed in all samples. It also required a reference sample to which all other samples are compared. The advantage of this method is that it is very simple to use, but the limitation is that, It is

based on the assumption that the control and reference sample have real Ct values and that these sample represent the true expression. Like housekeeping gene β-actin expression will remain same in treated vs untreated samples. There are studies which indicate these housekeeping genes (β-actin and GAPDH) significantly varies in expression in experiment (Schmittgen and Zakrajsek 2000, Rho, Lee et al. 2010).

Table 2-6 Primer sequences

Primer name	Location	Sequences
HCV-qRT-QPCRF	nt62-nt81	CTTCACGCAGAAAGCGTCTA
HCV-qRT-QPCRR	nt307-nt-288	CAAGCACCCTATCAGGCAGT
Actin-QF	nt267-nt286	AGCACAGAGCCTCGCCTTT
Actin-QR	nt1103-nt1083	TCATCATCCATGGTGAGCTG

2.5.9 miRNA cDNA synthesis

mir-122, miR-21 and miR-26a cDNA synthesis was done by using Taqman micro RNA specific RT kit (Applied Biosciences) in 15.5µl reaction with 0.15 µl of dNTPs, 1.5 µl of buffer, 0.19 µl of RNAse inhibitor, 1 µl of Multiscript reverse transcriptase enzyme, 3 µl of specific primer and 2.5 µl of 0.1 µg RNA mix with thermal conditions of 30minutes at 16^{o}C, 30 minutes at 42^{o}C and 5 minutes at 85^{o}C.

2.5.10 microRNA qRT-QPCR

qRT-QPCR was performed using 10μl Taqman No Amperase UNG mix, 7.67μl water, and 1μl miRNA-specific qRT-QPCR mix. The mastermix was aliquoted into a 96 well RT-QPCR plate and 1.33μl of RT product was added in triplicate. The reaction was performed in a Stratagene Mx3005P qRT-QPCR machine with cycle parameters of 95^{o}C for 10 min, then 40 cycles of 95^{o}C for 15sec and 60^{o}C for 60minutes.

2.6 Northern Blotting

2.6.1 Solutions

10X MOPS buffer: 200 mM MOPS, 10 mM EDTA, 50 mM Na Acetate, pH 7.0

.

37% (v/v) formaldehyde.

RNA Sample Buffer: 1X MOPS buffer, 50% v/v deionised formamide, 2.2 M formaldehyde

RNA loading dye: 50% glycerol, 0.02% Bromophenol blue, 0.02% Xylene cyanol FF.

Methylene Blue stain: 0.02% methylene blue, 0.3M Na acetate pH 5.2.

Church-Gilbert's hybridization buffer: 1mM EDTA, 1% BSA, 0.5M sodium phosphate monobasic, 7% SDS, pH 7.2.

20X SCC: 3M NaCl, 300mM sodium citrate pH 7.

Wash Solutions: 2X SCC + 0.1% SDS, 1X SCC + 0.1% SDS and 0.1X SCC + 0.1% SDS.

2.6.2 RNA agarose gel electrophoresis

1% agarose was boiled in 73ml of filtered water, cooled to ~50°C, and 10ml of 10X MOPS buffer and 17ml of 37% formaldehyde added, then poured into a clean gel casting assembly in a fume hood and left to solidify. The gel was transferred to a gel tank containing gel running buffer (1X MOPS buffer, 10% formaldehyde buffer) and soaked for 10 minutes before loading. 15.5 µl of RNA sample buffer was added to 2.5 µg of RNA sample and heated at 65°C for 15 minutes then placed on ice and 2µl of RNA loading dye added. The RNA samples were loaded into wells and the gel was run at 100V for 1-2 hours until the bromophenol blue dye had migrated ~2/3 of the length of the gel (Figure 2-1). The gel was soaked in 0.05M NaOH (200-400ml) for 20 minutes and then rinsed with distilled water and soaked in 20X SSC buffer for 30-40 minutes.

2.6.3 Blotting

One piece of Zetaprobe nylon membrane (BioRad) and three pieces of blotting paper the size of the gel, and a longer piece of blotting paper to use as a wick, were cut. The blotting paper pieces were soaked in 20X SSC buffer. A glass plate was placed across the 20 X SSC buffer container and the wick was draped across it such that both ends of paper were dipped in buffer. The gel was carefully transferred onto the wick, then the nylon membrane was placed on the gel, and then the 3 blotting paper pieces were placed onto the membrane one by one. Each layer was rolled with a pipette to remove any

trapped air bubbles. Pieces of parafilm were placed along with the edges of the gel to block the direct transfer of buffer above into the paper towels without passing through the gel and membrane. Finally, a stack of paper towels and second glass plate were placed on top with a weight to compress the stack (Figure 2-1). The apparatus was left overnight.

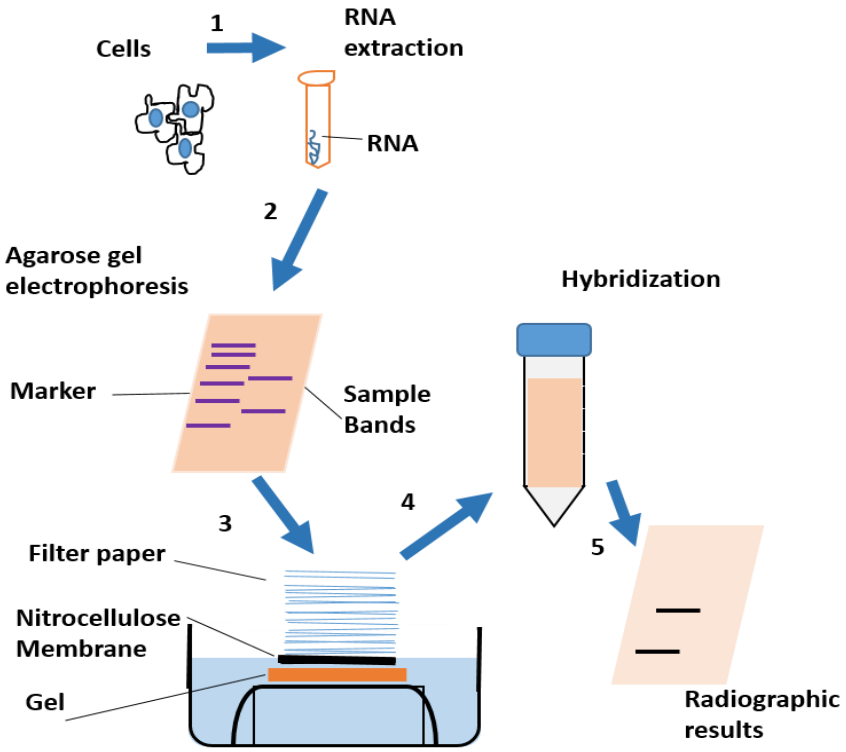

Figure 2-1 Northern blot procedure

The figure describes the basic steps involve in northern blotting. RNA is extracted and after the electrophoresis, the RNA is blotted onto a nitrocellulose membrane. The membrane is hybridized with the radio labelled probe and result is detected after exposing it to X-ray film.

2.6.4 Hybridization

The next day, the paper towels and blotting papers were removed carefully and the membrane was immediately cross-linked in a UV-cross linker for 1200 sec (default). The membrane was then stained in methylene blue stain for about 1 minute and rinsed with deionised water several times to visualize the bands. 18S and 28S rRNA positions were marked. The membrane was pre-hybridised in 5ml of Church-Gilbert Hybridisation solution at 65^{o}C with rotation for 1h. The pre-hybridisation solution was replaced with 5ml fresh pre-warmed Church-Gilbert solution and ^{32}P-labelled probe and the membrane was rotated overnight at 65^{o}C. After probing, the membrane was washed sequentially with 2X SSC/0.1%SDS, 0.5X SSC/0.1%SDS and 0.1X SSC/0.1%SDS for 10 minutes each at RT. The membrane was blotted on tissue paper, wrapped in saran wrap and exposed to a phosphor screen overnight, and the screen was scanned using a STORM phosphorimager (GE Healthcare). To strip, the membrane was incubated three times in boiling 0.5% SDS for 30 min with shaking.

2.6.5 ^{32}P Probe preparation

An HCV monocistronic IRES vector was digested by *Ncol*, while an *EcoRI* digested fragment from RT-qPCR2.1actin vector were used to make radiolabelled probes. 25-30ng of template DNA and 12μl of water was heated at 95°C for 3minutes, then transferred to ice and briefly centrifuged. Then 5μl of 5X labelling buffer (Promega), 0.5μl of dNTP mix (20mM each dATP, dGTP and dTTP), 1μl of BSA (400μg/μl), 1μl of Klenow fragment polymerase and 2.5μl of α-^{32}P-dCTP were added, spun and incubated at

37°C for 1 hour. The probe was cleaned up by spinning through a G50 sephadex column at 4000rpm for 2 minutes and boiled at 95°C for 3minutes, then added to the hybridisation solution.

2.7 Protein Extraction

2.7.1 Solutions

SDS loading buffer: 100mM Tris-HCl, pH 6.8; 20% glycerol; 8% SDS; 20% β-mercaptoethanol; 2mM EDTA; 0.2% Bromophenol blue

Western blot stripping solution: 100mM β-mercaptoethanol, 2% SDS, 62.5 mM Tris-HCl pH6.7.

10X SDS-PAGE Running Buffer: 250mM Tris, 1.92M glycine, 1% SDS, pH 8.3.

TBST buffer: 10mM Tris pH 8.0, 0.9% NaCl, 0.1% Tween.

Western blotting buffer: 50mM Tris, 192 mM glycine, 20% methanol.

Ponceau stain: 0.5% (w/v) Ponceau, 5% (w/v) trichloroacetic acid (TCA)

RIPA buffer: 25 mM Tris•HCl pH 7.6, 150 mM NaCl, 1% NP-40, 1% sodium deoxycholate, 0.1% SDS

2.7.2 Protein quantification

Cells were washed with chilled PBS and scraped in chilled PBS on ice, then centrifuged at 500g for 3 minutes at 4°C. The supernatant was discarded and the pellet was re-suspended in 1XSDS buffer or in RIPA buffer. To disrupt the viscous DNA, lysates were passed through a fine syringe needle ten times and stored at -80°C.

2.7.3 Bradford assay

In order to ensure the equal loading of protein in SDS-PAGE electrophoresis, Bradford assay was used to determine the protein concentration of sample in RIPA buffer. 1-2 µl of sample was mixed with 1X Bradford assay reagent (Bio-rad), incubated for 5 minutes at room temperature and absorbance was read at 595 nm using Eppendorf photometer. The absorbance was compared to BSA standards to estimate the concentration of the protein in a given sample.

2.8 SDS PAGE and western blotting

2.8.1 SDS-PAGE

Glass plates were cleaned thoroughly by scrubbing in water, then wiped with 70% industrial methylated spirit (IMS) and dried. Plates were fixed into a casting assembly and checked for any leakage using water. A 10% resolving gel was prepared as shown in Table 2-7. After adding the 10% APS (ammonium per sulphates) and TEMED (Tetramethylethylenediamine), the gel was immediately poured into the casting unit and a water layer was applied for levelling and monitoring the polymerisation. Water was removed and soaked with tissue and a stacking gel was prepared (30% acrylamide 0.8% bis-acrylamide, 1M Tris-HCl, 10% SDS, 10% APS and 20µl TEMED) and poured above the resolving gel. A clean comb was placed in the stacking gel and the gel was left to polymerise. The gel was transferred into 1XSDS running buffer and the comb was removed carefully. Wells were

washed with running buffer to remove air bubbles. Protein samples were heated at 95^{o}C for 15 minutes. Samples and protein marker were loaded and run for 2-3 hours at 150V for optimal separation of proteins.

Table 2-7 SDS-PAGE resolving gel composition

Chemical		**10%**
Acrylamide/bis-acrylamide sol. (30%/0.8%) (ml)	2gel	5
	1gel	2.5
1.5M Tris-HCl pH8.8 (ml)	2gel	3.75
	1gel	1.875
10% SDS(ul)	2gel	150
	1gel	75
Water (ml)	2gel	6.1
	1gel	3.05
10% APS (ul)	2gel	100
	1gel	50
TEMED (ul)	2gel	20
	1gel	10

2.8.2 Western blotting

6 pieces of blotting paper and one piece of PVDF membrane were cut to a larger size than the gel. Blotting papers were soaked in blotting buffer and PVDF were first soaked in methanol and then in blotting buffer. The gel blotter surface was cleaned and three layers of blotting papers applied one

by one and rolled over to remove air bubbles, then the PVDF membrane was placed on top and rolled. The resolving gel was separated from the stack and carefully removed from the plates and placed over the membrane and rolled. The remaining three pieces of blotting paper were placed over the gel one by one and rolled over. The membrane was blotted for 1.5h at a constant current of 70mA. The membrane was then transferred into 5% milk TBST solution and blocked for 30-60 minutes on a rocking shaker. The membrane was then transferred into (1:2500) primary antibody (anti-eIF4AI/II, rabbit, Abcam) in 5-10ml 5% milk solution and incubated at 4^{o}C overnight with rotation. The next day, the membrane was washed in TBST buffer for 10 minutes and transferred into secondary antibody (1:5000) in 5% milk/TBST and place on a rotating shaker at room temperature for 1-2hours. The membrane was washed three times in TBST buffer for 10 minutes each and exposed to ECL detection solution (GE Healthcare, Amersham Biosciences) for about 1 minute, then visualised using a Fuji image analyser system. The membrane was stripped by rotation in stripping solution for 30 minutes at 50°C followed by 3 washes in TBST for 10-15 minutes at room temperature.

2.9 Immunoprecipitation (IP)

2.9.1 Stock Solutions

NET2 (50mM Tris-HCl pH 7.5, 150mM NaCl, 0.5% NP-40)

2.9.2 Procedure

For each sample 25µl of protein A/G agarose beads, 2.5µl glycogen (10mg/µl), 25µl BSA (10mg/ml) and 2.5µl of Yeast tRNA (10mg/ml) were added to 500µl of NET2 (without NP-40) and incubated for 30 minutes with rotation at 4^{o}C to block the beads and reduce non-specific binding. The beads were then centrifuged and washed in another 500µl of NET2 (without NP-40) at 200g for 3minutes at 4^{o}C. Transfected cells (as described in section 2.3.2) were washed with PBS, scraped in 10ml of chilled PBS on ice and centrifuged at 500xg for 5minutes at 4^{o}C. The cell pellet was re-suspended in 400µl of NET2 with 0.5% NP-40 in the presence of protease inhibitor (Thermo Scientific) and RNAse Inhibitor and incubated for 5-10 minutes on ice to allow lysis. The lysate was centrifuged at high speed for 5 minutes at 4^{o}C to remove cell debris, and the supernatant was transferred into a fresh tube. 10% of each lysate was added to 1ml of TRI reagent and frozen at -20^{o}C as total cell lysate. 180µl of the remaining supernatant was transferred into each of two tubes containing the washed beads. For each lysate, 1µl (1ug/µl) of specific anti-FLAG antibody or anti-eIF4AI/II (for endogenous eIF4AI/II) was added to one tube and 2.5µl(0.4ug/µl) of anti-mouse IgG (for FLAG) or anti-Rabbit IgG (for endogenous eIF4AI/II) as a control to the other tube (Figure 2-2). Tubes were incubated O/N with rotation at 4^{o}C. The following day, the tubes were centrifuged at 200g for 3minutes at 4^{o}C and beads were washed 3 times in 500µl NET2 (with protease inhibitor). After the last wash, the supernatant was discarded and 1ml of TRIZOL reagent was added to the beads pellet. RNA was extracted and HCV and miR-122 cDNA

and qRT-QPCR performed as described in previous sections (2.5.4, 2.5.7 ,2.5.8, 2.5.9, 2.5.10).

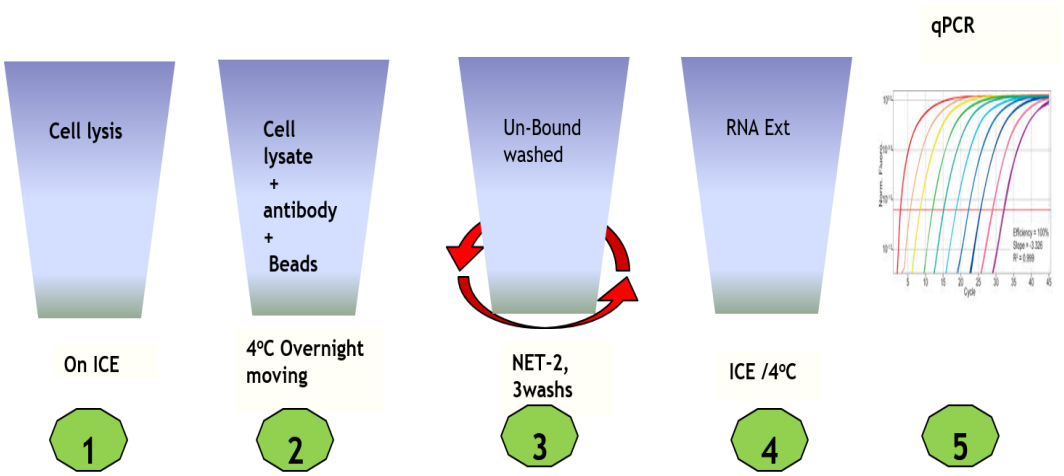

Figure 2-2 Immunoprecipitation of RNA

The figure shows the basic steps in RNA immunoprecipitation. These steps are represented by number. Cells were lysed and mixed with antibody bond protein A/G beads for overnight at 4°C. The unbound complexes were washed and removed by centrifugation followed by RNA extraction and RT-qRT-QPCR based detection of the target RNA.

2.10 Luciferase Assay

Cells transfected with luciferase reporters were harvested by washing twice in PBS and addition of 50 µl passive lysis buffer.

5µl of each lysate was assayed for firefly and Renilla luciferase enzyme activities using Promega's dual luciferase reporter assay system according to the manufacturer's protocol. Dual luciferase assays were performed using a GLOMAX luminometer (Promega) by addition of 25µl *LAR II* reagent to assay firefly luciferase activity, then 25µl of *Stop & Glo* reagent to assay *Renilla* luciferase activity.

2.11 Biophysical techniques

2.11.1 Confocal Microscopy

To study the localization of eIF4AI, eIF4AII in liver cells, confocal microscopy (CM) was used. All images were taken using the Carl Zeiss Laser Scanning System LSM 510 (Carl Zeiss, AG).

2.11.2 Sample preparation for CM imaging

NNeo/C-5B (5B), Huh7 and Hela cells were transfected with control, anti-eIF4AI and anti-eIF4AII siRNAs to knock down the two eIF4A proteins or control siRNA as described in section (2.3.3.1). After 24 hours, cells were counted and 7500 cells per well were cultured into the 8 well µ-Slide (Ibdi GmbH, Germany) chambers. Next day cells were washed 2XPBS and fixed with 4% paraformaldehyde solution for 10 min at room temperature. Cells

were washed 4-5 times with PBS and permeabilised with 0.2% Triton-X100 in PBS for 2 min at room temperature. Cell were again washed 4-5 times with PBS and blocked with 3% freshly made BSA for 30 min at room temperature. BSA was removed and cells were incubated with respective primary antibodies (PAb) against eIF4AI and eIF4AII (ab31217 anti-eIF4A1 1:100 and ab31218 anti-eIF4A2 1:200) in BSA, for 1 hour at room temperature. Cells were again washed 4-5 times with PBS and incubated with *Alex Fluor* 488 (green) and *DRAQ5* 1:5000 (red) antibodies for 5 min to stain eIF4A proteins and nucleic acids. Cell were washed 4-5 minutes with PBS and mounted with fluoromount (Sigma) by directly adding two drops per well. Wells were covered with aluminium foil and kept at 4^{o}C until microscopy. To scan Alexa Fluor green 488 nm wavelength was used while for *DRAQ5* 633 nm wavelength was used.

3 Investigation of the effects of eIF4A proteins on HCV RNA levels

3.1 Introduction

eIF4A is the most studied and characterized DEAD-box helicase protein. It belongs to the SFII domain of the helicase family and all other members of the DEAD-box family are identified on the basis of structural homology or functional similarities to the eIF4A (Rogers, Richter et al. 1999, Linder and Jankowsky 2011). Among eIF4A proteins, eIF4AI is the most studied isoform, perhaps due to the assumption that both eIF4AI and eIF4AII function are indistinguishable as they share 91% amino acid similarity.

As a member of the eIF4F complex eIF4A has a role in the bidirectional unwinding of the 5' UTR secondary structures in both cap-dependent and cap-independent mRNAs, which are both translated in an ATP-dependent manner (Rozen, Edery et al. 1990). eIF4A interacts with other translation initiation factors to execute its activities in translation. It binds with the HEAT domain of eIF4G, which results in close configuration of eIF4A with mRNA, while both eIF4B and eIF4H stimulate eIF4A helicase activity to unwind longer and more stable secondary structures. It is also thought that eIF4B and eIF4H prevent the refolding of the mRNA strand and help the eIF4A in 5' to 3' movement (Lindqvist, Imataka et al. 2008). This helicase activity of eIF4A is also considered to be inversely linked to the stability and the length of the secondary structures (Rogers, Richter et al. 1999). Despite the

homology, both eIF4AI and eIF4AII isoforms showed significant differences not only in tissue specific expression (Nielsen and Trachsel 1988) but also in their requirement in different cellular mechanisms and developmental stages (Williams-Hill, Duncan et al. 1997, Galicia-Vazquez, Cencic et al. 2012, Meijer, Kong et al. 2013). In a recent study in *Arabidopsis*, the knockdown of eIF4AI results in slow growth, delayed flowering and defective ovulation while the knockdown in eIF4AII did not show any phenotype (Bush, Crowe et al. 2015). Using an *in vitro* binding assay, it has been demonstrated that eF4AII, but not eIF4AI, interacts with HCV NS5B protein. It was suggested that eIF4AII helps NS5B-mediated RNA synthesis by unwinding the RNA secondary structure present in the HCV genome (Kyono, Miyashiro et al. 2002). In another study, knockdown of eIF4AII resulted in a reduction miRNA based protein repression via the 3' UTR (Meijer, Kong et al. 2013). Helicases are also implicated in both viral replication and in activation of innate host response against viral infections (Ranji and Boris-Lawrie 2010). eIF4AII has been shown as binding partner of HCV RNA polymerase (Kyono, Miyashiro et al. 2002). miR-122 binds to HCV 5'UTR and plays a vital role in HCV replication/translation (Henke, Goergen et al. 2008, Jopling 2008) but the proteins involve in this regulation are unknown so in the present study, the role of eIF4A protein was investigated in HCV regulation.

3.2 Results

3.2.1 eIF4AII knockdown reduces HCV mRNA to lower levels than eIF4AI knockdown

To study the effect of eIF4A helicase proteins on HCV regulation, siRNA based knockdown of both eIF4A isoforms (eIF4AI and eIF4AI) was performed in Huh7 5B (NNeo/C-5B) HCV replicon cells (Figure 1-12) and HCV RNA levels were monitored by qRT-QPCR. These Huh7 cells consist of bi-cistronic autonomously replicating complete HCV genome. Due to the high degree of variability in gene expression over a passage of time and lack of transfer of nucleic material to next generation in transient transfection, the above described cell system was used to ensure the reproducibility in the experiments. (Figure 3-1A). Cells were seeded in duplicate in 6cm plates in DMEM medium as described previously (see section 2.3.2. and 2.3.3.). Depletion of both eIF4AI and eIF4AII was performed by siRNA as used in (Meijer, Kong et al. 2013), while non-targeting siRNA were used as a control. Protein was extracted and western blot analysis (figure 3-1 B) was performed to confirm the knockdown of eIF4AI and eIF4AII (Performed by Catherine Jopling) while 3-1 C shows WB performed by me (CSA) but it shows unequal loading control. Figure 3-1 B and C show effective knockdown of eIF4AI and eIF4AII by siRNAs. It also shows that knockdown of eIF4AI results in an increase in eIF4AII expression (Galicia-Vazquez, Cencic et al. 2012). The qRT-QPCR results (figure3-1B) also show that the knockdown of eFI4AI and eIF4AII result in reduction in HCV RNA levels compared to control. Total RNA was extracted from the cells and reverse transcribed to cDNA using random

primer. The primers used for HCV qRT-QPCR were first checked for their ability to amplify the target (HCV) RNA in linear range by standard curve analysis and amplified products were run on the gel to confirm the product size (performed by Catherine Jopling). HCV specific primers HCVF and HCVR, which bind to nt62-81 and nt307-288 in the HCV 5'UTR were used to determine the HCV RNA levels by qRT-QPCR (figure 3-1A). The Ct values of triplets were averaged and HCV RNA levels were calculated by 2^-ΔΔCt method relative to actin mRNA. Although eIF4AI depletion resulted in 32% reduction (P=0.06) in HCV RNA levels compared to control, eIF4AII knockdown strongly repressed the HCV RNA level to just 30% (70% reduction, P=0.005) compared to control cells. The change in HCV RNA levels in eIF4AI and eIF4AII knockdown cells were also confirmed by northern blot analysis (figure 3-2). These results show that knockdown of both eIF4AI and eIF4AII decrease HCV RNA in replicon cells, but eIF4AII knockdown has a stronger effect.

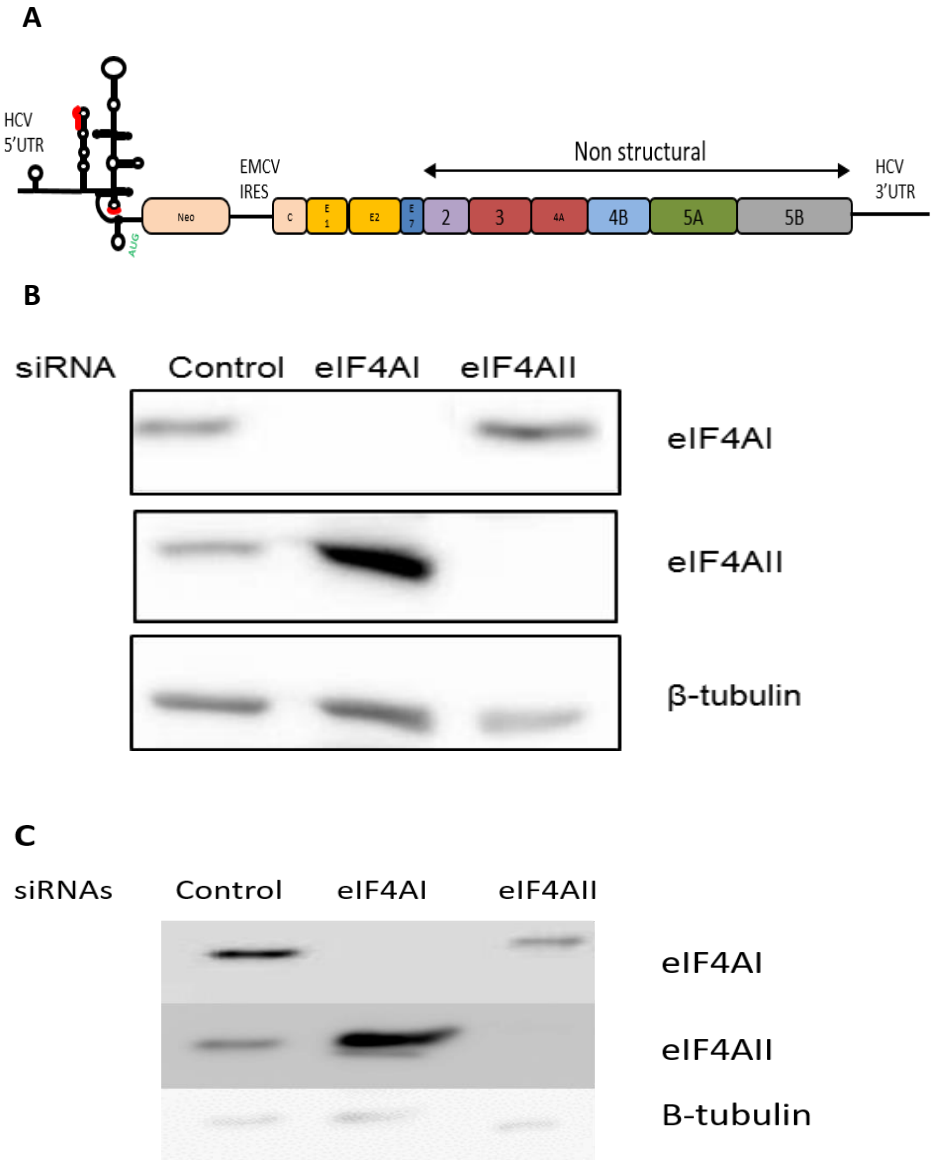

Figure 3-1 Conformation of eIF4AI and eIF4AII knockdown by western blot analysis.

A) Schematic diagram of Huh7 5B HCV replicon. The red marks in HCV 5' UTR regions indicate the RT-qRT-QPCR primer binding sites while the start codon is shown in green AUG letters. **B)** Both eIF4AI and eIF4AII proteins were knockdown by siRNAs in 5B cells. Western blot showing eIF4AI and eIF4AII expression, checked using specific antibodies, while β-tubulin was used as loading control. **C)** as B, except that shows unequal β-tubulin control loading.

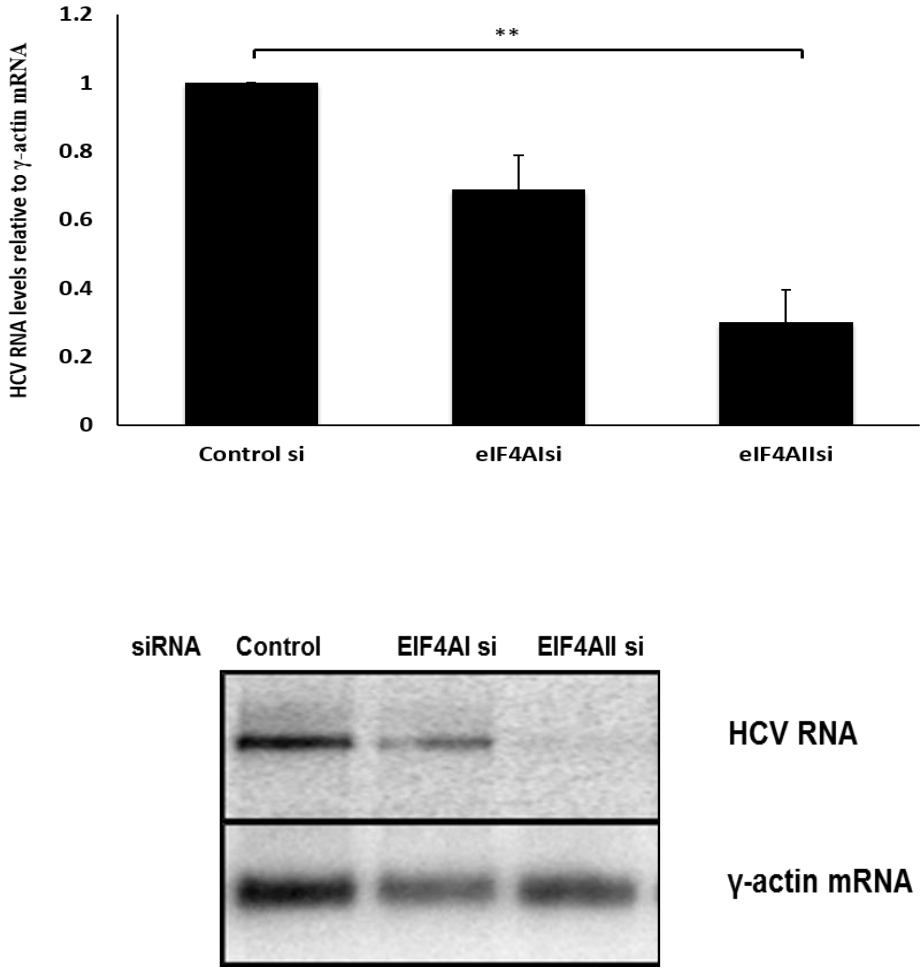

Figure 3-2 HCV RNA levels in eIF4AI and eIF4AII knockdown HCV replicon (5B) cells.

A) HCV RNA RT-qRT-QPCR levels in non-targeting siRNA control, eIF4AI and eIF4AII HCV RNA RT-qRT-QPCR levels in non-targeting siRNA control, eIF4AI and eIF4AII knockdown cells relative to γ-actin mRNA. The error bars represent the standard deviation (SD) in at least sixteen independent experiments. Statistical significance was determined by t.test **P<0.01 **B)** Northern blot analysis of HCV RNA levels in eIF4AI and eIF4AII knockdown cells compared to HCV RNA in non-target control. γ-actin was used as loading control.

3.2.2 Confirmation of effects of eIF4AII knockdown on HCV using different siRNAs

Although the simplicity and convenience of the use of siRNAs in studying the function of protein has made this technique very popular, off target effects could result in false positive results (Jackson, Burchard et al. 2006). In order to confirm that the results of siRNA based eIF4AII knockdown shown previously are real and that this knockdown leads to reduction of HCV RNA, we used siRNAs (eIF4AII si B and eIF4AII si C) with different target sites in eIF4AII mRNA (figure 3-3A). eIF4AII was knocked down by different siRNAs and RT-qRT-QPCR was performed to measure the HCV RNA levels as described already (see sections 2.3.3.1 and 2.5.4.). eIF4AII si B has the lowest repression of HCV as the HCV RNA levels were higher than the normally used eIF4AII si A (Figure 3-6). The average of the nine independent biological replicate shows that the eIF4AII siRNA A and siRNA B repress HCV RNA to 22-23%. While eIF4AII siRNA C represses HCV RNA to 8.7% compare HCV RNA levels in non-target control cell. Although this indicates that eIF4AII siRNA C has most effective repression among all three siRNAs used against eIF4AII but considering the size of errors in these siRNAs it seems that all siRNAs have similar level of repression. These results of eIF4AII repression by different siRNAs show that the eIF4AII repression in previous experiments was actual repression and that the decrease in HCV RNA was due to eIF4AII repression and not to off-target effect of these siRNAs.

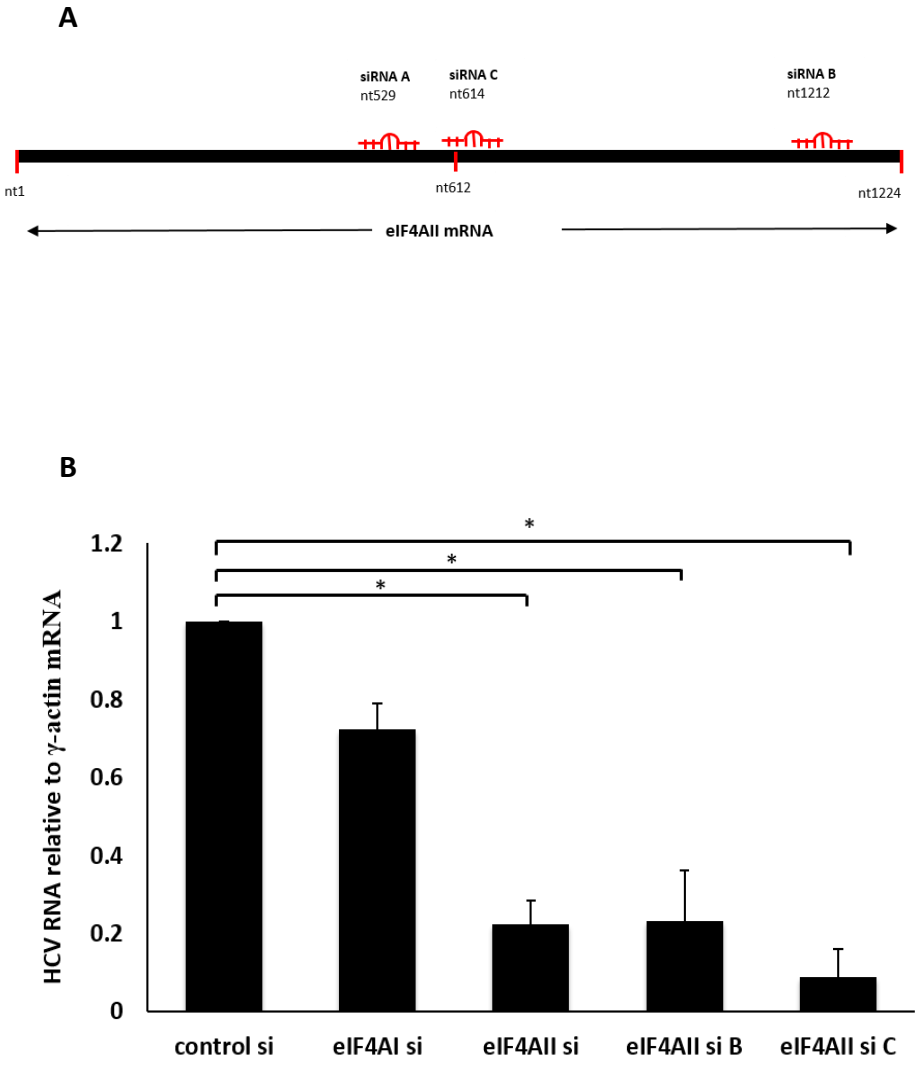

Figure 3-3 Confirmation of effects of eIF4AII knockdown on HCV by other anti-eIF4AII siRNAs.

A) Schematic diagram of eIF4AII mRNA showing the binding sites of siRNA A, siRNA B and siRNA C. **B)** To rule out possible off-target effects of eIF4AII knockdown, eIF4AII was depleted by two additional siRNAs B and C with different target sites as shown in (A). The RT-qRT-QPCR analysis of HCV RNA relative to γ-actin mRNA in this graph indicates decreased HCV RNA levels upon eIF4AII depletion by siRNAs with different targets in eIF4AII compared to non-targeting control siRNA. The data represent the average of four independent experiments. The error bars show the SD and *P<0.05 (t.test). furthermore, the ANOVA test indicate that there is no significant difference (P>0.05) between eIF4AIIsi, eIF4AIIsiB and eIF4AIIsiC.

3.2.3 Exogenous expression of eIF4AI and eIF4AII do not increase HCV RNA levels

After establishing that eIF4AI and eIF4AII knockdown reduce the HCV RNA level in HCV replicon cells, both eIF4AI and eIF4AII were overexpressed to see whether this increases HCV RNA levels. For this, 5B cells were transfected with plasmids containing FLAG-eIF4AI and FLAG-eIF4AII (figure 4-1) (Meijer, Kong et al. 2013). The empty pcDNA4/TO plasmid was used as control. Total RNA was extracted and HCV RNA qRT-QPCR was performed to determine the HCV RNA levels in eIF4AI and eIF4AII overexpressing cells.

Figure 3-4 represents the HCV RNA qRT-QPCR levels in eIF4AI and eIF4AII overexpressing 5B cells relative to HCV RNA levels in control cells. The data is representative of at least three independent experimental replicates. The overexpression of FLAG tagged eIF4AI and eIF4AII did not show any effect on HCV RNA levels when compared to HCV RNA level in control. This could be due to the fact that FLAG tagged eIF4A proteins were not functional or weren't incorporated into the correct complex. The northern blot analysis also shows similar HCV RNA levels in eIF4AI and eIF4AII overexpressing cell compared to control.

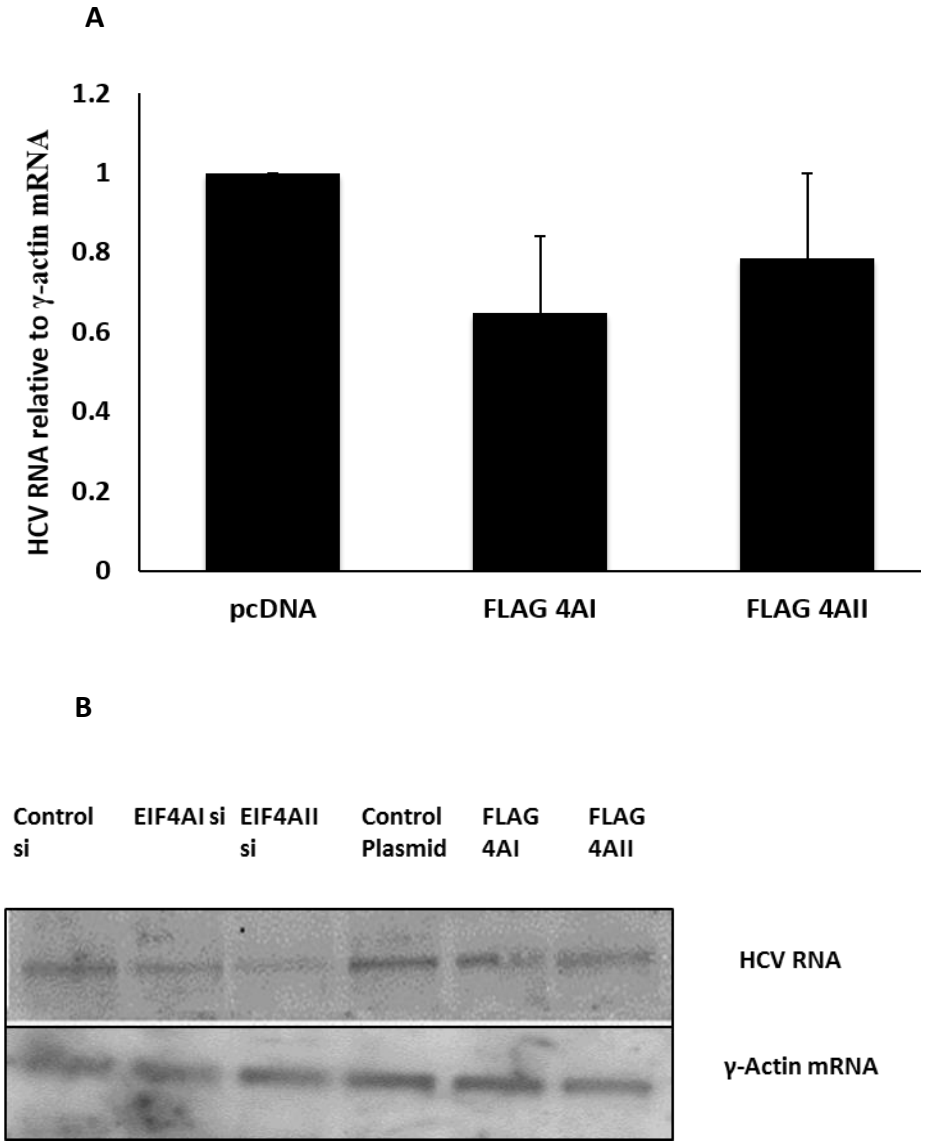

Figure 3-4 HCV RNA RT-qPCR in FLAG eIF4AI and FLAG eIF4AII overexpressing cells

eIF4AI and eIF4AII were overexpressed in 5B cells while pcDNA was used as control plasmid **A)** HCV RNA RT-qRT-QPCR levels relative to γ-actin mRNA in eIF4AI and eIF4AII overexpressing cells compared to cells transfected with control plasmid. **B)** HCV RNA levels measured by northern blot while lower row shows γ-actin mRNA as loading control.

3.2.4 Effect of exogenous expression of siRNA resistant eIF4AII on HCV RNA levels in eIF4AII depleted cells

It was already shown in previous results (section 3.2.1), that the knockdown of eIF4AII represses HCV RNA. In order to assess if the restoration of eIF4AII could restore the knockdown effects on HCV RNA levels, an siRNA-resistant version of eIF4AII (thankfully got form Martin Bushell lab) which have mutations at siRNA A binding sites in eIF4AII mRNA) was used (Meijer, Kong et al. 2013). 5B cells were transfected with eIF4AII specific siRNA A and non-target scrambled siRNA as control and after 24 hours siRNA-resistant eIF4AII plasmid (4AII-SR), or a control empty plasmid (pCTO) were introduced into same cells. RNA was harvested after 48 hours and RT-qRT-QPCR was performed to measure the HCV RNA levels. Figure 3.5 represents data from three independent experiments. The effect of eIF4AII knockdown (in the absence of over expressing plasmid) was similar to the knockdown result shown earlier (figure 3.1) confirming that eIF4AII depletion reduces HCV RNA. In the presence of the DNA transfection control (pCTO), there was no significant difference in HCV RNA levels between knockdown cells and pCTO containing cells observed (figure 3-5 middle panel). The overexpression of eIF4AII by siRNA resistant eIF4AII plasmid (right panel) restored the HCV RNA levels in both control and eIF4AII overexpressed cells even further than the levels in siRNA knockdown cells. The increase in HCV RNA levels in eIF4AII overexpressed cells compared to eIF4AII si is significant, which indicates that the restoration of HCV RNA level in eIF4AII knockdown cell is due to the overexpression of eIF4AII.

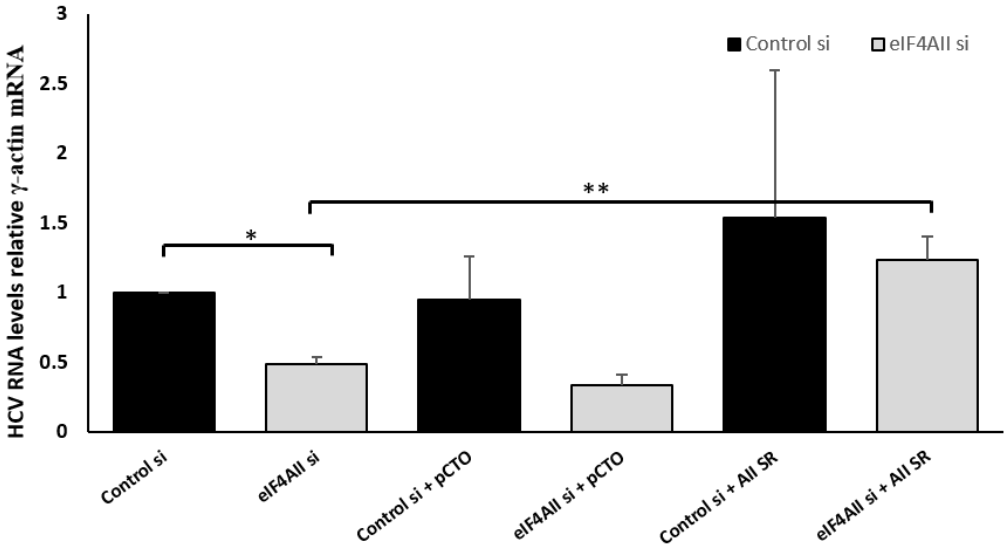

Figure 3-5 Relief of effects of eIF4AII knockdown on HCV RNA by expression of siRNA resistant eIF4AII

eIF4AII was overexpressed by using siRNA resistant eIF4AII plasmid (AII SR) in control and eIF4AII knockdown cells. The pCTO plasmid was used as a transfection control. The graph represents the HCV RNA measured by RT-qRT-QPCR relative to γ-actin mRNA following eIF4AII knockdown and siRNA-resistant eIF4AII expression. The data is representative of at least three independent biological replicates and bars represent the standard deviation (SD). T.test was used to determine the significance level *P<0.05, **P<0.01

3.2.5 eIF4AI knockdown has variable effects on HCV RNA levels

Both eIF4AI and eIF4AII have been knocked down to study the effects on HCV RNA. It has already been shown in section 3.2.1 that both eIF4AI and eIF4II knockdown reduce HCV RNA levels. The knockdown of eIF4AII always resulted in reduction of HCV RNA but eIF4AI knockdown showed variable effects as in some cases the knockdown of eIF4AI resulted in an increase of HCV RNA even further to that of control (figure 3-6). Although the data is not statistically significant due to high variability among the repeats, it shows that knockdown of eIF4AI could increase the HCV RNA levels. In a previous study it was shown that knockdown of eIF4AI result in increase in eIF4AII expression but eIF4AI function was not restored which indicate that both eIF4AI and eIF4AII work differently (Galicia-Vazquez, Cencic et al. 2012). Due to the difference in results between two experiments (this data and the data shown in figure 3-2), the two sets of data are presented separately to avoid the masking of the differences between the two data sets. These differences in the results could be due to the subtle differences in the confluence level of the cells or due to experimental variability. This could also be due to the passage number of cells or used and this experiment as it was performed a year later than the previous. Further experiments are required to draw a firm conclusion.

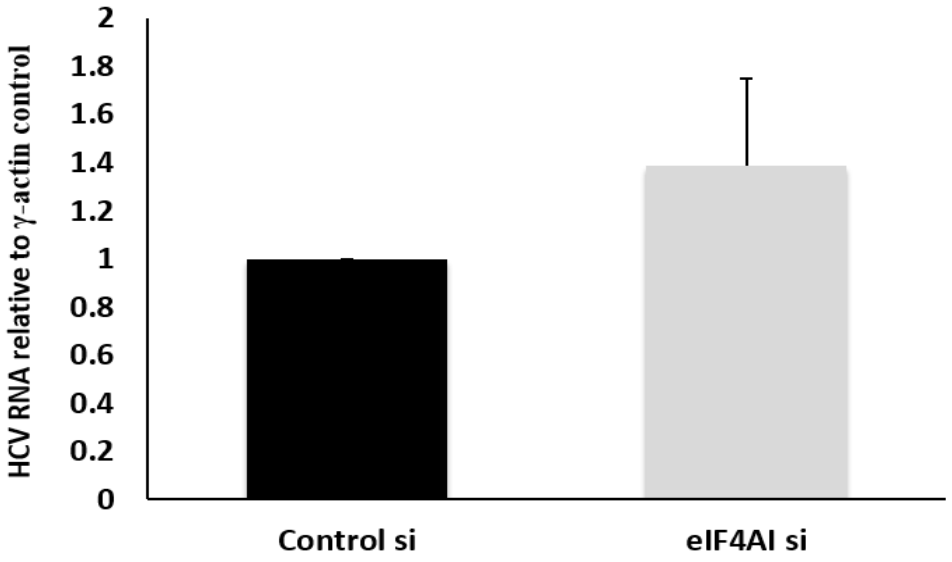

Figure 3-6 Variable effects of eIF4AI knockdown on HCV RNA levels in

The figure represents the HCV RNA qRT-QPCR levels in six independent experiments which showed very different effect of eIF4AI knockdown compared to data in section 3.2. The qRT-QPCR levels are relative to γ-actin mRNA in eFI4AI knockdown cells compared to cells treated with control siRNA. The data is presented separately to avoid the masking of the differences between the two sets. The error bar shows the SD.

3.2.6 miR-122 overexpression and inhibition do not affect HCV RNA levels in eIF4AII depleted cells

It has been shown in the previous studies that miR-122 binds to two sites in the HCV 5'UTR and positively regulates the HCV virus (Jopling, Yi et al. 2005). The mechanism by which miR-122 regulates HCV RNA abundance is still unknown. In the previous section (3.2.1) it is observed that eIF4AII is involved in HCV regulation. To determine whether the eIF4AII regulation of HCV also required miR-122 involvement or not, pre-miR-122 and 122 2'OMe (miR-122 inhibitor) were used to overexpress and inhibit the miR-122 in eIF4AI and eIF4AII depleted 5B cells. Pre-miR-122 is recognized by the Dicer enzyme in the cytoplasm and processed into mature miR-122, which binds to HCV 5'UTR and upregulates the HCV virus. 122 2' OMe is miR-122 complimentary sequence in which a methyl group (CH_3) is attached at 2' hydroxyl position in each nucleotide (figure 4-8). This 2'-O-methylation at each position which leads to stable binding to miRNA through complementarity between the bases. The binding of 122 2'OMe to miR-122 (RNA sequence) prevent the miR-122 binding to target sequence (i.e. HCV RNA) (Jopling 2010, Roberts and Jopling 2010).

Both eIF4AI and eIF4AII were knocked down in N/Neo C-5B cells as described previously (section 2.3.3.1) and treated with pre-miR-122 and miR-122 2'OMe at the same time. RNA was harvested after 72 hours and HCV mRNA levels were determined by qRT-QPCR and northern blot.

In figure 3-7, HCV qRT-QPCR levels following miR-122 overexpression and inhibition are shown in eIF4AI and eIF4AII knockdown cells. When the HCV

RNA levels in eIF4AI and eIF4AII knockdown cells are compared to control cells, eIF4AII depletion resulted in more decrease in HCV RNA levels compare to eIF4AI knockdown. This is similar to the result presented already in figure 3-2. In the presence of overexpressed miR-122, there is an increase in HCV RNA levels in control and eIF4AI knockdown cells but in eIF4AII knockdown cell the HCV RNA levels remain unchanged. The overexpression of miR-122 showed no effect on HCV RNA in eIF4AII knockdown cells. Similarly, the inhibition of miR-122 does not affect the level of HCV RNA in eIF4AII depleted cells. Although the addition of miR-122 increases the HCV RNA levels in control and eIF4AI knockdown cells, due to the high error the increase in HCV RNA following miR-122 overexpressing in conditions of eIF4AI knockdown is not statistically significant. The inhibition of pre-miR-122 by 122 2'OMe significantly decreases the HCV RNA levels in control cells. While, there was no significant difference observed between HCV RNA levels with or without miR-122 inhibition in eIF4AI and eIF4AII knockdown cells. HCV RNA analysis by northern blot (figure 3-8) shows a similar pattern of HCV RNA levels to HCV levels in qRT-QPCR. miR-122 overexpression significantly increases the HCV RNA levels in control cells and the inhibition of miR-122 by miR-122 2'OMe also significantly decrease the HCV RNA qRT-QPCR levels in control cells. These results indicate that in the presence of endogenous eIF4AII (control si cells) the overexpression and inhibition of miR-122 significantly affect the HCV RNA levels, while in eIF4AII knockdown cells the presence and absence of miR-122 do not affect the HCV RNA levels.

Although the error is quite high these results suggest that functional eIF4AII is required for miR-122-mediated regulation of HCV.

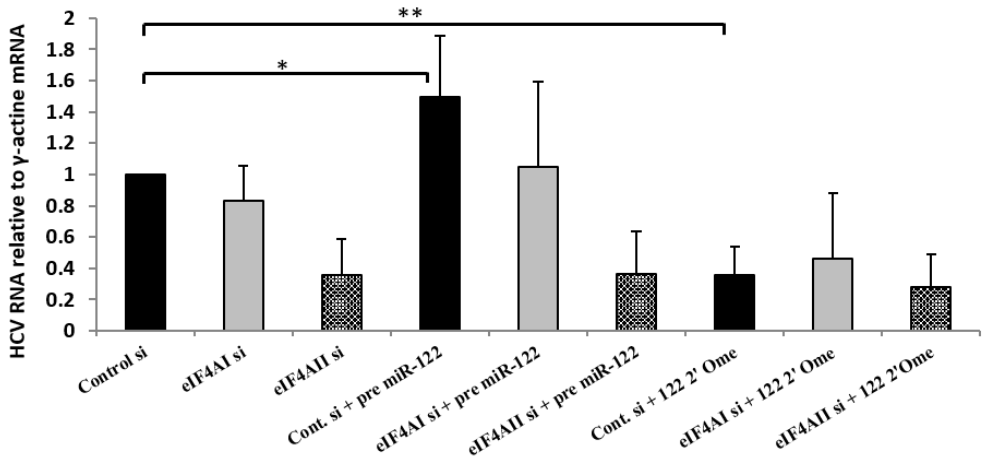

Figure 3-7 Overexpression and depletion of miR-122 in eIF4AI and eIF4AII knockdown cells.

To observe the effect of miR-122 in eIF4AI and eIF4AII depleted cells, miR-122 was overexpressed and depleted in Huh7 5B cells using pre-miR-122 and 122-2'OMe, respectively. RNA was harvested after 72 hr and used for qRT-QPCR detection of HCV RNA relative to γ-actin mRNA. Graph is representative of at least three independent biological replicates and the SD is denoted by error bars. t.test was used to determine the significance level. *P<0.05 and **P<0.01

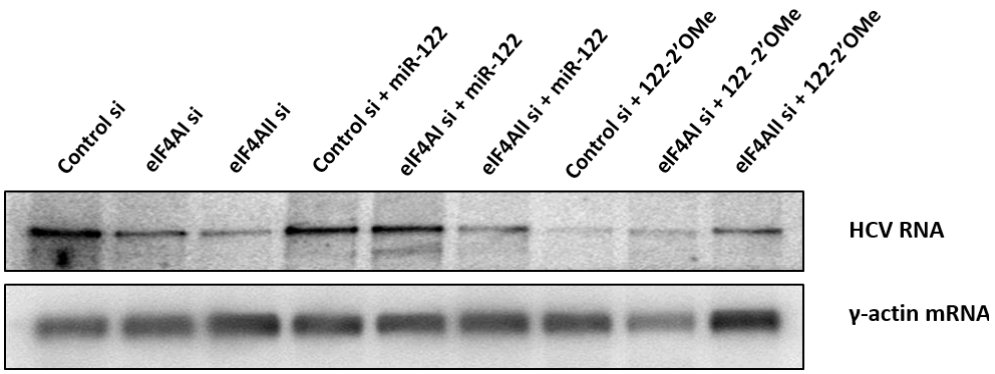

Figure 3-8 Northern blot detection of HCV RNA following overexpression and depletion of miR-122 in eIF4AI and eIF4AII knockdown cells.

Figure showing northern blot analysis of HCV RNA levels upon miR-122 overexpression and depletion in eIF4AI and eIF4AII depleted cells. Lower bands show the γ-actin mRNA loading control.

3.2.7 eIF4AI knockdown relieves repression of HCV RNA in eIF4AII knockdown cells

In the previous sections, it has been shown that the knockdown of eIF4AII reduces HCV RNA levels. The eIF4AI knockdown has lesser effect on HCV RNA level as in one set of experiments the knockdown of eIF4AI resulted in reduction in HCV RNA levels (figure 3-2) while in another set it leads to slight increase in HCV RNA levels (figure 3-6). The overall results presented in previous sections indicate that eIF4AI and eIF4AII have different effects on HCV RNA levels. In the present section, the double knockdown of eIF4AI and eIF4AII was performed to study the effect of complete loss of eIF4A activity on HCV RNA levels. Two different eIF4AII siRNAs (eIF4AIIsi A and eIF4AIIsiC) with different target binding sites alone and in combination with eIF4AI siRNA were used to study the double knockdown effect of eIF4AI and eIF4AII on HCV RNA levels. RNA was harvested and qRT-QPCR was performed to determine the HCV RNA levels as described previously (2.5.4). The knockdown of only eIF4AI and eIF4AII reduce the HCV RNA levels as shown in previous section. eIF4AII siRNA C reduces the HCV RNA to even lower levels then siRNA A (figure 3-9) as seen already in figure 3-3. Surprisingly, when both eIF4AI and eIF4AII were knocked down in combination the HCV RNA levels were restored compared to single eIF4AII knockdown cells. Although, due to high error the restoration of HCV RNA in double knockdown cells was statistically not significant, similar type of effect in monocistronic H77 system was also observed (performed by Catherine Jopling). This indicates that the restoration of HCV RNA in double knockdown cells is likely to be a genuine biological effect.

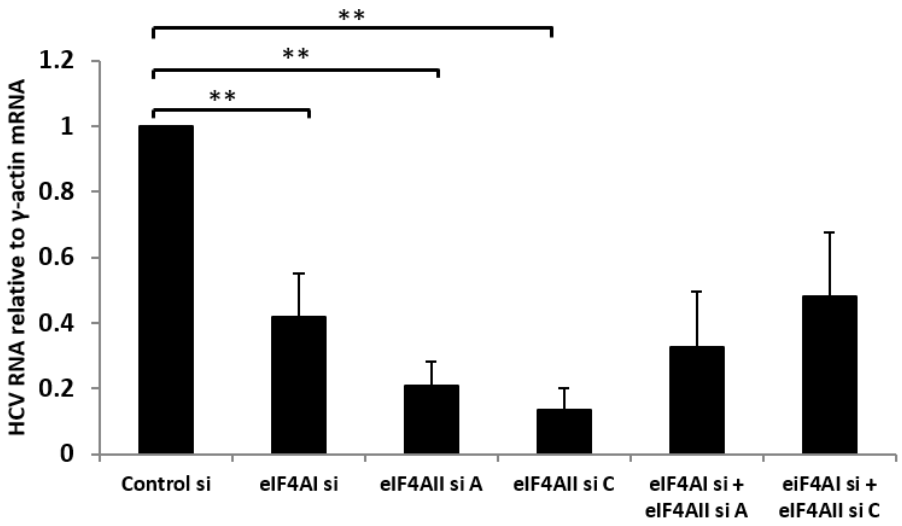

Figure 3-9 eIF4AI depletion relieves HCV RNA inhibition by eIF4AII knockdown.

Huh7 5B cells were treated with siRNAs against eIF4AI, eIF4AII or both and RNA was harvested post 72hr. Bar graph represents HCV RNA RT-qPCR levels relative to γ-actin mRNA of at least five independent experiments. The error bars represent mean +SD. Statistical significance level was determined by t.test where **P<0.01

3.3 Discussion

The techniques and results presented here demonstrate the successful knockdown of both eIF4AI and eIF4AII proteins. The siRNA-mediated knockdown of eIF4A proteins was consistent and reproducible among different experiments and confirmed by western blot analysis.

It was also demonstrated that eIF4AII knockdown decreases the HCV RNA levels to 80% and that eIF4AI has no or variable effect. Difference in HCV RNA levels in eIF4AI knockdown cells was also observed which could be due to the difference of cell confluency as the concentration of siRNAs was kept same in all experiments. The high HCV RNA levels in some experiments in eIF4AI knockdown cells compared to control could be due to compensatory overexpression of eIF4AII (Galicia-Vazquez, Cencic et al. 2012). More experimentation work is required to study the underlying mechanism.

The knockdown of eIF4AII resulting in repression of HCV RNA could be due to of the involvement of eIF4AII in HCV replication by interacting with NS5B or its involvement in miRNA-mediated regulation of protein synthesis (Kyono, Miyashiro et al. 2002, Meijer, Kong et al. 2013).

To see whether the overexpression of eIF4A proteins (especially eIF4AII) could increase the HCV RNA in HCV replicon cells, both eIF4AI and eIF4AII were overexpressed by plasmids containing FLAG tagged eIF4AI and eIF4AII.

There was no increase in HCV RNA levels observed in eIF4AI or eIF4AII overexpressing cell compared to control cells. This could be due to failure of FLAG tagged eIF4A proteins incorporation into functional complex or failure of expression system (expression plasmid) in producing functional eIF4A proteins. eIF4AII overexpression with different conditions, time of expression, amount of plasmid and different plasmid constructs followed by western blot analysis of protein expression levels are required to study the effect of eIF4AII expression on HCV RNA levels.

The role of miR-122 in HCV regulation is already established so to determine the effect of miR-122 in the eIF4AI and eIF4AII depleted cells, miR-122 was overexpressed and depleted by pre-miR-122 and miR-122 inhibitor (122 2' OMe) respectively. No significant difference in HCV RNA following miR-122 overexpression and inhibition was observed in eIF4AII depleted cells, while miR-122 overexpression significantly increased the HCV RNA levels in control and eIF4AI depleted cells and miR-122 inhibition decreased the HCV RNA levels in these cells. This indicates that the miR-122 regulation of HCV is dependent on eIF4AII. These results are similar to the previous results in which eIF4AII has been shown to play a role in miRNA-mediated repression via 3'UTR. These results also indicate that eIF4AII is involve in an increase of target mRNA when micro RNA binding sites are present in 5'UTR.

After establishing that eIF4AII knockdown reduces HCV RNA levels and that eIF4AI knockdown has variable effects on HCV RNA, both eIF4A proteins were depleted to study the effects of double knockdown on HCV regulation. The double knockdown of eIF4AI and eIF4AII resulted in relief of HCV RNA repression compare to eIF4AII single knockdown. This could be due to the fact that knockdown of eIF4AI increases the eIF4AII expression beyond the eIF4AII knockdown levels. Such a change in eIF4A protein levels in single and double knockdown would need to be investigated by western blot analysis.

After establishing that eIF4AII is involved in HCV regulation in a replicon system, the effects of knockdown of both eIF4A proteins were tested in live virus infections. The Huh7.5 were depleted for eIF4AI and eIF4AII individually or in different combinations followed by addition of two different strains of HCV genotype 2a. HCV RNA levels were determined by qRT-QPCR (data not shown) but due to the high degree of variability among the experiments it was not possible to draw a conclusion. More repeats of these experiments are required to investigate the role of eIF4AII in live virus system. This will also help in knowing if there is any difference in eIF4AII role between replicon system and infectious virus system. Study of the role of eIF4AII in the live virus will also give a more realistic picture as this system is more representative of the real virus infection.

In this chapter the role of eIF4AII in HCV regulation was studied and it was established that eIF4AII but not eIF4AI positively regulates HCV RNA in replicon cells while more experiments are required to study this role in live virus systems. Further studies are also required to investigate the mechanism of eIF4AII regulation and to know at what stage of HCV replication this regulation occur.

In the next chapter, the association of HCV RNA with eIF4AII and miR-122 is investigated.

4 eIF4AII associates with HCV and miR-122 in a miR-122 dependent manner

4.1 Introduction

In the previous chapter the role of eIF4AI and eIF4AII in HCV regulation was investigated. Both eIF4AI and eIF4AII were depleted in HCV replicon cells by specific siRNAs and it was found that eIF4II knockdown decreases the HCV RNA levels. However, eIF4AI knockdown moderately reduces HCV RNA levels in some experiments but in contrast, in other experiments an increase in HCV RNA levels was observed, so it was difficult to conclude whether there was any effect. These findings led to the conclusion that eIF4AII positively regulates HCV. An important question is the mechanism by which eIF4AII regulates HCV, and this chapter aims to address this question. Specifically, it was important to determine whether eIF4AII directly associates with HCV RNA and whether miR-122 is involved in this regulation.

During the initiation of protein translation, eIF4A helps the 40S ribosomal subunit in binding and scanning of the mRNA to recognize the start codon by removing the secondary structure present in the mRNA. MiR-122 binds to two binds sites in the HCV 5' UTR region and enhances the abundance of HCV virus (Jopling, Yi et al. 2005). A number of other host factors like DDX3 and DDX6 are also involved in HCV regulation (Ariumi, Kuroki et al. 2007, Jangra, Yi et al. 2010). DDX6 helicase regulates HCV replication in a miR-122 independent (Huys, Thibault et al. 2013) manner. The potential involvement

of eIF4AII in HCV replication as a binding partner of HCV NS5B protein (Kyono, Miyashiro et al. 2002) and its role in miRNA based repression of protein translation (Meijer, Kong et al. 2013) with our data on eIF4AII suggested that eIF4AII might be part of complex in which HCV RNA and miR-122 are also present. To test the hypothesis that eIF4AII directly interacts with HCV RNA and/or miR-122, RNA immunoprecipitation (RIP) was performed with first FLAG-eIF4AI and FLAG-eIF4II and later on with anti-EIF4AI and anti-EIF4AII antibodies and the immunoprecipitated complexes assayed for the presence of HCV RNA and miR-122.

4.2 Results

4.2.1 HCV RNA immunoprecipitation with FLAG-eIF4AI/AII

To further investigate the role of eIF4AI and eIF4AII in HCV regulation, RNA immunoprecipitation (RIP) was used to isolate the eIF4AI and eIF4AII complexes. The rationale behind selecting this technique was to determine if HCV RNA and miR-122 are present in the eIF4AI and eIF4AII bound complexes. For this, the plasmid pCMV-Entry containing eIF4AI or eIF4AII (provided by Dr. Martin Bushell, MRC Toxicology Unit, Leicester, UK) upstream of a FLAG tag was used to express FLAG-eIF4AI or FLAG-eIF4AII in Huh7 HCV replicon cells (figure 4-1). Transfected cells were lysed in NET-2 buffer in the presence of protease inhibitor cocktail and RNAse inhibitor and incubated with anti-FLAG antibody overnight at 4 °C. The following day, lysates were washed with NET-2 to remove unbound complexes and RNA

and protein were extracted. qRT-QPCR was used to determine the HCV RNA and miR-122 levels.

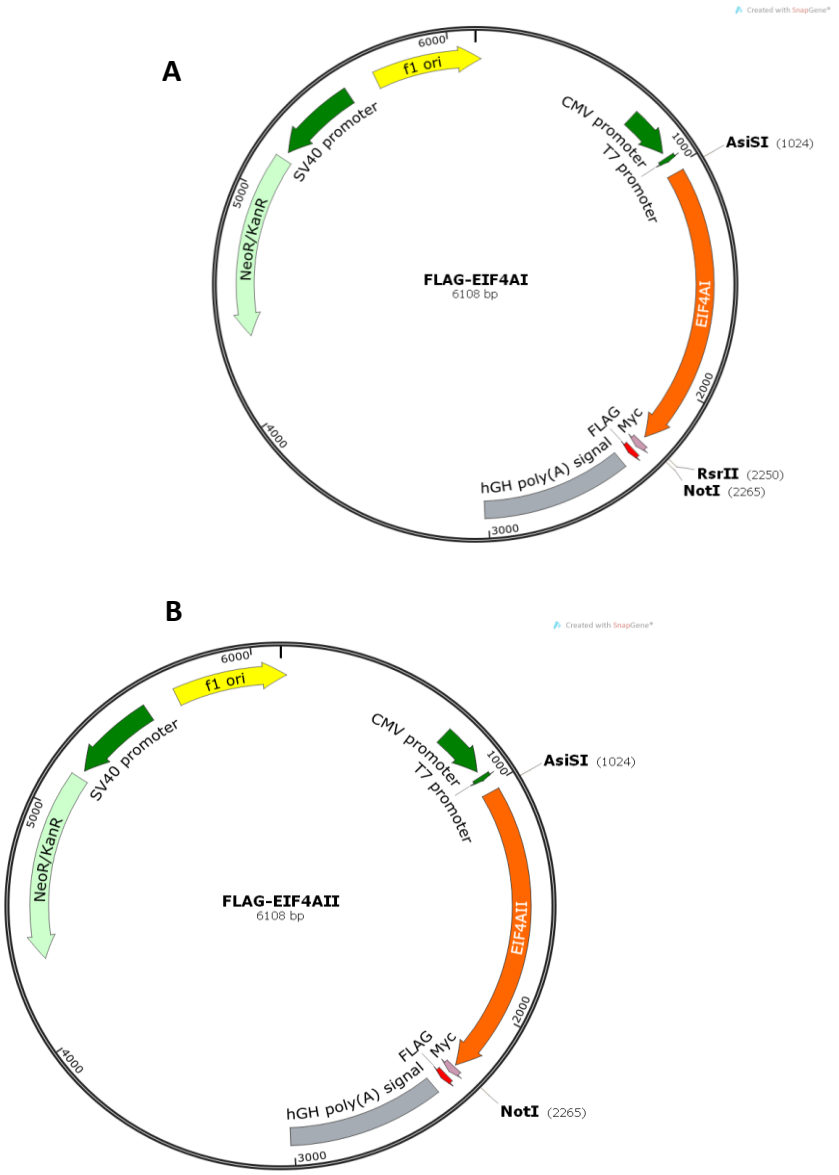

Figure 4-1 FLAG-eIF4A plasmids

A) Schematic representation of pCMV-Entry vector with eIF4AI inserted upstream to FLAG tag using AsiSI and RsrII restriction sites. **B)** eIF4AII was inserted in the same vector as **A** using AsiSI and NotI restriction sites.

RNA was extracted from the IP samples and cDNA synthesis was carried out. qRT-QPCR was performed in triplicates to determine the HCV RNA levels in FLAG-eIF4A1, FLAG-eIF4AII and FLAG-pCTO IPs. The CT values of the triplicates were averaged and HCV RNA levels were calculated by 2^-ΔCt method relative to 10% input. Figure 4-2 represents the HCV RNA qRT-QPCR levels in FLAG-pCTO, FLAG-peIF4AI and FLAG-peIF4AII input (black bars) and in FLAG IPs (grey bars). The two-fold increase in HCV RNA levels in FLAG-eIF4AII plasmid compared to FLAG-pCTO control plasmid might suggest low level association of HCV RNA with eIF4AII. When FLAG-eIF4AI and FLAG-eIF4AII HCV RNA levels were compared to their input levels it was noted that FLAG eIF4AI and eIF4AII and the FLAG control (figure 4-3) have very low association with HCV RNA, Furthermore, there was no enrichment of HCV RNA with anti-FLAG compared to IgG control. Figure 4.3 shows data from a single experiment. Data from other experiments was not included due to the problems with sample loss. As no enrichment of HCV RNA in FLAG-IPs was detected, this experimental approach was not pursued further. These data suggest that eIF4AI and eIF4AII do not interact with HCV. However, there are several other possible explanations for the lack of pulldown. It is possible that FLAG-tagged proteins were not expressed. Western blotting was not carried out to test this due to the time constraints. The lack of interaction observed could also be due to a failure of FLAG-eIF4AI and FLAG-eIF4AII protein association with cellular partners to form a functional complex.

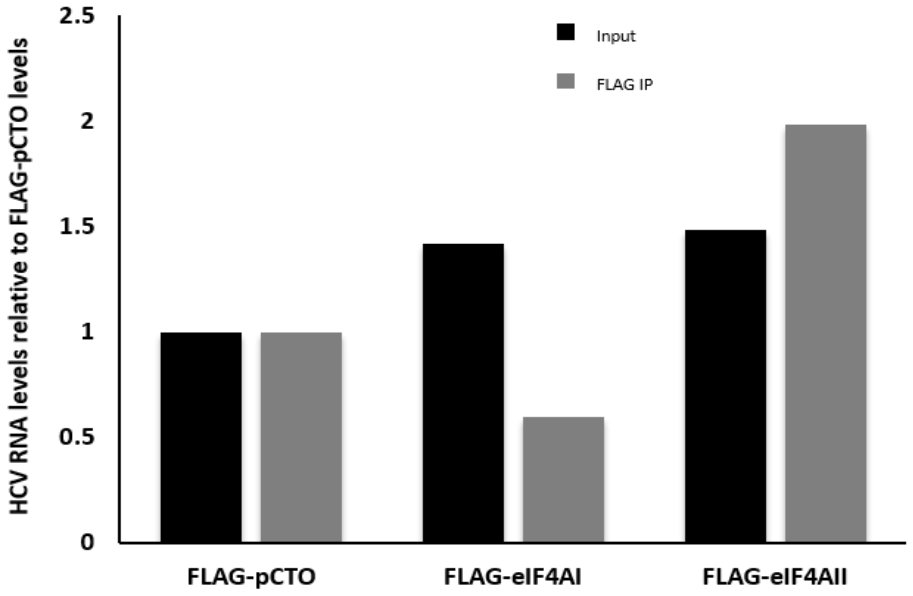

Figure 4-2 HCV RNA does not associate with FLAG-eIF4A proteins

The graph shows the HCV RNA levels detected by qRT-QPCR in 10% input RNA and anti-FLAG IP from 5B cells transfected with FLAG-eIF4AI and FLAG-eIF4AII, compared to the FLAG-pCTO empty vector control. The data represent a single experiment.

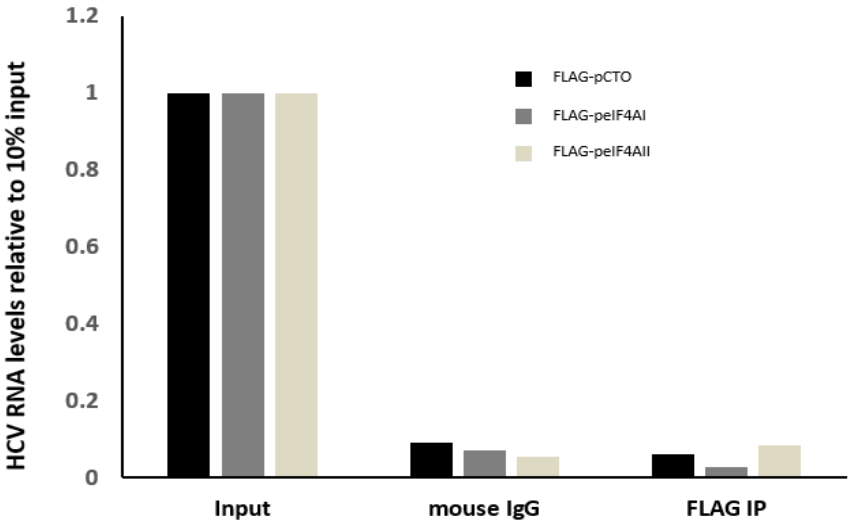

Figure 4-3 HCV RNA levels in FLAG IPs

HCV RNA levels from the FLAG IPs in figure 4-2 are shown relative to 10% of input. Mouse IgG was used as a control. FLAG IPs do not show enrichment of HCV RNA. The data represent the single repeat of this experiment.

4.2.2 miR-122 immunoprecipitation with FLAG-eIF4AI and FLAG-eF4AII

Similar to the determination of HCV RNA qRT-QPCR levels in FLAG IPs shown in previous section, miR-122 levels were also determined in FLAG-eIF4AI/AII IPs while FLAG-pCTO was used as control plasmid. Immunoprecipitated RNA was used as template for miR-122 cDNA synthesis followed by qRT-QPCR based detection of miR-122 levels in FLAG-eIF4AI and FLAG-eIF4AII IPs.

Figure 4-4 represents the data from four independent biological replicates and shows the levels of miR-122 in FLAG IPs from pCTO, peIF4AI and peIF4AII and in mouse IgG control compared to 10% input. FLAG-peIF4AII shows higher levels of miR-122 association compared to miR-122 levels in FLAG-peIF4AI IP but the high error bars, especially in FLAG eIF4AII IP, indicate a high degree of variability among the experiments. Also, there is little enrichment compared to the IgG control, so these data do not support a direct interaction between eIF4AII and miR-122. As discussed in the previous section, optimization of FLAG based immunoprecipitation would be required to repeat these experiments to draw a firm conclusion. The high variability in the results might also indicate the lack of association of FLAG versions of these proteins into functional complex.

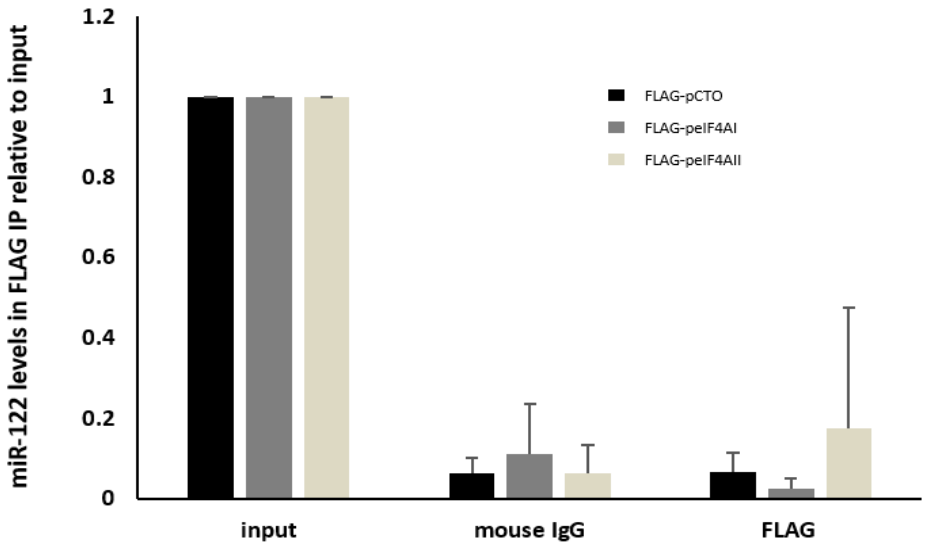

Figure 4-4 miR-122 does not associate with FLAG-eIF4A proteins

pCTO, eIF4AI and eIF4AII FLAG tag plasmids were transfected into 5B cells and FLAG IP was performed. The figure represents the miR-122 levels, determined by RT-qRT-QPCR in FLAG pCTO, eIF4AI and eIF4AII IPs relative to 10% of the respective input. Mouse IgG was used as IP control. The data is representative of four independent biological experiments. The error bars represent the SD.

4.2.3 HCV RNA associates with endogenous eIF4AII

Although the previous experiments do not show an interaction between FLAG-eIF4AII and HCV RNA, there are potential problems with the approach of using FLAG tagged proteins. As an alternative approach, antibodies specific to the endogenous eIF4A proteins were used to immunoprecipitate replicon cell lysates, and the immunoprecipitates were assayed for HCV RNA. Cell lysate was incubated at 4^{o}C overnight with protein A/G agarose beads in the presence of antibodies to eIF4AI, eIF4AII or an IgG control. Next day RNA was extracted and cDNA was synthesised. HCV RNA levels were determined by qRT-QPCR.

Figure 4-5 shows the average 2^-ΔCt of more than ten biologically independent replicates compared to 10% of input. The bars show the HCV RNA level with endogenous eIF4AI, eIF4AII and IgG control compared to 10% input. HCV RNA showed high levels of enrichment (28% of the input) with eIF4AII and this enrichment was statistically significant ($P<0.05$) compared to IgG control. Endogenous eIF4AI didn't show any binding to HCV RNA compared to the input, while the negative control using IgG isoform also showed no association. These results indicate that HCV RNA and eIF4AII interact with each other and that eIF4AI has no interaction with HCV RNA. Although the eIF4AI and eIF4AII antibodies are validated for IP by manufacturer (Abcam), there was only one band detected with eIF4AI and eIF4AII antibodies on western blot (blot not shown), so it is very unlikely that these antibodies are bringing down any other proteins in the IPs.

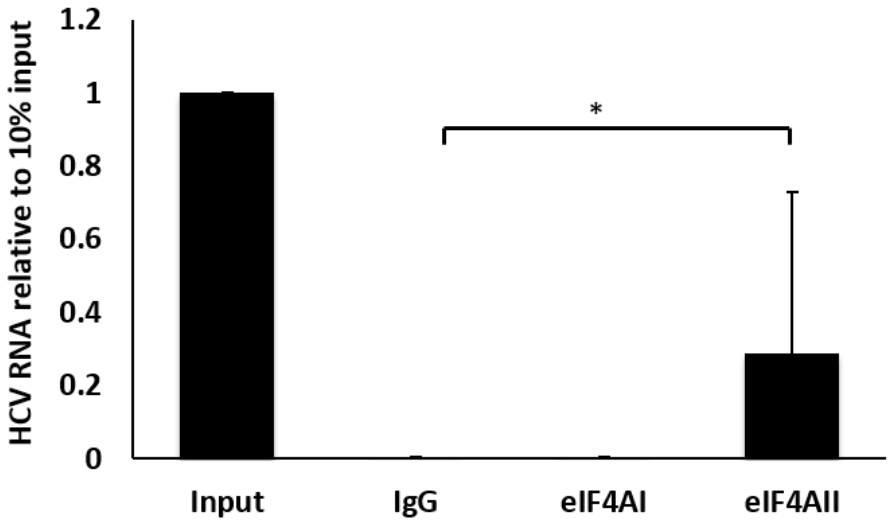

Figure 4-5 HCV RNA is immunoprecipitated by an antibody to endogenous eIF4AII, but not eIF4AI

The figure represents the qRT-QPCR levels of HCV RNA following immunoprecipitation of 5B cell lysate with antibodies specific to endogenous eIF4AI and eIF4AII proteins, relative to 10% input. Normal mouse IgG was used as an IP control. The bars show the SD. The data represent the mean of more than ten independent experiments with *P<0.05 (Student's t test).

4.2.4 miR-122 interacts with endogenous eIF4AII

As mentioned in above section (4.2.3), antibodies to endogenous eIF4A proteins were used to pull down HCV RNA. The same approach and the same RNA was used to detect the miR-122 levels associated with the endogenous eIF4AI and eIF4AII proteins, while rabbit IgG was used as IP control. The miR-122 qRT-QPCR levels were detected by using specific primers following cDNA synthesis.

Figure 4-6 represents the average miR-122 enrichment in eIF4AII IP with endogenous eIF4AII protein from at least ten biologically independent experiments.

The black bars represent the miR-122 enrichment levels with endogenous eIF4AI and eIF4AII or IgG control relative to 10% of input. The eIF4AII shows 60% miR-122 enrichment compared to input. The enrichment is also statistically significant ($P<0.01$) compared to IgG control. The endogenous eIF4AI immunoprecipitate didn't show any enrichment of miR-122, while eIF4AII interacts with miR-122 and these enrichment levels are double the HCV RNA enrichment levels shown in figure 4-5. The absence of miR-122 in eIF4AI immunoprecipitate indicates that eIF4AI doesn't interacts with miR-122, or may be due to the possibility that the eIF4AI antibody doesn't immunoprecipitate effectively. But the important point is that it is not certain that the absence of HCV RNA (figure 4-5) and miR-122 in eIF4AI IP means there is no interaction unless it is further confirmed that eIF4AI is immunoprecipitated. The high error bars in eIF4AII IP show the high

variability among the biological replicates but the P value ($P<0.01$) indicates the statistical significance of enrichment of miR-122 in the eIF4AII IP.

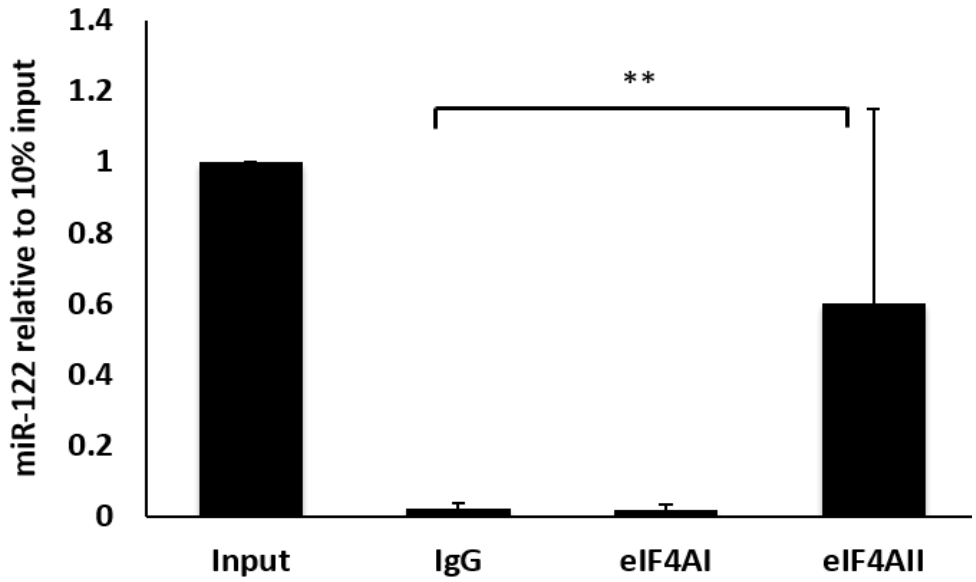

Figure 4-6 miR-122 RNA is immunoprecipitated by an antibody to endogenous eIF4AII, but not eIF4AI

The figure represents the RT-qRT-QPCR levels of miR-122 following immunoprecipitation of 5B cell lysate with antibodies specific to endogenous eIF4AI and eIF4AII proteins, relative to 10% input. Normal mouse IgG was used as a control. The data represent the mean of at least ten independent experiments. The bars show the SD while **P<0.01 (Student's t test).

4.2.5 eIF4AII also interacts with miR-21 and miR-26a

eIF4AII has already been shown to be involved in miRNA-mediated repression of protein synthesis via the 3'UTR sites (Meijer, Kong et al. 2013). The miR-122 data presented in section 4.2.4 is the first evidence of eIF4AII interaction with miRNA. So apart from miR-122 levels in eIF4AII IP, two other miRNAs present in the liver were also investigated in eIF4AI and eIF4AII IPs. For this, RT-qRT-QPCR was used to determine the presence of miR-21 and miR-26a in eIF4AII IP.

As observed for miR-122, both miR-21 and miR-26a were detected in eIF4AII IP but not in eIF4AI IP (figure 4-7). The interaction of eIF4AII with miR-21 and miR-26a but not eIF4AI supports the previous observation that eIF4AII, but not eIF4AI, is required for miRNA-mediated repression of translation (Meijer, Kong et al. 2013) and the notion of that eIF4AI and eIF4AII proteins have different roles and functions. Although eIF4AII IP show enrichment of both miR-21 and miR-26a, the level of enrichment of these microRNAs were less than the level of miR-122 enrichment with endogenous eIF4AII as shown in previous section 4.2.4. The higher level of miR-122 enrichment with eIF4AII compared to miR-21 and miR-26a levels could be due to the presence of HCV RNA-miR-122 complex in eIF4AII IPs. It is possible that eIF4AII is binding with this complex and strengthening the interaction between HCV RNA and miR-122, but this need to confirm by further experiments.

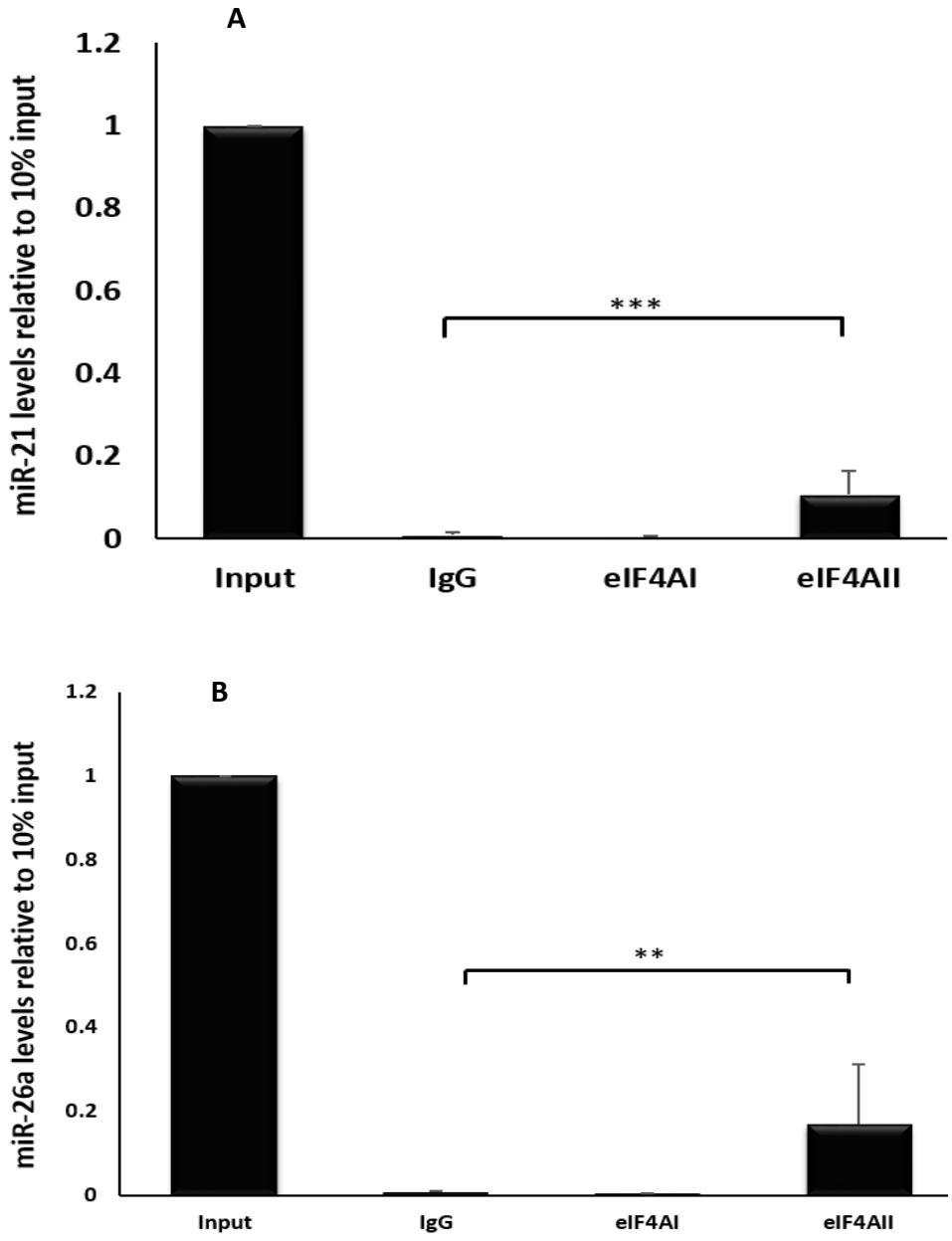

Figure 4-7 miR-21 and miR-26a are immunoprecipitated by an antibody to endogenous eIF4AII, but not eIF4AI

miR-21 levels determined by RT-qRT-QPCR in immunoprecipitated 5B cell lysates with antibodies specific to endogenous eIF4AI and eIF4AII IPs, relative to 10% input. Normal mouse IgG was used as an IP control. B). As (A), except that miR-26a levels were determined by qRT-QPCR. The data represent the mean of at least five independent experiments, and error bars represent the SD. Statistical significance was determined by Student's t-test where **P<0.01 and ***P<0.001.

4.2.6 miR-122 sequestration reduces HCV RNA association with eIF4AII

In the previous sections (4.2.3, 4.2.4) both HCV RNA and miR-122 were shown to interact with eIF4AII. eIF4AII has also been shown to be involved in miRNA-mediated repression of protein translation via the 3' UTR (Meijer, Kong et al. 2013). To study whether the HCV RNA and eIF4AII association is miR-122 dependent or not, miR-122 was sequestered by miR-122 2'oMe. The miR-122 2'-O-methylated (2'OMe) inhibitor is an RNA oligonucleotide complementary to normal miR-122 sequence with a methyl group attached to 2' position (figure 4-8).

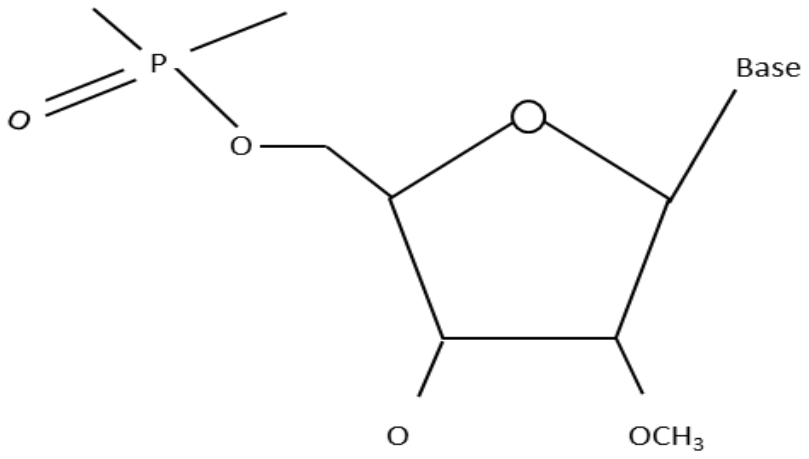

Figure 4-6 Structure diagram of 2' OMe nucleotide

The addition of a methyl group at position 2 of a nucleotide increases the stability against RNase (Wu, Yang et al. 2014) and the complementary sequence of mIR-122-2'OMe binds to miR-122 and block its binding to the target sequence (Jopling, Yi et al. 2005). To investigate the role of miR-122 in HCV RNA association with eIF4AII, HCV replicon cells were transfected with miR-122 2'OMe (miR-122 inhibitor) or mock transfected. The idea was

that if miR-122 is involved in HCV RNA and eIF4AII associations, then sequestration of miR-122 by miR-122 2'OMe should result in a decrease in HCV RNA levels in eIF4AII IPs. Figure 4-9 represents average 2^-ΔCt from more than five biologically independent experiments relative to 10% of input. The black bars represent the HCV RNA levels in endogenous eIF4A IPs while IgG was used as control. Endogenous eIF4AII binds to significantly high levels ($p<0.05$) of HCV RNA in the presence of wt miR-122 (black bars) compared to IgG control while eIF4AI didn't show any enrichment of HCV RNA as previously seen in Figure 4-5. When miR-122 binding to its target was blocked by 122 2'OMe (grey bars), the HCV RNA enrichment in eIF4AII IP was reduced to 24% of HCV RNA enrichment with wt miR-122. Although the HCV RNA levels in eIF4AII does not significantly reduced compare to HCV RNA in mocked eIF4AII IP (black bars) but there was strong average decrease and clear trend in all the experiments. The HCV RNA levels in eIF4AI IP do not change in the presence (miR-122 wt) or absence (122 2'OMe) of functional miR-122. This is likely to be due to the fact that eIF4AI do not interact with HCV RNA, but it is possible that eIF4AI was not immunoprecipitated effectively. The eIF4AII IP results show that eIF4AII binds to HCV RNA in a miR-122 dependent fashion. Although this data suggests that eIF4AII, HCV RNA and miR-122 are part of same complex but it need further work to confirm this idea. Experiment like using the mutant miR-122 binding sites followed by IP can give further information about the interaction.

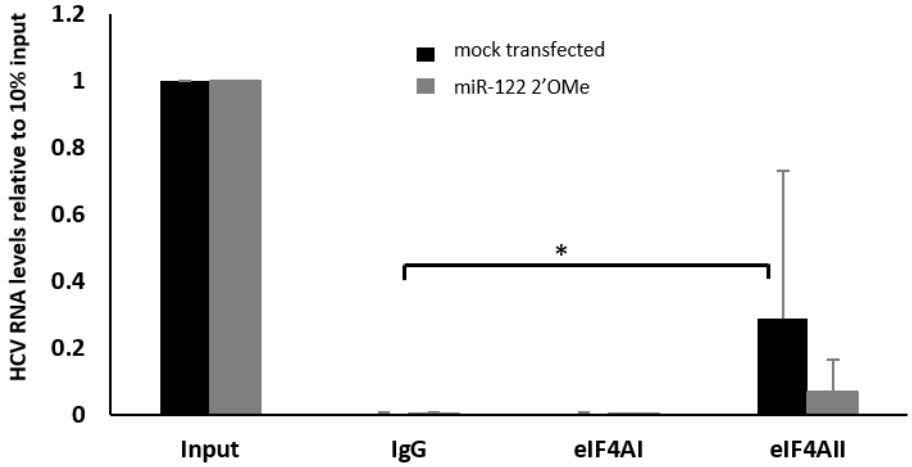

Figure 4-7 HCV RNA association with eIF4AII is reduced by miR-122 sequestration

5B cells were transfected with miR-122 inhibitor (122 2'Ome) and RNA was immunoprecipitated with antibodies specific to endogenous eIF4AI and eIF4AII. The figure shows HCV RNA levels in eIF4A IPs in the presence (black bars) and following inhibition (grey bars) of miR-122, determined by RT-qRT-QPCR relative to 10% input. The data are representative of more than five biologically independent replicates. The error bars show the SD. P*<0.05 (Student t.test).

4.2.7 miR-122 inhibition reduces miR-122 association with eIF4AII

To observe the effect of miR-122 sequestration on the miR-122 association with eIF4AII, miR-122 RT-qRT-QPCR was also performed on the IP RNA samples described above in section 4.2.6.

As expected, miR-122 sequestration significantly ($P<0.05$) reduces miR-122 in eIF4AII IP (figure 4-10). These results confirm the successful inhibition/sequestration of miR-122. It also suggests that miR-122 only interacts with eIF4AII when it is free to bind its targets.

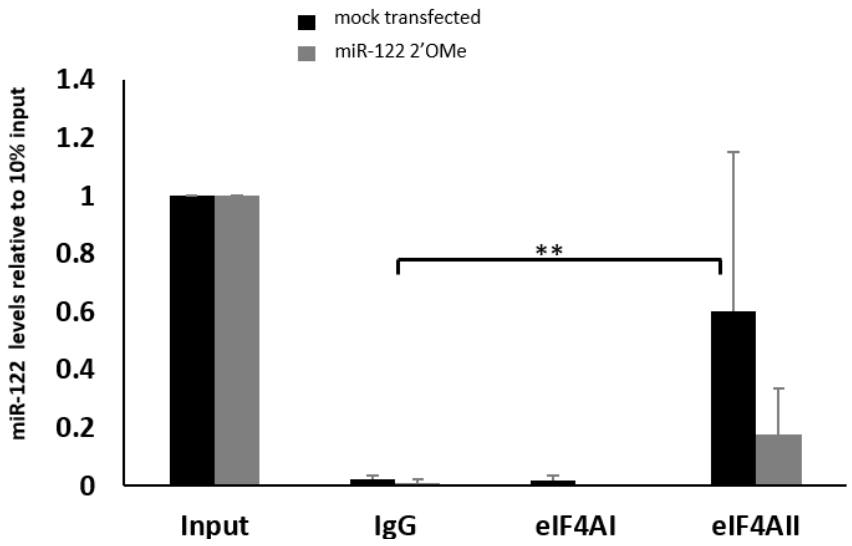

Figure 4-8 miR-122 association with eIF4AII is reduced by miR-122 sequestration

RT-qRT-QPCR was used to detect the miR-122 levels relative to 10% input following IP with antibodies specific to endogenous eIF4AI and eIF4AII, in control (black bars) and miR-122 inhibitor-treated (grey bars) 5B cell lysates. miR-122 sequestration significantly reduces the amount of miR-122 in eIF4AII IP. The data represent average of more than five independent biological replicates. Error bars represent the Standard deviation (*SD*). *P<0.01 (Student t.test).

4.2.8 miR-21 and miR-26a association with eIF4AII is independent of miR-122

As described earlier (4.2.5) eIF4AII also interacts with other miRNAs present in liver. To see if miR-122 sequestration by miR-122 2'Ome also affects the miR-21 and miR-26a association with eIF4AII, RT-qRT-QPCR to detect miR-21 and miR-26a was also performed on the IP samples described in section 4.2.6.

Figure 4-11 shows that the levels of both miR-21 and miR-26a in the eIF4AII are not affected by miR-122 sequestration. This indicates that both miR-21 and miR-26a association with eIF4AII is independent of miR-122, and shows that the effects of miR-122 sequestration on HCV and miR-122 association are specific and not due to other effects of the 2'OMe transfection.

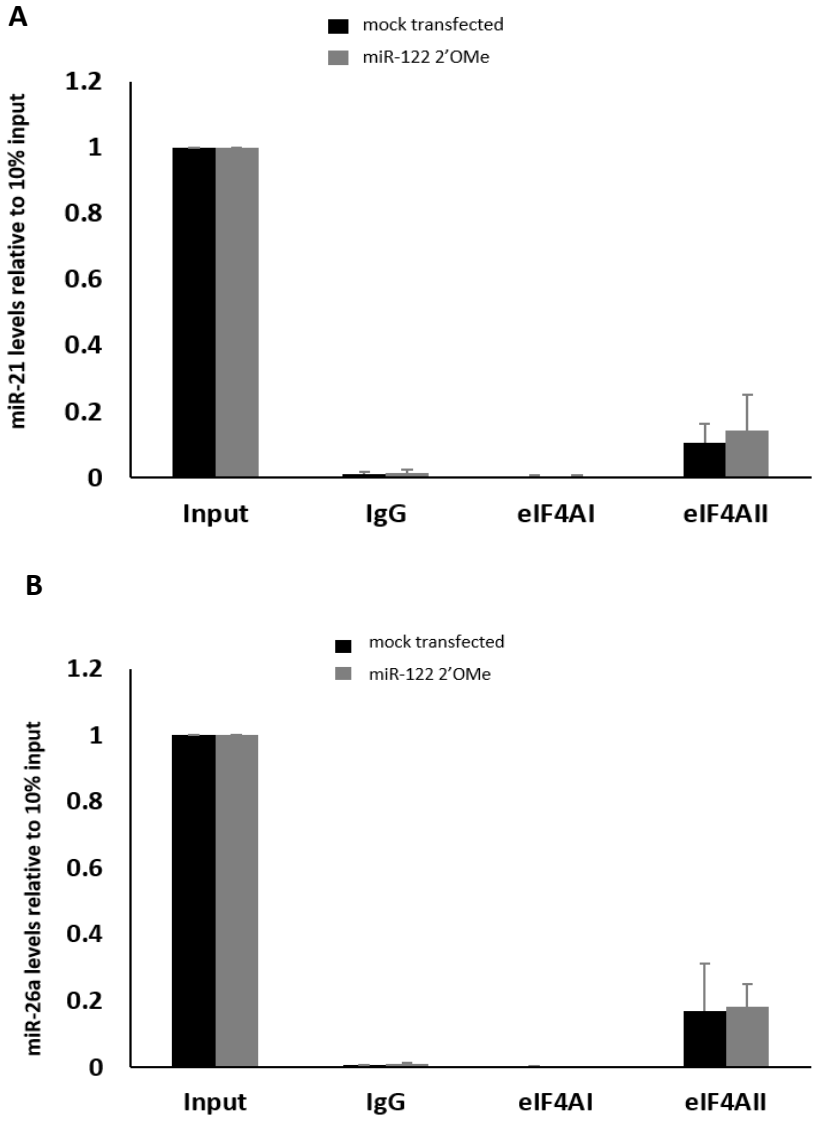

Figure 4-9 miR-21 and miR-26a association with eIF4AII are unaffected by miR-122 sequestration

A) miR-21 levels in eIF4AI and eIF4AII immunoprecipitates of 5B cell lysates, relative to 10% input, in the absence of miR-122 inhibitor (black bars) and in the presence of miR-122 inhibitor (grey bars). **B)** As (A) except the bars represent qRT-QPCR levels of miR-26a. Both figures are representative of more than five biologically independent experiments. The error bars represent the Standard deviation (SD).

4.2.9 eIF4AII binds to luciferase reporter RNA with four miR-122 binding sites in the 3'UTR

In the above sections, it was demonstrated that eIF4AII binds to HCV, miR-122 and other miRNAs in the HCV replicon system when miR-122 binding sites are present in HCV 5'UTR. To determine whether eIF4AII interacts with other miR-122 target RNAs, a plasmid (Luc122x2) containing four miR-122 binding sites in the 3'UTR of the firefly luciferase gene, and a control plasmid (Luc122x2m4) (figure 4-12 A) ((Jopling, Schutz et al. 2008) in which a TC to AG mutation was introduced at position 3-4 in each of the miR-122 seed matches (figure 4-12 B), were used. In this experiment approach two different reporter were used to test if eIF4AII interacts with other miR-122 targets, as well as HCV RNA. The use of Huh7 cell will allow to test whether the eIF4AII interaction with miR-122 is dependent on the presence of HCV 5' UTR.

Plasmids (luc122x2 and luc122x2m4) were transfected into two 10 cm plates containing Huh7 cells, which were subjected to immunoprecipitation with the eIF4AII antibody or an IgG control as described above, after 48h RNA was extracted. Luciferase mRNA and miR-122 RNA levels were determined by qRT-QPCR. The endogenous eIF4II showed higher binding to luciferase compared to the IgG control (figure 4-13A). When miR-122 binding was abolished by seed mutation, eIF4AII binding was decreased, while there was no difference in IgG control binding in the presence or absence of miR-122 binding sites (figure 4-13B). The data represents a single repeat of the experiment, so to draw a firm conclusion, further repeats are needed to

validate the above data. However, these results suggest that eIF4AII binding to luciferase RNA is dependent on the presence of miR-122 binding sites and that this binding is independent of location of the miR-122 binding sites.

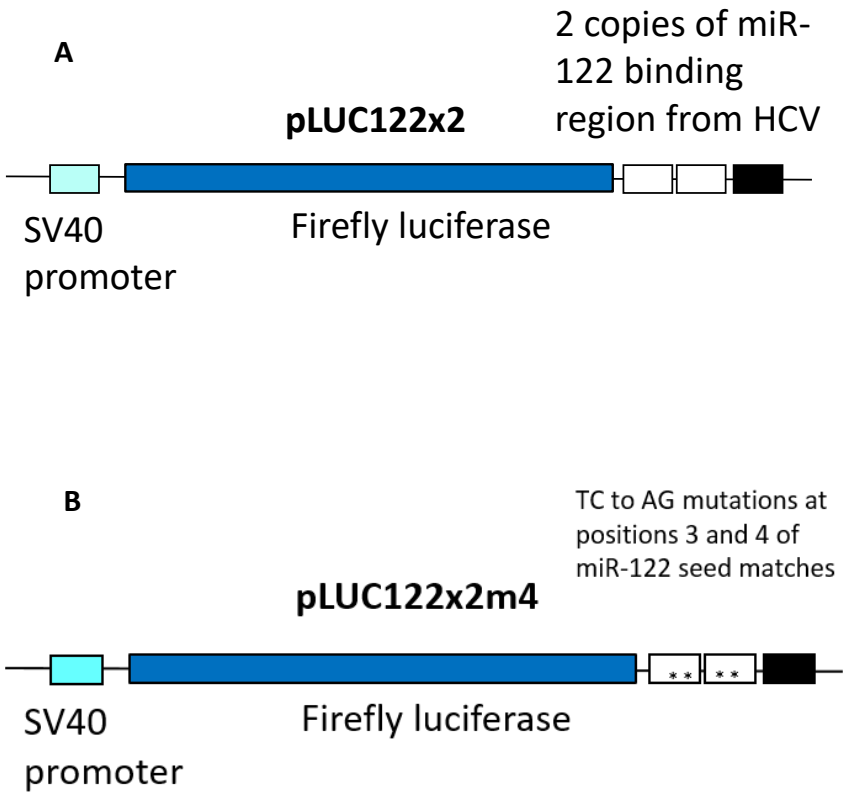

Figure 4-10 Structure of pLuc122x2 and pLuc122x2m4 plasmids

A). The structure of pLuc122x2, which contains 2 copies of the miR-122 binding region (nt 1-45) from the HCV 5' UTR in the 3'UTR of firefly luciferase. **B).** The Luc122x2m4 luciferase reporter containing mutations at positions 3-4 in each of the four miR-122 seed matches.

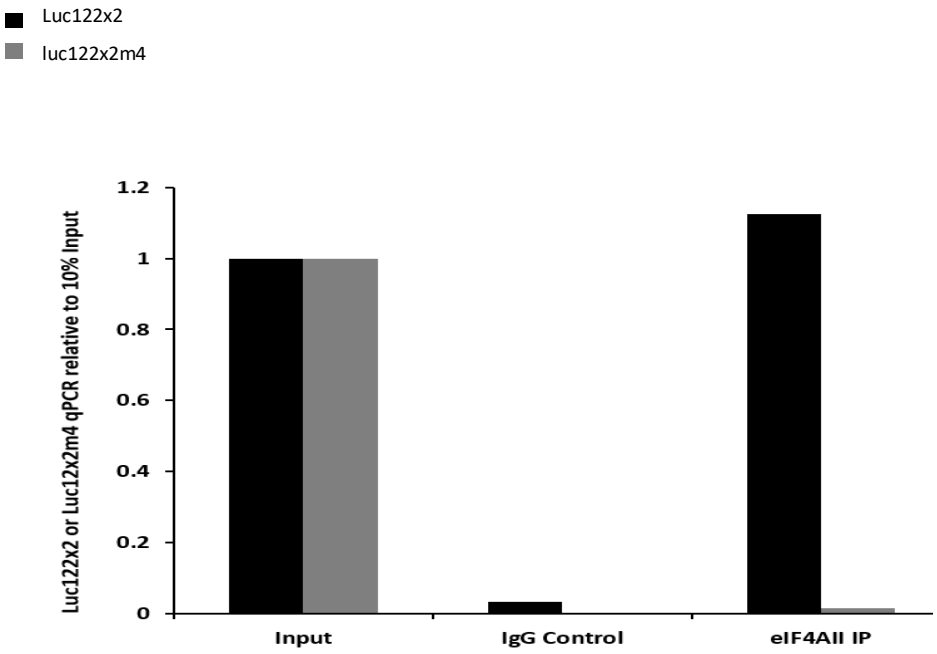

Figure 4-11 miR-122 targeted firefly luciferase associates with eIF4AII

The plasmids pLuc122x2 and pLuc122x2m4 were transfected into Huh7 cells and lysates were immunoprecipitated with an antibody to endogenous eIF4AII. Luciferase mRNA levels were determined by RT-qRT-QPCR in eIF4AII IPs or in IgG control IP relative to 10% input. The figure represents data from a single biological repeat.

4.2.10 The eIF4AII-miR-122 interaction is maintained in the absence of HCV RNA

To check whether the eIF4AII and miR-122 interaction is maintained in Huh7 cells transfected with luc122x2 (a luciferase reporter containing 2 miR-122 binding sites in the 3'UTR), and luc122x2m4 plasmids were transfected into Huh7 cells and immunoprecipitation carried out as described in the above section (4.2.9). RNA was purified and miR-122 levels were measured by RT-qRT-QPCR in eIF4AII IP and IgG control relative to 10% input. Figure 4-14 A shows that eIF4AII was binding to higher amounts of miR-122 compared to the IgG control. This indicates that eIF4AII not only interacts with RNA when miR-122 binding sites are present in the HCV 5'UTR, but it also interacts when miR-122 binding sites are present at 3'UTR of target mRNA (luciferase mRNA). Mutation at the miR-122 seed match position 3 and 4 has been reported to abolish the miR-122 binding to the binding sites (CLJ paper). When cells were transfected with luc122x2m4, the RT-qRT-QPCR result showed a decrease in miR-122 binding with eIF4AII (figure 4-14 B). Although the result shows that loss of miR-122 binding to its target results in decrease in eIF4AII interaction and eIF4AII interacts with miR-122 when miR-122 binds to its target, but as this data is form a single experiment, it is not possible to dram a frim conclusion. It is possible that low levels of luciferase RNA and miR-122 in luc122x2m4 eIF4AII IPs could be due to the loss of sample (figure 4-13, 4-14).

There results expand the previous findings indicating that eIF4AII associates with other miR-122 targets in addition to HCV RNA.

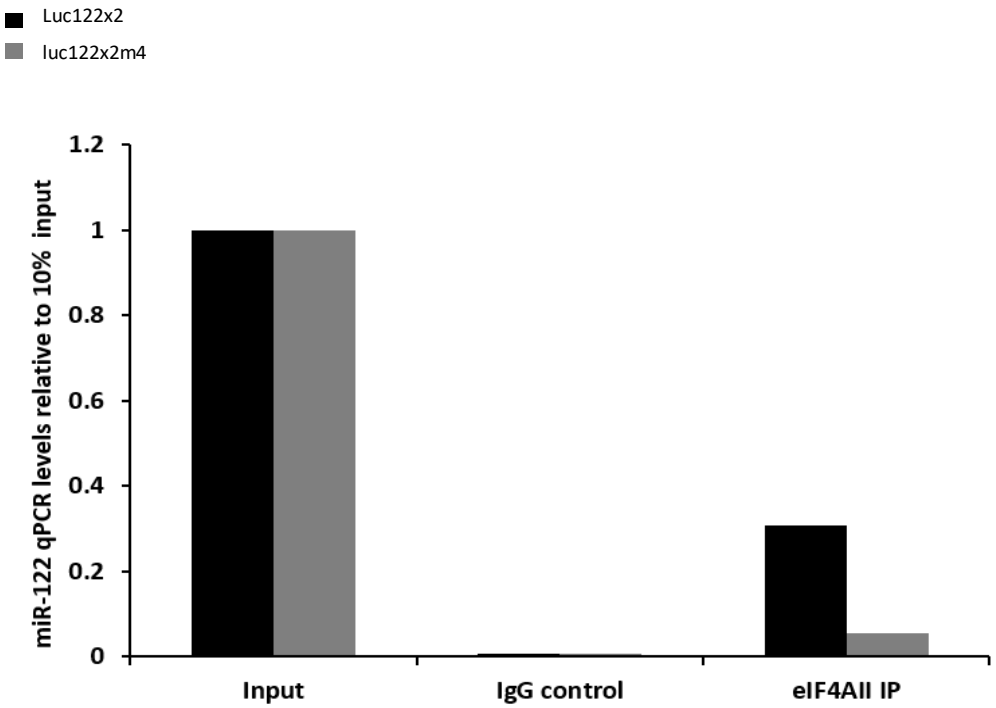

Figure 4-12 miR-122 association with eIF4AII following transfection of luciferase plasmids.

miR-122 levels in eIF4AII IP relative to 10% input in lysates of Huh7 cells transfected with pLUC122x2 and pLUC122x2m4.

4.2.11 Effects of eIF4AI and eIF4AII knockdown on eIF4AII IP

After establishing that eIF4AII is binding to HCV RNA and miR-122 in a miR-122 dependent manner, siRNA-mediated knockdown of eIF4AI and eIF4AII was performed. The rationale of these experiments was that if eIF4AII is interacting with HCV RNA and mIR-122, then the knockdown of eIF4AII should result in a decrease of HCV RNA and miR-122 in eIF4AII IPs.

4.2.11.1 eIF4AI knockdown effects on HCV RNA and miR-122 levels in eIF4AI IP

Huh7 5B replicon cells were seeded into 10 cm plates and the next day the eIF4AI knockdown was performed by siRNA transfection in one plate, while another plate was used as a control in which scrambled siRNA with no target was transfected. After 48 hours of siRNA transfection, the cells were subjected to an overnight eIF4AI IP or an IgG control. Next day RNA was extracted and RT-qPCR was performed to determine the HCV RNA and miR-122 RNA levels.

The HCV RNA levels in control (no eIF4AI knockdown) in eIF4AI IP were very low so it was not possible to measure and compare the effect of eIF4AI knockdown (data not shown). Similarly, there was no difference detected between the miR-122 levels in normal and eIF4AI knockdown cells (data not shown). This could be either due to the fact that there is no enrichment of HCV RNA in eIF4AI IP or due to the fact that eIF4AI IP did not work.

4.2.11.2 HCV RNA levels do not change in eIF4AII IPs in eIF4AI knockdown cells

Suppression of eIF4AI has been suggested to result in increased eIF4AII mRNA and protein levels (Galicia-Vazquez, Cencic et al. 2012). The results described in this chapter and in chapter 3 indicate the potential role of eIF4AII in HCV regulation. So, the cell lysates described in above section (4.2.11.1) were subjected to immunoprecipitation by eIF4AII antibody to see the effect of eIF4AI knockdown on eIF4AII with HCV RNA and miR-122.

Figure 4-15 represent the data from at least seven independent replicates. The bar graph represents HCV RNA levels in control (black bars) and eIF4AI knockdown (grey bars) cells in eIF4AII IPs. In control conditions, eIF4AII shows significantly high binding to HCV RNA compared to IgG control ($P<0.05$). There was no difference in HCV RNA levels in eIF4AII IPs in control and eIF4AI knockdown cells. The actual increase in eIF4AII mRNA and protein expression in eIF4AI knockdown cells were not observed by western blot parallel to this experiment but effective knockdown of eIF4AI by siRNA has been already shown in (chapter 3 Figure 3-1)

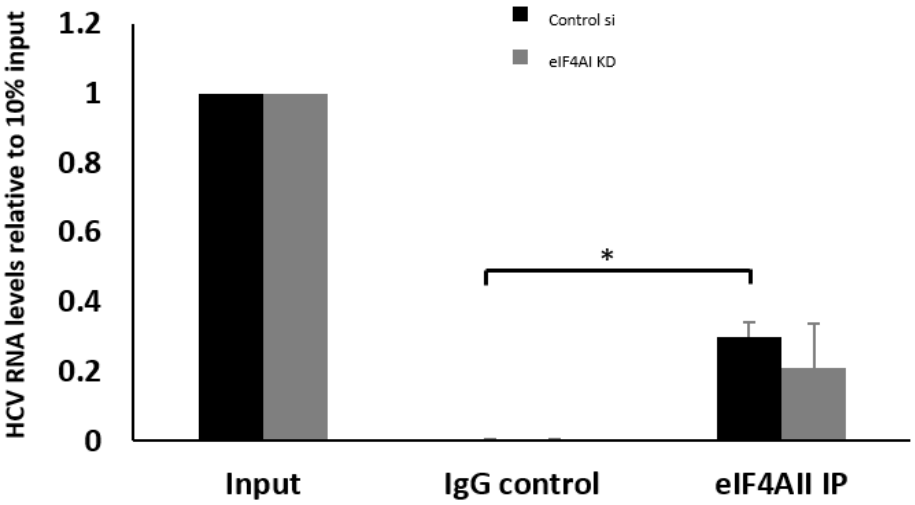

Figure 4-13 eIF4AI knockdown does not affect association of eIF4AII with HCV RNA

5B cells were transfected with a non-targeting control siRNA or an eIF4AI specific siRNA, followed by immunoprecipitation by eIF4AII antibodies or IgG control. The figure represents the HCV RNA levels in control cells (black bars) and eIF4AI knockdown cells (grey bars) relative to 10% input. Data are the mean of seven independent experiments, and the error bars represent SD. *P<0.05 (Student's t test).

4.2.11.3 miR-122 levels appear higher in eIF4AII IP in eIF4AI knockdown cells

As described above in section 4.2.11.2, knockdown of eIF4AI did not change the level of HCV RNA in eIF4AII IPs. To study the effect of eIF4AI knockdown on miR-122 association with eIF4AII, qRT-QPCR of miR-122 was also performed on RNA from eIF4AII IPs in eIF4AI knockdown cells.

Figure 4-16 represents the miR-122 Rt-qRT-QPCR levels in eIF4AII IPs in eIF4AI knockdown cells. The data represent at least seven biological repeats. The black bars represent the miR-122 levels in control cells while the grey bars represent miR-122 in eIF4AI knockdown cells. Although the knockdown of eIF4AI results in an increase in miR-122 levels in eIF4AII IPs compared to the control cells, due to the high error between the experiments, it is not statistically significant.

The results shown in section 4.2.11.2 and 4.2.11.3 show that the knockdown of eIF4AI does not affect HCV RNA in eIF4AII IPs, but may lead to an increase in miR-122 association with eIF4AII.

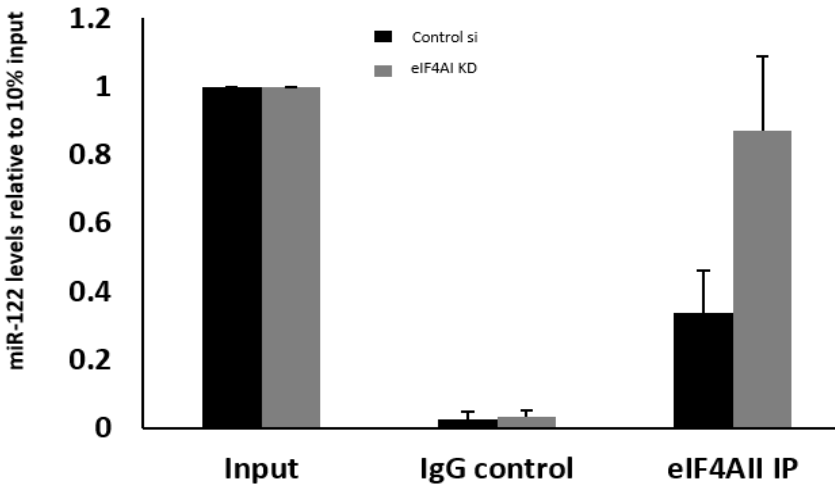

Figure 4-14 miR-122 association with eIF4AII is increased following eIF4AI knockdown.

The figure represents the miR-122 levels in eIF4AII IPs in control (black bars) and eIF4AI knockdown (grey bars) 5B cells relative to 10% input. The data is representative of at least seven independent biological replicates. The error bar is SD.

4.2.11.4 eIF4AII knockdown reduces HCV RNA levels in eIF4AII IP

To study the effect of eIF4AII knockdown on HCV RNA and miR-122 interaction with eIF4AII, cells were plated into 10 cm plates and transfected with either scrambled siRNAs or eIF4AII specific siRNA to knock down eIF4AII, as described in the previous section (4.2.11.1). After 24 hours, the cells were lysed and subjected to overnight IP with eIF4AII antibodies while IgG was used as control. After immunoprecipitation, RNA was extracted and RT-qRT-QPCR was used to determine the HCV RNA and miR-122 levels in the control and eIF4AII knockdown cells.

Figure 4-17 represents HCV RNA levels in eIF4AII IP or IgG control IP relative to HCV RNA level in input. The eIF4AII binding to HCV RNA compared to IgG control indicates that eIF4AII does interact with HCV RNA, as previously shown in figures 4-9 and 4-15. HCV RNA levels significantly decrease in eIF4AII IP when eIF4AII is knocked down (figure 4-17). The loss of the HCV RNA in the absence of eIF4AII in eIF4AII IPs confirms that the eIF4AII antibody immunoprecipitates the correct protein, and clearly indicates that eIF4AII and HCV RNA interact with each other.

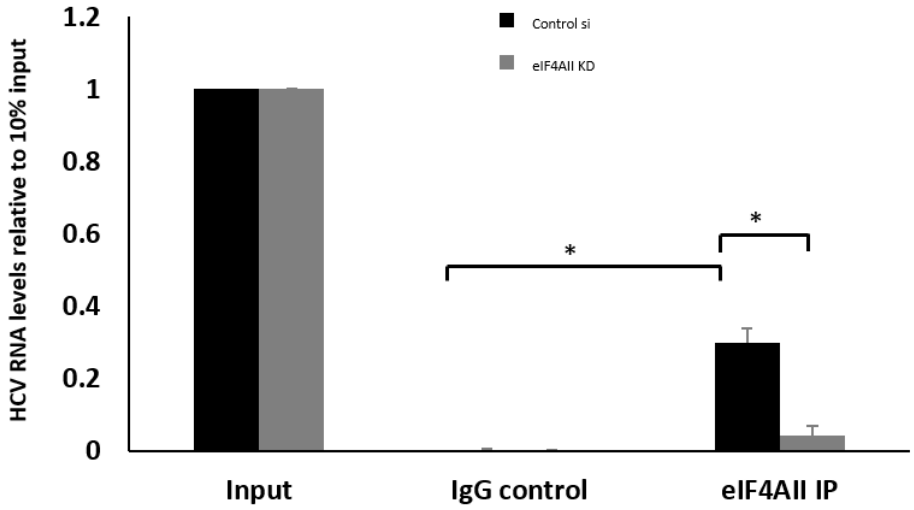

Figure 4-15 Reduction in HCV RNA in eIF4AII IP following eIF4AII knockdown shows that the antibody is specific

5B cells were either transfected with a non-targeting control siRNA or with an eIF4AII specific siRNA, and lysates were immunoprecipitated with eIF4AII antibodies or a normal mouse IgG control. HCV RNA levels were determined by RT-qRT-QPCR in IP relative to 10% input. Black bars show data from control siRNA-treated cells, while the grey bars show data from eIF4AII knockdown cells. The figure represents the data from at least five independent replicates. The error bars represent the SD. *P<0.05

4.2.11.5 Knockdown of the eIF4II reduces miR-122 levels in eIF4AII IPs

After the confirmation that eIF4AII interacts with HCV RNA and that this interaction is lost in the absence of eIF4AII, the same strategy of eIF4AII knockdown followed by eIF4AII immunoprecipitation was applied to study the effect of depletion of eIF4AII on miR-122 binding with eIF4AII.

In normal conditions when eIF4AII is present, miR-122 shows significantly high binding to eIF4AII (figure 4-18 black bars) compared to IgG control. This is similar to what already presented in previous sections (4.2.4 and 4.2.7). When eIF4AII is depleted by siRNA transfection, miR-122 levels in eIF4AII IPs significantly decrease compared to miR-122 levels in cells containing eIF4AII (figure 4-18 grey bars). The significant levels of miR-122 in eIF4AII IP and loss of miR-122 levels in the absence of eIF4AII confirms that eIF4AII interacts with miR-122.

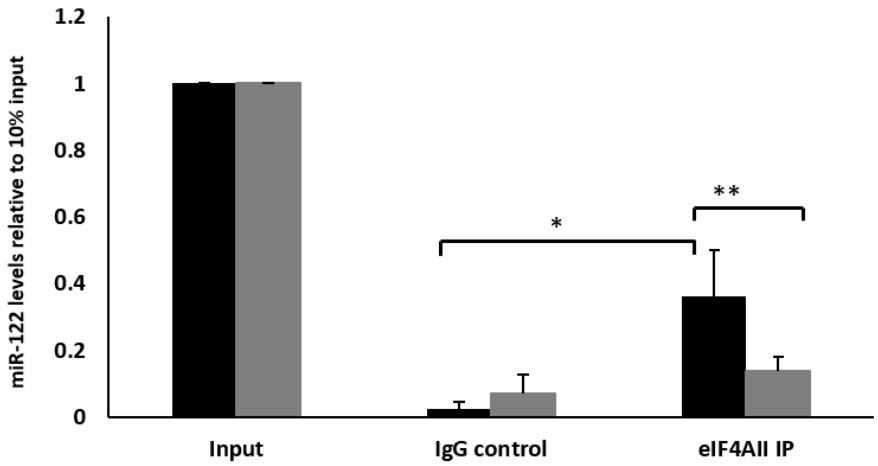

Figure 4-16 miR-122 association with eIF4AII is reduced by eIF4AII knockdown.

miR-122 levels were determined by RT-qRT-QPCR in eIF4AII IPs of cells transfected with control siRNA (black bars) or eIF4AII siRNA (grey bars), relative to 10% input. The data is representative of at least five independent biological replicates. The error bars represent SD. *P<0.05, **P<0.01 (Student t.test)

4.2.12 Knockdown of the Ccr4-Not complex subunit CNOT1 reduces the level of HCV RNA and miR-122 in eIF4AII IPs

As described in the introduction of this chapter, the Ccr4-Not complex subunit CNOT1 binds to eIF4AII (Meijer, Kong et al. 2013). A potential role for CNOT1 in eIF4AII interactions with HCV and miR-122 was investigated.

In parallel to the eIF4AI and eFI4AII knockdown experiments described above, CNOT1 was also depleted by a specific siRNA in replicon cells and eIF4AII IP carried out. The RNA was purified and the HCV RNA and miR-122 levels were determined by qRT-QPCR as described in previous IP experiments.

The figure 4-19 represents HCV RNA RT-qRT-QPCR data from at least four independent biological replicates in eIF4AII IPs in CNOT1 knockdown cells. In control cells (in the presence of CNOT1, black bars), eIF4AII showed significantly higher levels (P=0.02) of HCV RNA association compared to IgG control. The knockdown of CNOT1 resulted in reduction of HCV RNA in eIF4AII IPs, but this difference was not statistically significant (P= 0.067). However, the level of HCV RNA in CNOT1 knockdown eIF4AII IPs was 80% less than HCV RNA levels in the presence of CNOT1. This large difference suggests that CNOT1 has a role in eIF4AII binding to HCV RNA, possibly due to a direct interaction with eIF4AII.

After measuring the HCV RNA level in control and CNOT1 knockdown cells in eIF4AII IPs, miR-122 levels in eIF4AII IPs in CNOT1 knockdown and control cells were also measured (figure 4-20).

miR-122 levels in eIF4AII IPs in CNOT1 knockdown cells were significantly lower (p=0.019) than the miR-122 levels in control cells (figure 4-21 B). This indicates that CNOT1 is contributing to eIF4AII binding or interaction with both HCV RNA and miR-122. Both the HCV RNA and miR-122 qRT-QPCR levels in eIF4AI IPs in CNOT1 knockdown cells were also determined and there was no difference in both HCV RNA and miR-122 in both groups (data not shown).

Together, these results indicate that Ccr4-Not complex subunit CNOT1 has a role in eIF4AII association with both HCV RNA and miR-122.

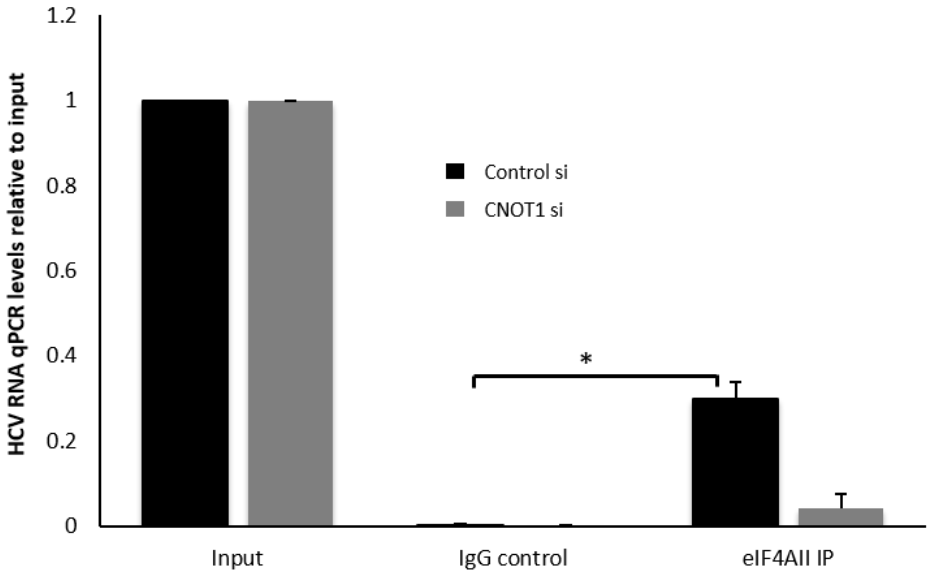

Figure 4-17 Association between HCV RNA and eIF4AII is reduced by CNOT1 knockdown

5B cells were treated with a non-targeting control siRNA or an siRNA specific to CNOT1 and HCV RNA was harvested 48hrs post transfection. HCV RNA levels were determined by RT-qRT-QPCR eIF4AII IPs of lysates of control cells (black bars) or CNOT1 knockdown cells (grey bars) relative to 10% input. The data is representative of at least four biologically independent replicates. The error bars show the SD, while t.test was used to determine the level of significance. *P<0.05

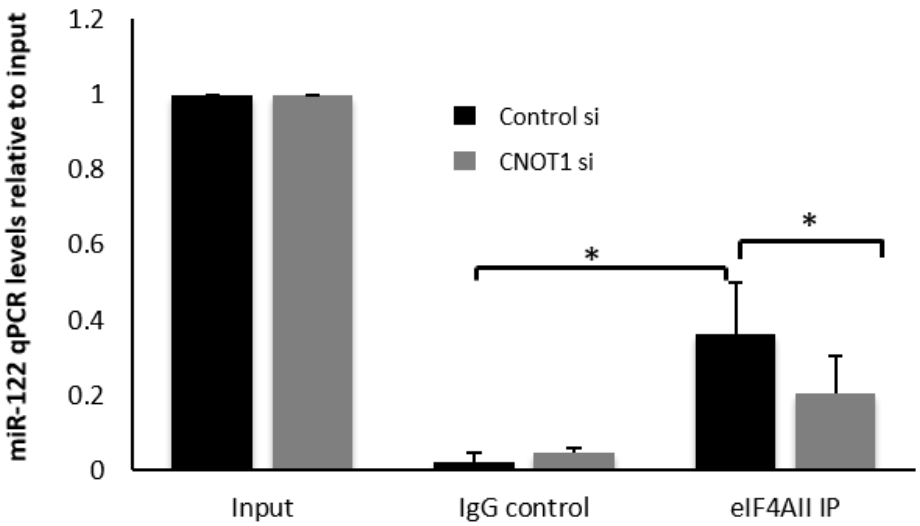

Figure 4-18 miR-122 association with eIF4AII is reduced by CNOT1 knockdown

miR-122 RNA levels were determined by RT-qRT-QPCR in eIF4AII IPs of lysates of 5B cells treated with control siRNA (black bars) or CNOT siRNA (grey bars), relative to 10% input. The data is representative of at least four biologically independent replicates. The error bars show the SD. *P<0.05 (t.test)

4.3 Discussion

The methods, approaches and results presented here in this chapter demonstrate successful immunoprecipitation of the HCV RNA and liver specific microRNA-122 with endogenous eIF4AII. The IP results also show binding of the endogenous eIF4AII with two other microRNAs, miR-21 and miR-26a, which are also present in liver. Having more than 90% sequence homology with eIF4AII, eIF4AI IP was also performed to see if there was also an interaction between eIF4AI and HCV RNA or miR-122. The results from immunoprecipitation of the HCV RNA and miR-122 by endogenous eIF4AI do not show any interaction or binding of this homolog. Taken together, these results indicate that the eIF4F component eIF4AII but not eIF4AI is interacting with both HCV RNA and miR-122. This also supports the results from recent past studies suggesting that eIF4AI and eIF4AII might have different functions. The suppression of eIF4AI has been suggested to increase the mRNA and protein level of eIF4AII without reciprocating the function of eIF4AI (Galicia-Vazquez, Cencic et al. 2012). So to study the effect of eIF4AI knockdown on HCV RNA and miR-122 association with eIF4AII, HCV RNA and miR-122 level were also measured in eIF4AII IPs in eIF4AI knockdown cells. The results from these IPs show that there is no increase in HCV RNA levels bound to eIF4AII but miR-122 association increase in eIF4AII in eIF4AI KD cells (figure 4-15 and 4-16). This could be due to the eIF4AII binding with different complexes but due to the lack of statistical significance it is not possible to draw and definite conclusion. Furthermore,

due to the lack of western blot data, the increase in eIF4AII expression in eIF4AI knockdown cells was also not confirmed. In another study eIF4AII, but not eIF4AI, has been shown to be involved in microRNA based repression of protein expression (Meijer, Kong et al. 2013). These studies and our finding indicate that although eIF4AI and eIF4AII have more than 90% homology, they have different functions.

miR-122 binds to two sites in the 5' UTR of HCV RNA and results in an increase in HCV RNA abundance (Jopling, Yi et al. 2005). In the previous chapter, it was shown that knockdown of eIF4AII leads to a decrease HCV RNA. In this chapter immunoprecipitation was performed with FLAG tagged eIF4AI and eIF4AII to investigate whether HCV RNA and miR-122 interact with eIF4A proteins or not, but unfortunately the FLAG-eIF4AI and FLAG-eIF4AII IPs did not work and HCV RNA and mir-122 interaction with eIF4AI and or eIF4AII could not be measured. There could be several reasons that FLAG-IPs failed to detect HCV RNA and miR-122, but this was not further investigated as the endogenous IPs were effective and a more biologically valid approach. Antibodies to the endogenous eIF4AI and eIF4AII proteins were used to determine the interaction between eIF4A proteins, HCV RNA and mIR-122 in the HCV replicon cells. The results of endogenous eIF4AI and eIF4AII IPs presented in this chapter show that eIF4AII but not eIF4AI binds to both HCV RNA and miR-122. Furthermore, when miR-122 was inhibited with miR-122 2' OMe inhibitor, the HCV RNA levels in endogenous eIF4AII IP were reduced which suggests that the association of eIF4AII with HCV RNA and miR-122 is miR-122 dependent. These results suggest that these three

molecules are part of the same complex. It would be very important to verify these results in different HCV system like full length HCV and live HCV virus infection. Full length HCV RNA was transfected into Huh7 cells but the IP results could not detect HCV RNA and miR-122 with eIF4AII. Due to the lack of time this experiment was not further optimized and repeated, which could limit the finding of Huh7 5B HCV replicon system. It would be very important to verify these results in other HCV replicon systems and by using other methods like *in vitro* binding assays.

The luciferase reporter RNA containing four miR-122 binding sites (from the HCV 5' UTR) in the 3' UTR was used to study the effect of location of miR-122 binding sites on eIF4AII binding. The reporter RNA was immunoprecipitated with endogenous eIF4AII antibodies in the presence of miR-122. The lack of association of the luciferase mRNA with mutant miR-122 binding sites results suggested that the ability of eIF4AII to bind to target RNA is dependent on miR-122 binding. It also indicates that eIF4AII also associates with miR-122 targets other than HCV RNA. More repeats are required to support these findings and the lack of enough reproducible data is a major limitation of these results.

It has been shown that eIF4AII is required for miRNA-mediated repression of protein translation and that Ccr4-Not complex subunit CNOT1 is required for eIF4AII binding to HCV RNA (Meijer, Kong et al. 2013). To study the effect of CNOT1 on HCV RNA and miR-122 binding with eIF4AII, siRNA-mediated knockdown of CNOT1 was performed and the HCV RNA and miR-122 levels

were measured in eIF4AI and eIF4AII IPs. Surprisingly, the knockdown of CNOT1 strongly decreases the miR-122 and the HCV RNA levels in eIF4AII IPs compared to the levels in control cells, but the levels were not affected in eIF4AI IPs. This could also indicate the interaction of eIF4AII with Ccr4-Not complex.

All the results presented in this chapter suggest that eIF4AII is involved in miR-122-mediated regulation of the HCV virus through its binding with HCV RNA and miR-122. In the next chapter a new approach to analyse the eIF4AII involvement in Hepatitis C virus regulation using reporter assays will be described.

5 Interplay between eIF4AII and miR-122 in HCV regulation

5.1 Introduction

In chapter 3 it was shown that eIF4AII regulates HCV, and eIF4AII was also shown to regulate miRNA activity (Meijer, Kong et al. 2013). The major question is whether it regulates HCV by controlling the activity of miR-122. Immunoprecipitation (IP) data presented in the previous chapter identifies a miR-122 dependent interaction between eIF4AII and HCV. This would support the above hypothesis, but does not test it directly. The effects of eIF4AII knockdown on HCV replication were also studied by combining the eIF4AII knockdown with inhibition or overexpression of miR-122 (chapter 3, figure 3-7). Inhibition or overexpression of miR-122 in eIF4AII depleted cells does not affect the HCV RNA level, which suggests that miR-122 regulation of HCV is dependent on eIF4AII. In this chapter, the role of eIF4AII in HCV regulation and how this relates to regulation by miR-122 is studied further. Different techniques were used, with luciferase reporter assays used to study the role of eIF4AI, eIF4AII and miR-122 in HCV translation, immunofluorescence (IF) to study the cellular localization of eIF4AII, HCV RNA and miR-122, and polysome profiling of whole cell lysates to study the effects of eIF4AII on miR-122-mediated activation of HCV translation.

5.2 Results

5.2.1 Effects of eIF4AII knockdown on luciferase activity in reporter containing miR-122 binding sites in 3'UTR in HCV replicon cells

To investigate the effect of eIF4AII on luciferase reporter expression in the N/Neo C-5B (5B) HCV replicon system, the cells were transfected with a reporter plasmid (pLUC122x2) in which firefly luciferase is flanked by four miR-122 binding sites from HCV 5'UTR in the 3'UTR (figure 4-12) and a *Renilla* luciferase transfection control plasmid. Luciferase expression from this reporter is repressed by miR-122 binding sites in the 3'UTR. 5B cells were seeded into plates and the following day siRNA transfection was performed to knock down eIF4AII. After 48 hours, a second transfection was performed to introduce the luciferase reporter (pLUC122x2) with miR-122 overexpression (pre-miR-122) or inhibition (miR-122 2'OMe), while random 2' OMe and pre-122p3+4 were used as control oligonucleotides as described previously in chapter 4 section 4.2.9. Cells were lysed in passive lysis buffer and a dual luciferase assay was performed to determine the firefly and *Renilla* luciferase activity in eIF4AII depleted and control cells.

Figure 5-1 represents the firefly luciferase activities relative to renilla control in eIF4AII depleted and control cells, during miR-122 inhibition (122 2'OMe), overexpression (pre-miR-122) and in control (Rand-2'OMe, pre-miR-122p3+4) treated cells that have endogenous miR-122 levels. In control oligonucleotide treated cells, the knockdown of eIF4AII significantly ($P<0.05$) increases firefly luciferase activity relative to Renilla luciferase activity. This

could be due to an increase in protein production from the reporter or a decrease in Renilla luciferase translation. In the absence of miR-122 (122 2'Ome), firefly/renilla luciferase activity increased compared to the Rand-2'OMe control, as expected due to the relief of miR-122 inhibition of the reporter. eIF4AII knockdown further increased the firefly/renilla luciferase ratio, similar to control conditions. The overexpression of miR-122 (pre-miR-122) decreases the firefly luciferase level in both untreated (control si) and eIF4AII depleted cells, as expected due to miR-122-mediated repression of the reporter. However, there is very little effect of eIF4AII knockdown in miR-122 overexpressed condition. This could suggest that maybe eIF4AII does have a role in miR-122 function, perhaps at the level of recruitment, and if sufficient miR-122 is present following pre-miR-122 transfection, the requirement for eIF4AII is overcome. In cells transfected with pre-miR-122, the knockdown of eIF4AII also significantly increases ($P<0.05$) luciferase production from the reporter, but this increase is very small.

The increase in firefly/renilla luciferase ratio following eIF4AII knockdown in miR-122 depletion (122 2'OMe) suggest that eIF4AII has a miR-122 independent effect, or it could also be due to a decrease in renilla control expression. There was also a similar increase in firefly luciferase in the presence and absence of miR-122 in eIF4AII knockdown cells. These data suggest that eIF4AII does not affect miR-122 repression via 3'UTR sites, in contrast to previous findings with different miRNAs (Meijer, Kong et al. 2013). These results also show that miR-122 acts like a canonical microRNA

with respect to repression when miR-122 binding sites are present in 3' UTR of the target genes as described previously (Jopling, Schutz et al. 2008).

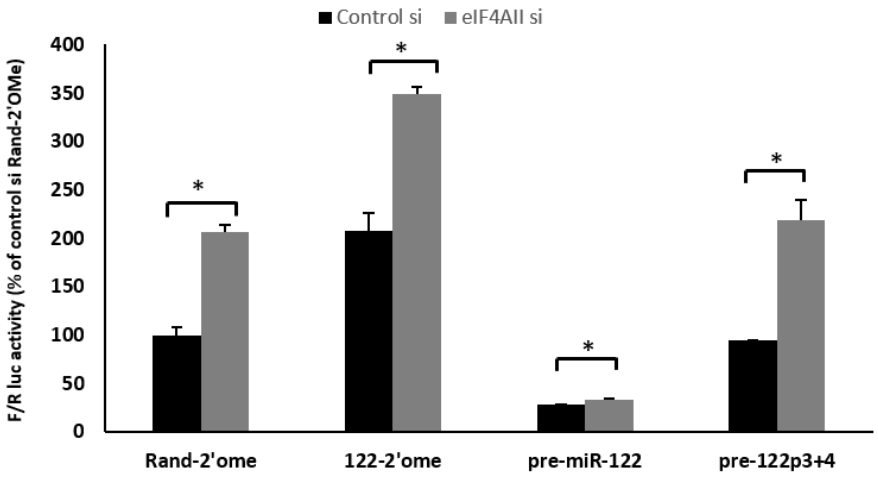

Figure 5-1 Knockdown of eIF4AII increases luciferase activity in reporter containing miR-122 binding sites in 3'UTR

Huh7 5B cells were treated with control or eIF4AII siRNA and after 48hrs pLuc122x2 together with Rand- 2'ome or 122 2'ome, pre-miR-122 or pre-122p3+4 were transfected. Firefly luciferase activity relative to renilla luciferase control is shown in the presence (Rand-2'OMe, pre-miR-122 and pre-122p3+4) and absence (122 2'OMe) of miR-122 in control and eIF4AII depleted cells. The black bars represent luciferase expression in control cells while grey bars represent levels in eIF4AII depleted cells. The figure represents data from at least three independent experiments. Error Bars represent the standard deviation (SD). Level of significance was measured by Student's t test where *P<0.05.

5.2.2 Effects of eIF4AI knockdown on luciferase reporter containing miR-122 binding sites in 3'UTR

The effect of eIF4AI knockdown on the pLUC122x2 luciferase reporter in HCV replicon cells was also investigated. Luciferase expression was measured in eIF4AI knockdown cells in the presence of endogenous (Rand-2'OMe and pre-122p3+4), overexpressed (pre-miR-122) and in the absence (122 2'OMe) of miR-122.

Figure 5-2 represents the data from at least three independent experiments. The knockdown of eIF4AI results in significant increase ($P<0.05$) in luciferase expression in all treatment groups. These results are similar to the result in above section (5.2.1). It is also observed that the presence or absence of miR-122 leads to similar changes in reporter luciferase expression in control, eIF4AI and eIF4AII depleted cells. This suggests that the eIF4A protein knockdown has a miR-122 independent, general effect on firefly and/or *Renilla* translation.

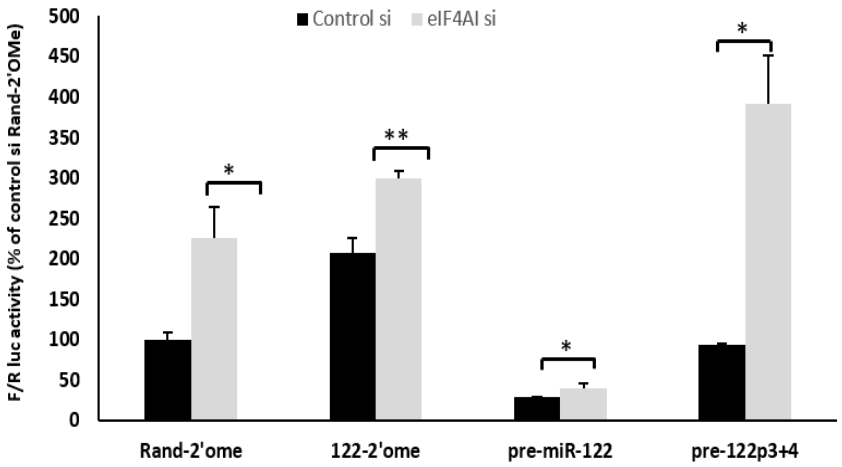

Figure 5-2 Knockdown of eIF4AI increases luciferase activity in reporter containing miR-122 binding sites in 3'UTR

Huh7 5B cells were treated with control or eIF4AI siRNA and after 48hrs pLuc122x2 together with Rand- 2'ome or 122 2'ome, pre-miR-122 or pre-122p3+4 were transfected in the cells. The bars represent the firefly luciferase activities relative to renilla luciferase control in control and eIF4AI knockdown cells in the presence (Random 2' OMe and pre-122 p3+4), absence (122-2' OMe) and overexpression (pre-miR-122) of miR-122. Error Bars represent the standard deviation (SD). Level of significance was measured by Student's t test where *P<0.05, **P<0.01.

5.2.3 Knockdown of eIF4AII increases luciferase activity from pLUC122x2 independent of miR-122 regulation in Huh7 cells

The presence of HCV RNA has been shown to sequester miR-122 which helps HCV propagation by de-repression of miR-122 targets (Luna, Scheel et al. 2015). So, to study the possible competition between HCV RNA and luciferase reporter for miR-122, and effect of eIF4AI and eIF4AII on this competition, the effects of eIF4A knockdown on luciferase expression from pLUC122x2 were also investigated in Huh7 cells that do not contain an HCV replicon. Luciferase expression was increased in eIF4AII and eIF4AI knockdown cells in the presence or absence of miR-122 in Huh7 cells (figure 5-3A and 5-3B). There was no cell specific difference observed in eIF4AI and eIF4AII depleted cells as the effects of eIF4AI and eIF4AII knockdown are similar in Huh7 (figure 5-3) and 5B cells (figures 5-1 and 5-2). One interesting observation is that pre-miR-122 reduces firefly luciferase activity more strongly in 5B cells then Huh7 cells (repression down to ~30%, compared to ~80%).

Together, the data from eIF4AI and eIF4AII depleted HCV replicon and Huh7 cells suggest that the knockdown of both eIF4AI and eIF4AII result in a miR-122 independent increase in firefly/renilla luciferase expression in the presence (HCV replicon cells) and absence of replicating HCV (Huh7 cells).

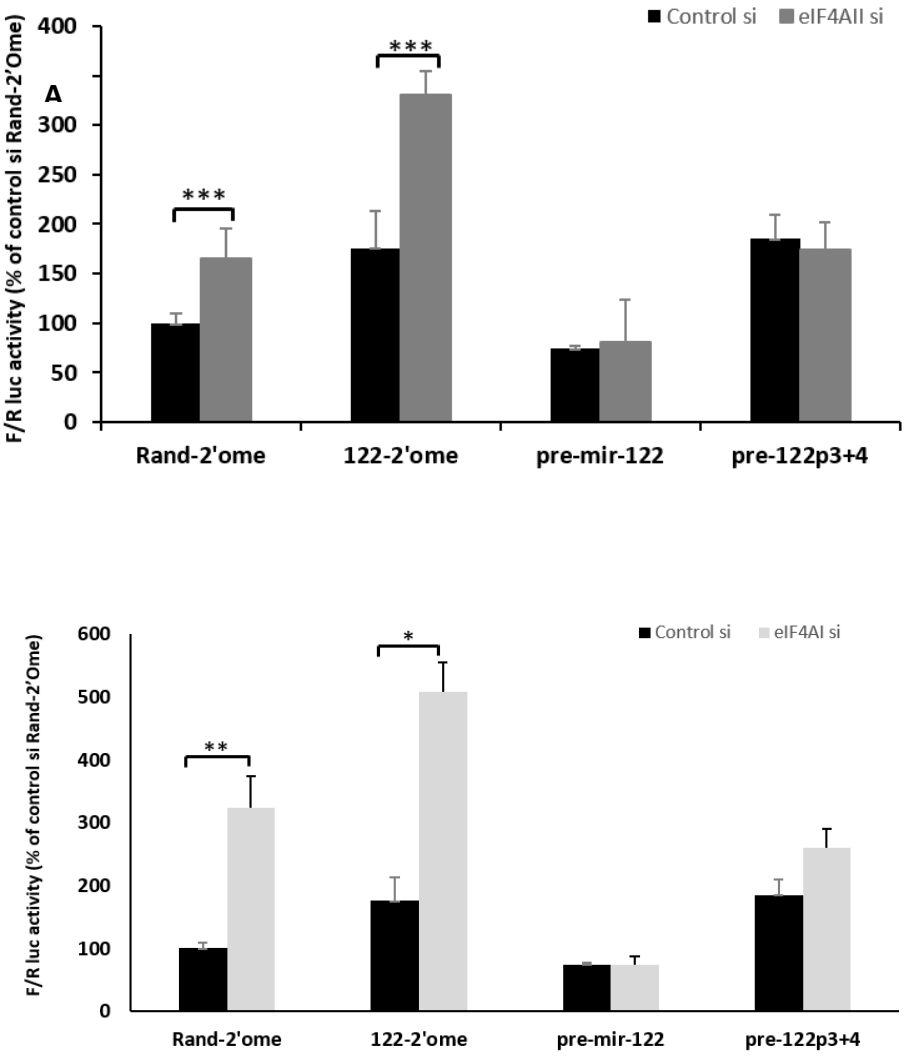

Figure 5-3 Knockdown of eIF4AII and eIF4AI increases luciferase activity in 3'UTR reporter in Huh7 cells

A) The data represents the firefly luciferase activities relative to renilla luciferase control in the presence (Random 2' OMe and pre-122p3+4), absence (122 2'OMe) and overexpression (pre-miR-122) of miR-122 in eIF4AI knockdown cells (light grey bars) compared to control siRNA treated cells (black bars). **B)** as A) except that B represents data from eIF4AII knockdown cells. Both figures represent the data form at least three independent experiments. The error bars represent the standard deviation (SD). Levels of statistical significance was determined by t test where *P<0.05, **P<0.01 and **P<0.001.

5.2.4 Knockdown of eIF4AII reduces miR-122-mediated activation of translation in sub-genomic JFH-1 and Con1b HCV luciferase reporters

After establishing that eIF4AII is not involved in miR-122 mediated repression of luciferase expression in HCV replicon and Huh7 cells, the role of eIF4A proteins, especially eIF4AII, was investigated in the HCV 5'UTR driven luciferase reporter RNA. The bicistronic system contains the firefly luciferase coding region under the control of the HCV 5'UTR while the EMCV IRES drives translation of the NS5B coding region, which is flanked by HCV 3'UTR (figure 5-4A, thanks to Andrew Tuplin and David Evans for kind gift of the plasmids). The HCV sequences are derived from either JFH1 (genotype 2a) or Con1b (genotype 1b) (Tuplin, Struthers et al. 2015). Luciferase production was measured relative to a capped, polyadenylated *Renilla* luciferase RNA transfection control in the presence of endogenous (Rand-2'OMe and pre-122p3+4), absence (122 2'OMe) and overexpressed (pre-miR-122) miR-122 in Huh7 cells.

Figure 5-4 represents luciferase expression from JFH1 and Con1b bicistronic RNAs. The knockdown of eIF4AII reduces the expression of luciferase in both reporters compared to the control siRNA in cells containing endogenous miR-122, although apart from cells overexpressing miR-122 (pre-miR-122) in JFH1 bicistronic system and endogenous miR-122 (pre-122p3+4) in Con1b cells, this reduction was not statistically significant. However, the same

pattern was observed in many independent experiments therefore it strongly suggests that knockdown of eIF4AII decreases the HCV IRES driven activation of luciferase translation. This suggests that eIF4AII regulates HCV, at least in part, at the translation stage of the replication cycle.

In cells containing the JFH1 reporter RNA, eIF4AII depletion appears to reduce luciferase activity to a lesser extent in cells containing the miR-122 inhibitor (122-2'OMe), which could indicate that eIF4AII may be involved in miR-122 based HCV regulation at a translational level, but as it lacks statistical significance, therefore it is difficult to drawn firm conclusion.

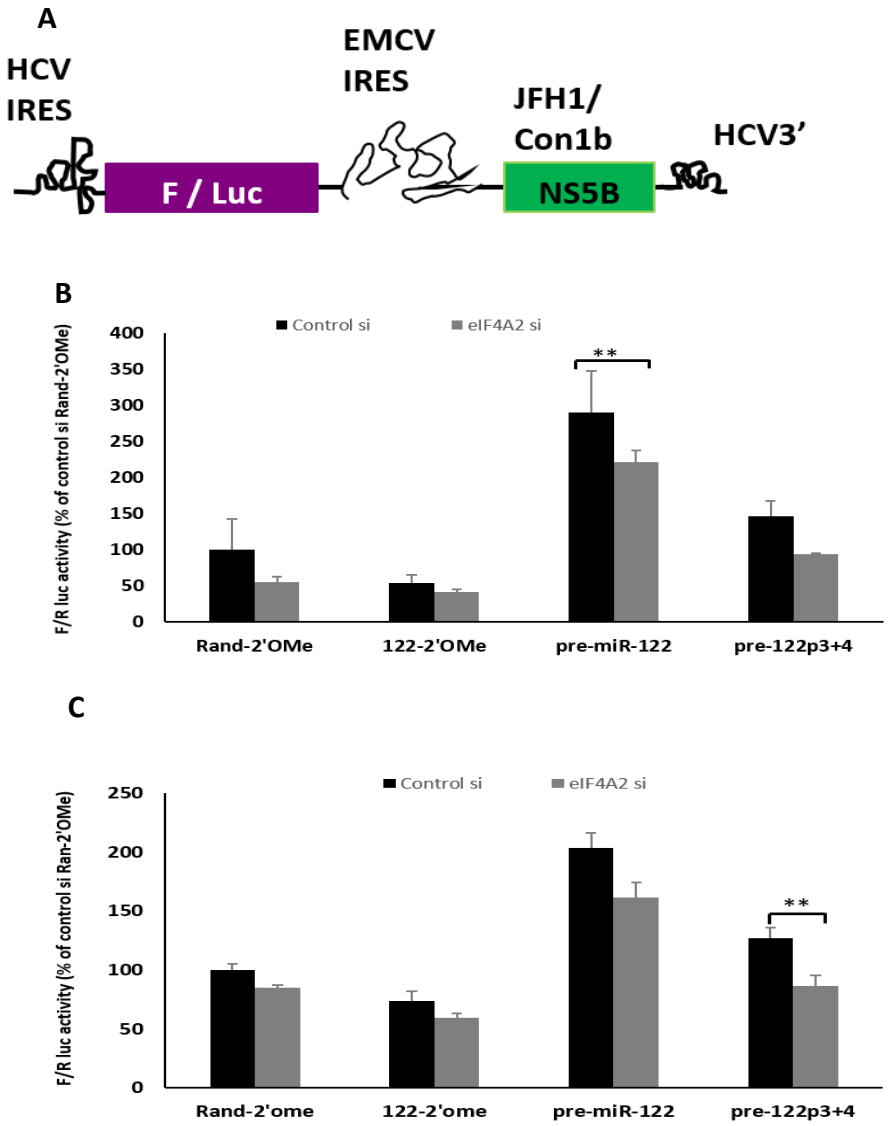

Figure 5-4 eIF4AII contributes to HCV IRES driven translation

A) Bicistronic luciferase reporter RNA containing firefly luciferase under HCV IRES and NS5B region from either JFH1 (genotype 2a) or Con1b (genotype 1b) under the EMCV IRES. **B)** Firefly luciferase expression relative to renilla (4hrs post expression) in JFH1 bicistronic RNA in eIF4AII depleted cells (grey bars) or control siRNA-treated cells (black bars) in the presence (Rand-2'OMe, miR-122p3+4), overexpression (pre-miR-122), and absence (122 2'OMe) of miR-122 in Huh7 cells. **C)** as (B) except the luciferase expression levels are measured in cells transfected with Con1b bicistronic RNA. The data is representative of at least 4 independent experiments. The error bars show the SD. The statistical significance was calculated by t test where ** $P<0.01$.

5.2.5 eIF4AI knockdown does not affect luciferase expression from JFH1 and Con1b bi-cistronic RNA reporters.

After establishing that eIF4AII may slightly contribute to HCV IRES driven translation (5.2.4), the role of eIF4AI was also investigated in HCV IRES driven translation of luciferase. The same experimental approach described in the above section was used.

In contrast to the results described in the above section in eIF4AII knockdown cells (5.2.4), the knockdown of eIF4AI instead slightly increases firefly/renilla luciferase expression in cells with or without miR-122 (figure 5-5A), except for cells containing the Con1b RNA reporter and overexpressing pre-miR-122. Although the increase in luciferase in response to eIF4AI knockdown is not statistically significant, these results were observed in all repeats of this experiment. The knockdown of eIF4AI tends to lead to increase in F/R luciferase ratio in cells transfected with either the 3'UTR reporter plasmid (figures 5-2 and 5-3B) or the HCV 5'UTR-driven reporter RNA (figures 5-5 A & B), but the effects on the plasmid are stronger. This indicates that the effects of eIF4AI are not dependent on presence of miR-122 binding sites at UTRs or on the presence or absence of the HCV IRES in two reporter systems. One possible explanation for these data could be that eIF4AI knockdown leads to a stronger decrease in Renilla than firefly luciferase translation, leading to an overall increase in F/R ratio in both 3'UTR and HCV 5'UTR reporters.

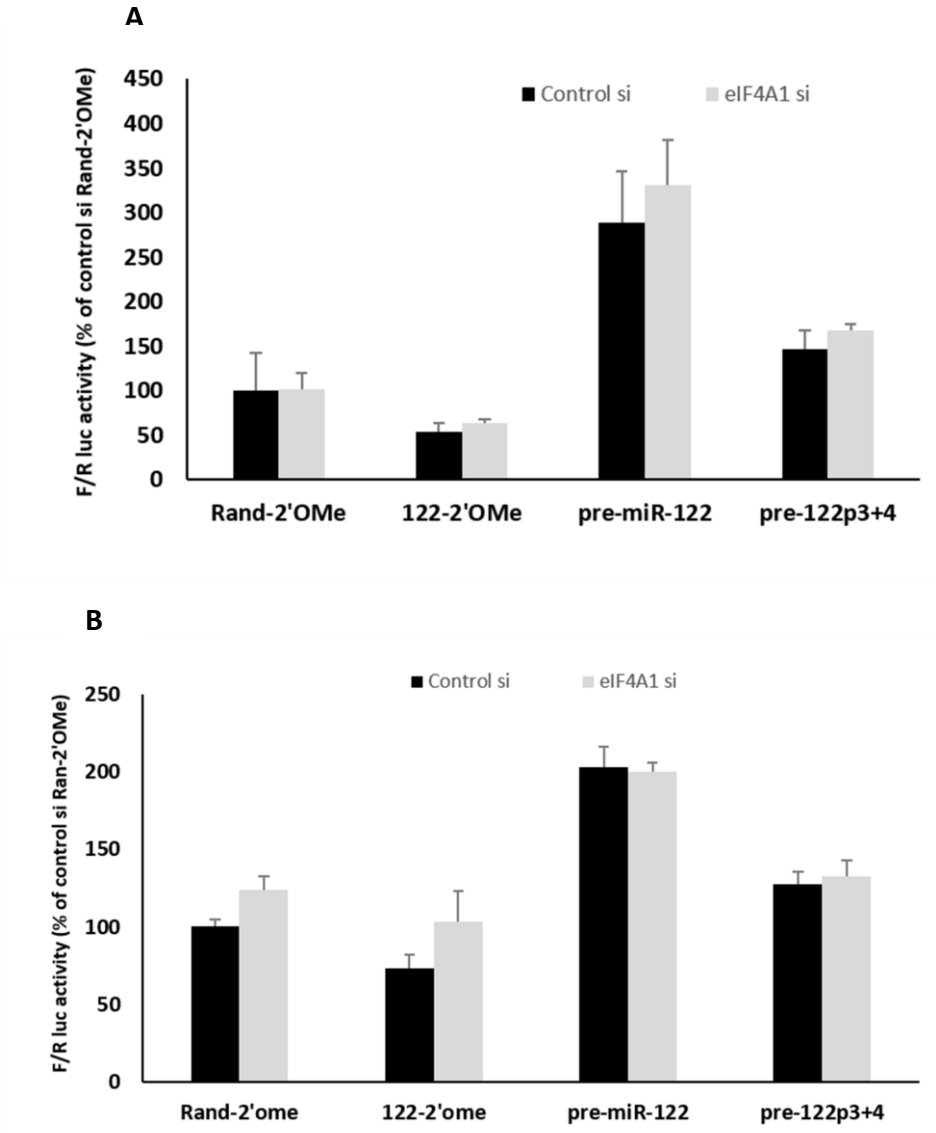

Figure 5-5 eIF4AI knockdown in HCV IRES driven luciferase reporter system

A) Firefly/renilla luciferase expression level in eIF4AI depleted Huh7 cells in the presence (Rand-2'OMe, pre-122p3+4), absence (122 2'OMe) and overexpression (pre-miR-122) of miR-122 following transfection of JFH1 bi-cistronic RNA. **B)** Same as (A) except that the luciferase level is from Con1b type HCV IRES driven luciferase reporter. The data is representative of at least four independent experiments and the error bars show SD.

5.2.6 Effect of eIF4AI and eIF4AII knockdown on HCV IRES and EMCV IRES driven translation of firefly luciferase in bicistronic reporter plasmids

To study the role of eIF4AI and eIF4AII in IRES driven translation, pRHCVF and pREMCVF plasmids were used (Coldwell, Mitchell et al. 2000) (figure 5-6 A). In both plasmids, renilla luciferase is translated in a cap dependent manner while firefly luciferase is translated in either an HCV or EMCV IRES driven manner. The HCV IRES lacks the initial 41 nucleotides which contain two miR-122 binding sites. The EMCV IRES requires eIF4A and eIF4G while HCV IRES has been reported to work without these proteins (Pestova, Shatsky et al. 1998).

Figure 5-6 B shows HCV IRES driven (black bars) or EMCV IRES driven (yellow bars) firefly luciferase translation in control or eIF4AI and eIF4AII knockdown cells relative to cap-dependent renilla luciferase translation. The eIF4AI knockdown shows a 60% ($p=0.051$) increase in HCV IRES driven firefly expression relative to renilla luciferase compared to control cells, while no change in firefly/Renilla expression in eIF4AII knockdown cells was observed. eIF4AI knockdown did not change the firefly expression under EMCV IRES compared to cap-dependent Renilla luciferase, while the reduction of firefly/renilla luciferase activity in eIF4AII knockdown was not significant but the clear increase suggest that this knockdown is likely to be a biological effect. These results suggest that, as the HCV IRES does not require eIF4AI, the increase in firefly/renilla expression observed could be due to the decrease in cap dependent Renilla expression in eIF4AI knockdown cells.

There was no difference observed between the EMCV IRES dependent firefly regulation in eIF4AI knockdown cells compared to control. This could be due to the regulation of IRES and cap mediated translation to the same extent. As eIF4AI was shown to be required for EMCV IRES driven translation (Pestova, Shatsky et al. 1998), it is possible that eIF4AI knockdown decreases both firefly and Renilla luciferase expression from the EMCV IRES bicistronic reporter plasmid, so that the ratio is unchanged. HCV IRES dependent firefly expression compared to cap-dependent Renilla luciferase expression in eIF4AII knockdown cells was also similar to control. This could indicate regulation of both the cap and the HCV IRES by eIF4AII, or could mean that neither is affected. The decrease in F/R in the EMCV IRES plasmid following eIF4AII knockdown suggests that eIF4AII contributes to EMCV IRES-driven, but not cap-dependent, translation. Overall, the data suggest that eIF4AII does not regulate translation via the HCV IRES in the absence of miR-122 binding sites, However, due to the confounding effects of eIF4A proteins on cap-dependent translation, it is not possible to draw firm conclusions from these experiments.

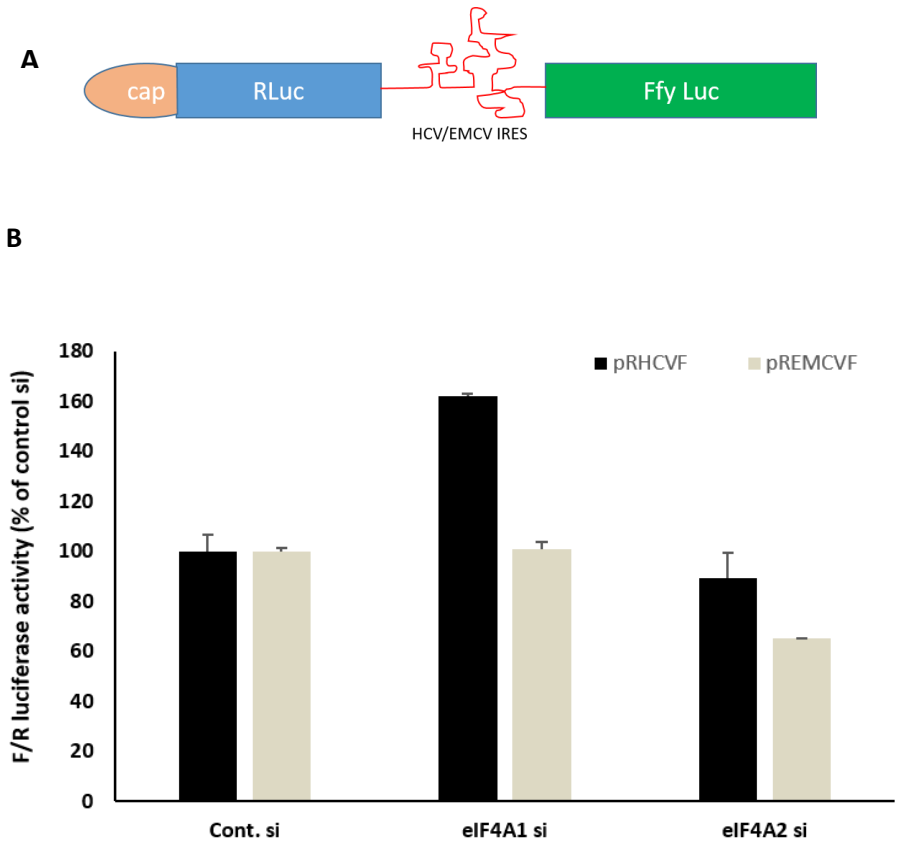

Figure 5-6 Effects of eIF4A proteins on HCV and EMCV IRES-driven firefly luciferase activity

A) Structure of bicistronic HCV or EMCV IRES driven luciferase reporters. **B).** HCV IRES driven (black bars) and EMCV IRES driven (yellow bars) bicistronic luciferase reporter activities in control, eIF4A1 and eIF4AII knockdown cells. Renilla and firefly activities were measured by dual luciferase reporter assay. The bars represent firefly activities relative to renilla in six independent experiments. Error bars show SD.

5.2.7 Subcellular localization of eIF4AI and eIF4AII

In the previous chapters 3 and 4, it was shown that eIF4AII regulates HCV in the presence of miR-122, and that eIF4AII associates with HCV RNA and miR-122 in a miR-122 dependent fashion. Based on these results, it was proposed that HCV RNA, miR-122 and eIF4AII might be part of same complex. To further investigate this and to visualize the presence of HCV RNA, miR-122 and eIF4AII in cells, first, eIF4AI and eIF4AII cellular localization was studied by an indirect immunofluorescent (IF) assay. Then, to confirm the specificity of the IF, the cells were depleted for eIF4AI and eIF4AII followed by IF based detection of eIF4AI and eIF4AII to see the loss of fluorescence signal.

5.2.7.1 eIF4AI and eIF4AII have different subcellular localization

Both 5B (Huh7 HCV replicon) and Huh7 cells were plated in wells slide and stained as described in chapter 2, section 2.13.1.1. Cells were first incubated with primary (eIF4AI and eIF4AII) antibodies and then with fluorescent tagged secondary antibody to visualize the subcellular localization of eIF4AI and eIF4AII. DRAQ5 was used for nucleic acid stain. DRAQ is far-red fluorescent stain which binds to DNA. The slide was mounted with Canada balsam oil and visualized under the Carl Zeiss laser scanning confocal microscope.

Figure 5-7 shows the localization of both eIF4AI and eIF4AII in 5B and Huh7 cells. Both cells show that eIF4AI and eIF4AII localize in different areas in the cells. eIF4AI signals (green dots) were only detected in the cytoplasm of both

cells (figure 5-7 upper panel) and there were no signals in the nucleus. Surprisingly, eIF4AII was not only visualized in the cytoplasm (low green signals) but it was mainly present in the nucleus (figure 5-7 lower panel). DRAQ5 signals (purple fluorescence) were detected in the nucleus and were positive in both types of cells. This was the first time that both eIF4AI and eIF4AII were visualized to determine their subcellular localization. To further investigate the difference in localization pattern and to confirm the results in Huh7 and 5B cells, the same experiment was repeated in the Hela cells (lower panel) and it was confirmed that both proteins exhibit different subcellular localization in Huh7, 5B and Hela cells. These experiments were repeated at least three times and similar results were obtained. If the antibodies used were specific, these results would clearly indicate that eIF4AI and eIF4AII localize to different locations in the cell. Therefore, it was essential to confirm that the antibodies were specific before drawing this conclusion. The difference in the subcellular localization could be due to the difference in the functions of both eIF4AI and eIF4AII.

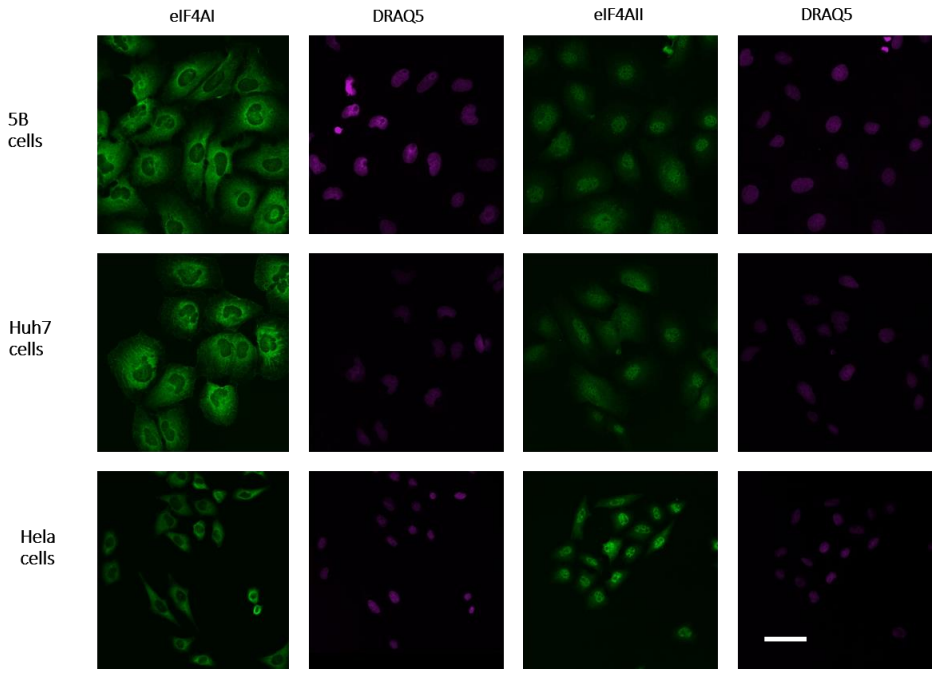

Figure 5-7 eIF4AI and eIF4AII subcellular localization in 5B, Huh7 and HeLa cell lines

The figure shows the confocal microscopy images of the eIF4AI and eIF4AII subcellular localization in 5B (upper panel), Huh7 (middle panel) and in Hela cells (lower panel). Both were visualized with green fluorescent tagged secondary antibody. DRAQ5 was used to visualize nucleic acid (purple). The white horizontal bar on the bottom right is equal to 57.21um on scale.

5.2.7.2 eIF4AII is not localizing in nucleus

To further verify the distribution of eIF4AI and eIF4AII from these results, eIF4AI and eIF4AII were depleted from the 5B cells followed by fluorescence based detection of eF4AI and eIF4AII. The idea was that the knockdown of these proteins would result in decrease or loss of fluorescence signal emission from eIF4AI and eIF4AII proteins.

Figure 5-8 shows the eIF4AI and eIF4AII fluorescence in control, eIF4AI and eIF4AII knockdown cells. eIF4AI and eIF4AII showed similar subcellular localization in as in figure 5-7. eIF4AI is localized in the cytoplasm, while eIF4AII is present in both the cytoplasm and nucleus, with higher fluorescence signal from nucleus. When eIF4AI was depleted in the cells (eIF4AI si), the eIF4AI signal dropped to background levels and fluorescence was dispersed. eIF4AII fluorescence increased in the cytoplasm and some signal was still detected in the nucleus. This increase in eIF4AII signals in eIF4AI knockdown cells is an interesting finding and needs further investigation to know the underlying mechanism. It could be due to the reciprocal increase in eIF4AII expression after eIF4AI knockdown (Galicia-Vazquez, Cencic et al. 2012), but the strong increase in the cytoplasm may suggest some re-localization of eIF4AII.

The knockdown of eIF4AII (figure 5-8 bottom row) did not affect the eIF4AI localization. The eIF4AII signals in eIF4AII depleted cells were completely absent from the cytoplasm but the depletion did not affect the eIF4AII signal

inside the nucleus. The presence of eIF4AII signals in the nucleus in eIF4AII depleted cells is therefore likely to be due to nonspecific binding of eIF4AII antibody to another protein in the nucleus. These results didn't confirm the previous observation of nuclear localisation of eIF4AII (5.2.7.1), which indicates that there is no difference in subcellular localization of the both proteins. These experiments could not be completed due to the lack of time, therefore further experiments would be necessary to investigate the localization of HCV and miR-122.

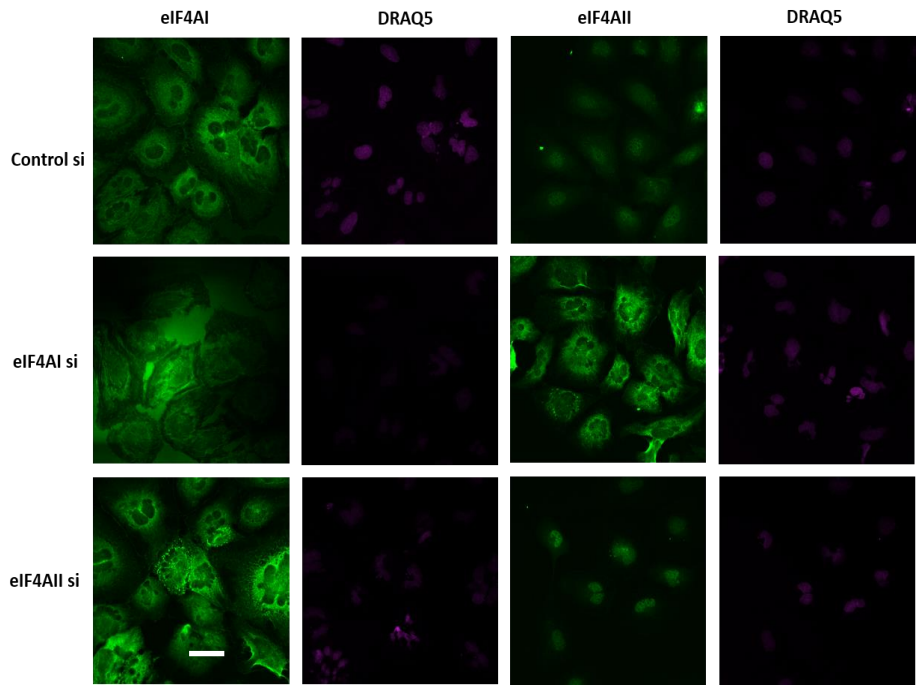

Figure 5-8 Subcellular localization of eIF4AI and eIF4AII in eIF4AI and eIF4AII depleted cell

The figure shows the fluorescence levels in eIF4AI and eIF4AII depleted 5B cells. The top row shows eIF4AI and eIF4AII levels in control siRNA-treated cells, while the middle and bottom rows represent the fluorescence levels in eIF4AI and eIF4AII knockdown cells. The horizontal bar at the bottom left figure is equal to 51.27µm on scale.

5.2.8 Polysome profile analysis of HCV RNA translation in the presence and absence of eIF4AII

Polysome analysis is used to investigate the translation activity of mRNAs and effects of different factors on mRNA translation. The reporter analysis described above suggest the effect of eIF4AII on HCV translation, so to further investigate which stage of HCV replication cycle was affected by eIF4AII, polysome profiling was performed. Studies showed that miRNAs, associating proteins and target mRNA all co-sediment in polyribosomes (Nottrott, Simard et al. 2006). To study the effect of the presence or absence of eIF4AII on HCV translation efficiency, and to see whether HCV RNA, miR-122 and eIF4AII are present in same fractions, polysome profile analysis was performed in HCV replicon 5B cells, while Huh7 cells were used as a control to determine whether there are differences in eIF4AII distribution in the presence of replicating HCV. The data from these experiments combined with luciferase analysis should provide further insight into whether eIF4AII regulation of HCV is related to miR-122 regulation.

Untreated Huh7 or HCV replicon (5B) cells were used to optimize the sucrose gradient fractionation and polysome profiling. Polysome profiling was performed by sucrose density gradient as described in section 2.12. A blank gradient tube without cell lysate was used as control. Fractions were divided into two parts for RNA and protein purification for qRT-QPCR, northern blot (NB) and western blot (WB) analysis of fractions.

The polysome analysis experiment (data not shown) shows that a clear polysome profile and successful fractionation were achieved in initial experiments. The RNA and protein were extracted from the fractions for qRT-QPCR and northern blot detection of HCV RNA and miR-122 and western blot detection on eIF4AII and HCV core in the same fractions.

HCV RNA signals were detected in both monosome and polysome fractions by northern blot. The presence of HCV RNA in 60S and 80S and polysome fractions indicate the active translation of HCV in 5B cells. Actin mRNA was also present in same fractions. The qRT-QPCR could not detect HCV RNA to confirm the northern blot results. Similarly, miR-122 could not be detected by either northern blot or qRT-QPCR. Western blot was also unsuccessful in detecting any eIF4AII and HCV signals. The reason for failure of qRT-QPCR based detection of HCV RNA and miR-122 could be the presence of heparin in cell lysis buffer, while miR-122 NB and eIF4AII WB could have been failed due to some technical issues and loss of RNA and protein by degradation.

Initial polysome profiling also worked well with Huh7 cells (data not shown). In the later repeats, due to the technical difficulties it was not possible to carry out the experiments following eIF4AII knockdown. Due to the time constraint it was not possible to re-optimize the apparatus and procedure. Therefore, it is not possible to draw any conclusions from these experiments and more repeats with a fully optimized procedure would be required to check the sedimentation of miR-122, HCV and eIF4AII in polysome profile analysis and the effects of eIF4AII depletion on this.

5.3 Discussion

In this chapter, the use of different techniques is described to further study the role of the eIF4AII helicase protein and miR-122 in HCV regulation. Dual luciferase assays were used to first study the role of eIF4A proteins in miR-122-mediated repression of firefly luciferase expression via the 3'UTR. Then, in another dual luciferase assay, the role of eIF4A proteins in miR-122-mediated activation of HCV-IRES driven translation were studied. Knockdown of both eIF4A proteins increased expression of firefly luciferase from the 3'UTR reporter plasmid in both HCV replicon and Huh7 cells. eIF4aII has been reported to be required for miRNA mediated translation repression (Meijer, Kong et al. 2013), but eIF4AII knockdown did not affect miR-122 regulation of the 3'UTR reporter. The difference in results between both studies could be the use of different cell types and miRNAs. It could also be due to the fact that eIF4AII regulation of miRNA mediated repression is not universal and affected by other variables like cell density or cell line specific. It is also possible that these effects are HCV specific, so more experimental work is needed to clearly define the role of eIF4A proteins especially eIF4AII in miRNA mediated repression. The knockdown of eIF4AI also increases the reporter expression independent of miR-122 binding. This indicates that eIF4AI is not involved in miR-122-mediated regulation via 3'UTR sites, but that its knockdown has differential effect on firefly and renilla translation. The knockdown of both proteins have similar effects on F/R ratio in

pLUC122x2 transfections. It is likely that the results from these experiments show a general effect of eIF4A proteins on translation.

The knockdown of eIF4AII also reduces the HCV-IRES driven translation of a luciferase reporter, which suggests that eIF4AII effect on the HCV replication cycle is at translation level. eIF4AI knockdown did not have the same effect as eIF4AII knockdown in these experiments, which indicates that the enhancement of HCV 5'UTR driven translation is eIF4AII-specific. IRES reporter plasmid analysis also suggest that eIF4AII only activates HCV IRES-driven translation in the presence of miR-122 binding sites, so it is possible that it is working via miR-122, but this was obscured in the data by other effects. The assessment of the effects of eIF4A proteins on luciferase reporter plasmids was difficult as the control used in these experiments was cap-dependent and likely to be affected by eIF4A protein depletion. However, these experiments allow us to look for the differences in regulation in the presence and absence of miR-122. More studies are required to know if the role of eIF4AII is specific to miR-122 binding at HCV 5'UTR or whether eIF4AII might also play a role in the life cycle of other RNA viruses.

Immunofluorescence and polysome profiling were also used to study the subcellular localization of eIF4A proteins and HCV, and to know whether the HCV RNA, miR-122 and eIF4AI or eIF4AII are present in same fractions. The initial IF experiment showed that both eIF4AI and eIF4AII localize to different areas in the cells. These results were very exciting as it was the first time that eIF4AI and eIF4AII cellular localization was studied. These results showed

that eIF4AI is localized to cytoplasm, while eIF4AII was detected in both cytoplasm and in nucleus. The cells were also depleted for eIF4AI and eIF4AII to confirm their localization by detecting the loss of fluorescent signals in knockdown cells. The eIF4AI knockdown results in overall loss of signal, which confirms that the antibody was specific and eIF4AI is present in cytoplasm. Although the eIF4AII knockdown slightly decreases the cytoplasmic signals, there was no change observed in nuclear signals of eIF4AII. This leads to the conclusion that the eIF4AII antibody used in these IF experiments was binding to a non-specific target in the nucleus. The knockdown of eIF4AI also result in increased cytoplasmic signals of eIF4AII which is very interesting finding and need further study to know the underlying mechanism. These results indicate that both eIF4AI and eIF4AII are present in cytoplasm. It would be a good idea to repeat these experiments with a different antibody to eIF4AII to get more specific signals. The results shown in chapter 4 indicate that eIF4AII interacts with HCV RNA and miR-122 in a miR-122 dependent manner and that they may be part of same complex. Here, eIF4A involvement in miR-122 mediated regulation of HCV was also studied, which indicates the eIF4AII is involved in HCV translation. The overexpression and sequestration of miR-122 (figure 3-7) did not have any effect on HCV RNA level in eIF4AII knockdown cells, which suggest that eIF4AII regulates HCV in miR-122 dependent manner. So to further study their presence and interaction, sucrose density based polysome profiling was performed in HCV replicon and Huh7 cells to see if HCV RNA, miR-122 and eIF4AII are present in same fractions. Huh7 cells were

used to compere the distribution of eIF4AII in the presence and absence of eIF4AII. The initial results showed resolved monosome and polysome peaks in both cells and HCV RNA signals were also detected by northern blot analysis in HCV replicon cells. The presence of HCV RNA in 60S, 80S and polysome peaks indicated the active translation of HCV in replicon cells. However, miR-122 and eIF4AII signals were not detected. The experiments were repeated several times but due to leakage of tracing solution (blue sucrose leakage from the top which disturbed the gradient) eIF4AII, HCV RNA and miR-122 levels were not detected. In future, the polysome profiling apparatus with option of piercing the gradient tubes from bottom can be used to avoid any leakage form the top of the gradient. This will not only help in confirming the association of eIF4AII with HCV RNA and miR-122 but the microarray or RNAseq analysis of the RNA collected from the polysome fractions will help in studying the effect of eIF4AII on expression levels of other genes.

6 Discussion

Besides the viral proteins, HCV is also heavily dependent on host factors to complete its life cycle. Several host factors have been identified, which are involved right from the start to the end of HCV life cycle. Examples of host factors include those that are involved in HCV entry into the hepatocytes (LDLR, CD81, SR-B1, OCLN and CLDN1), replication (PI4K-IIIα, Cyclophilin A and miR-122), assembly and release (lipid droplets, ApoB and ApoE) and tropism (OCLN, CLDN1 and CD81). The host factors include DEAD-box helicases, of which DDX1, DDX3, DDX5 and DDX6 have been implicated in HCV replication. At the start of this project, preliminary data from our lab (experiments performed by Catherine Jopling) showed that another DEAD box helicase, eIF4AII, contributes to HCV replication. The aim of this study was to investigate the role of eIF4AI and eIF4AII in HCV regulation. It was confirmed that eIF4AII contributes to the HCV regulation. It was further shown that eIF4AII interacts with HCV in a miR-122 dependent manner. It was also shown that eIF4AII interacts with two other miRNAs, miR-21 and miR-26a. A clear role of miR-122 in eIF4AII binding to HCV was shown, which suggests that these molecules work together. This was further confirmed by the lack of change in HCV RNA levels in miR-122 overexpressed or depleted eIF4AII knockdown cells.

6.1 Comparison between regulation of HCV by eIF4AII and other DEAD-box helicases

Several DEAD-box helicase proteins like DDX1, DDX3, DDX5 and DDX6 are involved in HCV replication. These helicases bind to HCV RNA or different viral proteins like HCV core and NS5B, and result in increase in HCV abundance. Intriguingly, it has also been shown that certain DEAD box helicases have roles in biogenesis or function of specific microRNAs (Ariumi, Kuroki et al. 2007, Jangra, Yi et al. 2010, Huys, Thibault et al. 2013, Kuroki, Ariumi et al. 2013).

Among HCV interacting DEAD-box helicases, DDX1 interacts with HCV UTRs, DDX6 and DDX3 interact with HCV core, while DDX5 and eIF4AII interact with NS5B polymerase. These enzymes are involved in HCV replication, while eIF4AII as binding partner of NS5B was suggested to facilitate the HCV replication by removing the HCV RNA secondary structures (Kyono, Miyashiro et al. 2002). Our data show that eIF4AII is involved in HCV replication and also suggest that it is involved in miR-122 mediated regulation of HCV, a role that has not been shown for any other DEAD box helicases.

DDX3 is a multifunctional protein and play roles in the life cycle of many viruses. In influenza virus it interacts with NS1 and NP proteins and acts as an antiviral factor by reducing the virus titre through regulation of stress granules (Thulasi Raman, Liu et al. 2016). DDX1 and DDX3 are also required for the viral Rev protein based transportation of HIV unspliced/partially

spliced mRNA from nucleus to cytoplasm (Kwong, Rao et al. 2005). DDX5 also enhance the HIV-1 replication by its function as a co-factor of Rev protein (Zhou, Luo et al. 2013). Due to their vital roles in HIV regulation, these helicases are considered as important drug targets in HIV infection.

DDX6 is a component of miRISC and interacts directly with Ago1-2. It is also involved in miRNA mediated silencing (Chu and Rana 2006). siRNA mediated knockdown of DDX6 reduces HCV replication but this does not affect the miR-122 regulation of HCV which suggests that both processes are mediated by separate mechanisms (Huys, Thibault et al. 2013).

6.2 Comparison of the role of eIF4AI and eIF4AII

eIF4A is another DEAD-box helicase and member of eIF4F complex. It unwinds double stranded RNA structure in the 5'UTR during ribosome scanning, and helps translation initiation by facilitating the ribosomal subunit binding to mRNA. eIF4AI and eIF4AII have more than 90% sequence similarity due to which these proteins have long been considered to be functionally interchangeable (Nielsen and Trachsel 1988). The vast majority of research of eIF4A has been done on eIF4AI. However, recent studies support the notion that eIF4AI and eIF4AII are functionally divergent. Cap analogue pull down assays resulted in more eIF4AI yield than eIF4AII, which suggested eIF4AI as preferred eIF4F binding partner compared to eIF4AII (Galicia-Vazquez, Cencic et al. 2012). eIF4AII depletion had no effect on cellular growth while eIF4AI depletion was shown to be inhibitory to cellular growth (Galicia-Vazquez, Cencic et al. 2012). This is a very important

difference between the two proteins and it shows that eIF4AII cannot perform all the same functions. eIF4AII, but not eIF4AI, was shown to play a critical role in miRNA mediated repression of protein translation (Meijer, Kong et al. 2013). In a recent study, it was shown that eIF4AII is not required for miRNA mediated repression (Fukao, Mishima et al. 2014, Galicia-Vazquez, Chu et al. 2015). The difference in the two studies could be due the difference in cell types and methodology used. siRNA mediated repression of eIF4AII did not affect the miRNA mediated repression of luciferase reporter (pLUC122x2) via 3'UTR and these findings are in contrast to the findings of previous study by Meijer, Kong et al. (2013). In chapter 3, it was shown that siRNA based knockdown of eIF4AII strongly reduces HCV RNA. This shows that eIF4AII is involved in HCV regulation. while the overexpression of eIF4AII by siRNA resistant eIF4AII could not significantly elevated the HCV RNA. This could be due to the non expression of siRNA resistant eIF4AII by the plasmid or lack of association of this protein with functional complex. More experiments are required to draw firm conclusion. eIF4AI knockdown had variable effects on HCV RNA levels. These variabilities could be due to the subtle differences in the confluence levels of cells or due to the experimental variability. These finding also support the idea that eIF4AI and eIF4AII function differently. Immunoprecipitation of HCV RNA with eIF4AII also indicate that eIF4AII interacts with HCV RNA and sequestration of miR-122 result in loss of HCV RNA pulldown in these IPs which indicates that this interaction is dependent on miR-122. While in contrast, HCV RNA and miR-122 were not detected in eIF4AI IPs, however,

as western blot was not performed to confirm that eIF4AI was immunoprecipitated, it is possible that this could be a false negative. Therefore, more experiments like eIF4A western blot and dominant negative mutant are required to draw a firm conclusion about the role of eIF4AI in HCV regulation.

6.3 Does eIF4AII regulate HCV by modulation of miR-122 function?

Sequestration and overexpression of miR-122 did not change the HCV RNA levels in eIF4AII depleted cells (figure 3-7), which suggests that eIF4AII contribution to HCV replication is linked with miR-122 regulation of HCV and functional eIF4AII is required for miR-122 mediated regulation of HCV. miR-122-HCV interaction is unusual: unlike canonical miRNA interaction with 3'UTR targets in mRNAs, leading to mRNA degradation and reduced production of the encoded protein, miR-122 binds to two tandem binding sites in HCV 5'UTR and promotes the accumulation of HCV RNA (Jopling, Yi et al. 2005, Jopling, Schutz et al. 2008). Although the mechanism of miR-122 promotion of HCV accumulation is still unknown, several mechanisms have been proposed which include the masking of HCV 5'UTR and hence protecting it from exonuclease degradation and from immune complexes (Machlin, Sarnow et al. 2011). Several miRISC and P-body components are also implicated in miR-122 mediated regulation of HCV (Wilson, Zhang et al. 2011, Zhang, Huys et al. 2012, Roberts, Doidge et al. 2014). We find miR-122 dependent interaction between eIF4AII and HCV RNA. We also find that eIF4AII interacts with two other miRNAs in Huh7 cell lines. This is the first

study indicating the interaction between eIF4AII, HCV RNA and other miRNAs including miR-122. More investigation using different assays like in-vitro binding assays would be necessary to find out whether the interaction between eIF4AII, HCV RNA and miRNAs is direct.

Both Ago and DDX6 are core components of miRNA mediated repression. Both proteins are also involved in HCV RNA accumulation, with Ago required for miR-122 mediated abundance of HCV RNA while DDX6 is involved in a miR-122 independent mechanism. These observations suggest that both miRNA based repression and activation share at least some of the same effectors. Similar to DDX6, eIF4AII has been proposed to be involved in miRNA mediated repression by Ccr4-Not complex via CNOT1 which leads to the blocking of ribosome scanning function and represses protein translation (Meijer, Kong et al. 2013). This model of silencing was questioned in a different study in which the interaction between eIF4AII and CNOT1 was not confirmed (Mathys, Basquin et al. 2014), and knockdown of eIF4AII could not repress the silencing (Galicia-Vazquez, Chu et al. 2015). It has been shown that DDX6 interacts with CNOT1 in a fashion similar to that of eIF4A and eIF4G (Petit, Wohlbold et al. 2012). Our data show that siRNA based knockdown of CNOT1 reduces both HCV RNA and miR-122 co-immunoprecipitation with eIF4AII, which indicates that Ccr4-NOT complex component CNOT1 contributes to eIF4AII association with miR-122 and HCV and may be part of same complex. Although this data supports the finding of previous study by Meijer *et al* (2013) it would be necessary to investigate these protein interactions with HCV RNA in more detail to determine the

mechanism of this interaction and to resolve the discrepancies. One reason for these controversial results could be that proteins have potential to interact with multiple partners in the cell but may favour particular interactions depending on the cell context.

6.4 eIF4AII effect on HCV translation

The bicistronic system containing HCV 5'UTR driven firefly luciferase coding region and the EMCV IRES driven-NS5B coding region, flanked by HCV 3'UTR was used to investigate the role eIF4AI, especially eIF4AII in translation via HCV 5'UTR driven reporter system. The results show that eIF4AII leads to translation activation in HCV IRES driven reporter expression (figures 5-4 and 5-5). Further investigation of eIF4AII role in HCV translation by analysis of composition of polysome fractions was unsuccessful due to experimental difficulties. With more time, this approach would be useful to determine whether eIF4AII affects the association of HCV RNA with translating ribosomes. The same question can also be addressed by using the replication-deficient (GND mutant) virus to measure the level of HCV proteins in the presence or following knockdown of eIF4AII. HCV completes its life cycle in different cellular entities and compartments. HCV translation occurs in detergent sensitive complexes, while replication occurs in double lipid bilayer containing detergent resistant complexes. The identification of different mRNPs members in these complexes could also provide insight into the contribution of these components in HCV regulation. So isolation of HCV

replication and translation complexes would be useful to determine whether eIF4AII interacts with HCV RNA and miR-122 in them or not.

It is possible that eIF4AII regulation of HCV might be related to previous roles identified for P bodies and stress granules in HCV infection. HCV infection has been reported to reduce the number of P-bodies and enhance the formation of stress granules (Pager, Schutz et al. 2013). P-bodies are cytoplasmic aggregates of proteins involved in translation repression and RNA decay associated with translationally repressed mRNAs (Cougot, Babajko et al. 2004). On the other hand, stress granules are aggregates of un-translating mRNAs and translation initiation factors, ribosomal subunits and RNA binding proteins, induced by cellular stress (Buchan and Parker 2009). The composition of P-bodies and stress granules mRNPs depend on the mRNAs present in these entities. P-bodies and stress granules interact with each other and exchange mRNPs, and a change in P-body component concentration could re-localize the mRNPs to stress granules. Many P-bodies components like miR-122, Lsm, DDX6, Ago are involved in either miR-122 mediated or miR-122 independent regulation of HCV replication. eIF4A proteins are components of stress granules while miR-122 is present in P-bodies. Furthermore, SUMO protein specifically binds to eIF4AII at position K226 and helps eIF4AII to induce the formation of stress granules (Jongjitwimol, Baldock et al. 2016). HCV infection increases the formation of stress granules containing mRNAs which preferentially translate through IRES dependent translation. It is possible that HCV infection induces a stress condition which generates stress granules and redistributes or re-localizes

P-bodies components like DDX6, Ago, miR-122 and Lsm, and at the same time takes advantage of highly concentrated stress granules components in its replication and translation.

Further investigations related to analysis of composition of polysomes, P-bodies and stress granules in the presence of absence of HCV interacting host factors like eIF4AII could help in understanding how these host factor-mediated mechanisms involved in HCV regulation.

siRNA based knockdown of target proteins is usually confirm by either western blot analysis and/or mRNA qRT-QPCR. These confirmatory experiments provide additional support to the findings and help in drawing the more firm and scientifically authentic conclusion about the results.

Although in the present study, the successful knockdown of both eIF4AI and eIF4AII was confirmed by western blot (Figure 3-1), the findings of later experiemnts especially immunoprecipitation of miR-122 and HCV RNA and increase in HCV RNA levels if double knockdown (eIF4AI and eIF4AII) were not confirm by western blot analysis. Several attemptes were made to get results form the western blot but due to some technical issues and time limitation it was not possible to further carry on these experiemtns. Therefore it is not possible to draw any firm conclusion about the positive role fo eIF4AII in miR-122 mediated regulation of HCV. In future these findings need to be confirm by western blot and ELISA experiemnts.

HCV has been shown to work as a sponge for miR-122 which result in sequestration of miR-122, which leads to dererepression of miR-122 target.

This derepression of miR-122 targets could help in HCV propagation in liver cells (Luna, Scheel et al. 2015). It is possible that eIF4AII interaction with miR-122 and HCV RNA works in similar fashion and sequester proteins like Pdcd4 which result in translation repression of specific protein like protein involve in immune function and apoptosis and lead to HCV specific favourable conditions in liver cells.

In future, the *in-vivo* knockdown of eIF4AII in HCV animal model followed by HCV RNA and protein detection will not only further support the findings of the present study but also provide an opportunity to study the eIF4AII protein as anit-HCV drug target.

6.5 HCV therapeutics

Interferon-alpha (INF-α) was used as the first anti-HCV drug during the 1990s and 8% -12% SVR was achieved. Later on the addition of ribavirin (RBV) enhanced the SVR to about 40%. Pegylated interferon (PEG-INF-a) combined with RBV increased the SVR up to 50% while the same regime failed to achieve SVR in of the remaining 50% of patients (Fried, Shiffman et al. 2002, Hadziyannis, Sette et al. 2004). The advent of the first direct acting agents (DAAs), the NS3/4A protease inhibitors telaprevir (TVR) and boceprevir (BOC) in combination with PEG-INF-α/RBV, further improved the SVR, but the adverse effects and low tolerance associated with these combination therapies and genetic variability of HCV reduced the effective use of these drugs. Recently, new DAAs including simeprevir (NS3/4A inhibitor), sofosbuvir (Nucleotide analogue NS5B polymerase inhibitor), ledipasvir

(NS5A inhibitor) in different combinations with other drugs and with IFN-α and RBV have been approved which allow highly effective treatment in shorter time duration compared to older IFN-α/RVB therapy. These drugs not only achieve more than 90% SVR but they also have shown minimal adverse effects and high tolerability. Very high prices, drug-to drug interaction (DDI) of new DAAs, increased risk of HBV virus activation and changes in levels of different chemicals in blood are the issues which need to addressed (Banerjee and Reddy 2016).

HCV virus mutates at the rate of 2.5 x 10^{-5} mutations per nucleotide per genome replication which is highest mutation rate among all RNA viruses (Ribeiro, Li et al. 2012). Inter and intra genotypic recombinations also increase the HCV genome variability. Due to this highly variable positive sense RNA genome, a possible problem associated with direct-acting antiviral agents is the development of antiviral resistance in HCV. There is also a possibility of other side effects as some of the therapies also require ribavirin in combination, which is known to be associated with anaemia, although newer therapies which only use a combination of DAAs should avoid this problem. Low levels of naturally occurring resistance associated substitutions (RASs) have already been reported against some of new DAAs like boceprevir, telaprevir, simeprevir and grazoprevir (Eltahla, Rodrigo et al. 2016, Marascio, Pavia et al. 2016). Therefore, an alternative therapeutic approach could be to interfere with host factors required for HCV pathogenesis. This could provide the promising solution to this issue and may provide superior treatment due to host-targeting agents (HTAs) ability

of i) providing higher genetic barrier to resistance, ii) antiviral activity against all HCV genotypes and iii) can be used in combination to complement the DAAs. Two HTAs, Cyclophilin A inhibitor and the miR-122 antagonists Miravirsen and RG-101 are already in clinical trials and may become available as anti-HCV treatment options (Zeisel, Lupberger et al. 2013, Gebert, Rebhan et al. 2014, Pawlotsky 2014). Many host factors including DEAD-box helicases have been implicated in HCV regulation. Viral and cellular helicases have been considered as drug targets for the treatment of viral infections.

DEAD-box helicases are implicated in many cancers and diseases and therefore are very promising targets for novel therapies. Inhibition of DDX3 by synthetically designed compounds has shown inhibition of HIV-1 replication. Several inhibitors like hippuristanol, pateamine A, silvestrol and rocaglate have been reported to inhibit both eIF4AI and eIF4AII isoforms (Low, Dang et al. 2005, Bordeleau, Mori et al. 2006, Bordeleau, Robert et al. 2008). This non-specificity is due to high sequence similarity between eIF4AI and eIF4AII. To date, it hasn't been possible to develop eIF4AI or eIF4AII specific inhibitors. However, the involvement of eIF4AII in HCV regulation make it very promising host target for anti-HCV drug design which may provide a better alternative to treat HCV infection.

7 References

Aitken, C. E. and J. R. Lorsch (2012). "A mechanistic overview of translation initiation in eukaryotes." Nat Struct Mol Biol **19**(6): 568-576.

Alexopoulou, A. and S. P. Dourakis (2005). "Genetic heterogeneity of hepatitis viruses and its clinical significance." Curr Drug Targets Inflamm Allergy **4**(1): 47-55.

Alter, H. J. (1996). "The cloning and clinical implications of HGV and HGBV-C." N Engl J Med **334**(23): 1536-1537.

Alter, H. J., R. H. Purcell, P. V. Holland and H. Popper (1978). "Transmissible agent in non-A, non-B hepatitis." Lancet **1**(8062): 459-463.

Arch, R. H., R. W. Gedrich and C. B. Thompson (1998). "Tumor necrosis factor receptor-associated factors (TRAFs)--a family of adapter proteins that regulates life and death." Genes Dev **12**(18): 2821-2830.

Ariumi, Y., M. Kuroki, K. Abe, H. Dansako, M. Ikeda, T. Wakita and N. Kato (2007). "DDX3 DEAD-box RNA helicase is required for hepatitis C virus RNA replication." J Virol **81**(24): 13922-13926.

Arnaud, N., S. Dabo, D. Akazawa, M. Fukasawa, F. Shinkai-Ouchi, J. Hugon, T. Wakita and E. F. Meurs (2011). "Hepatitis C virus reveals a novel early control in acute immune response." PLoS Pathog **7**(10): e1002289.

Aspinall, E. J., G. Hawkins, A. Fraser, S. J. Hutchinson and D. Goldberg (2011). "Hepatitis B prevention, diagnosis, treatment and care: a review." Occup Med (Lond) **61**(8): 531-540.

Balayan, M. S., A. G. Andjaparidze, S. S. Savinskaya, E. S. Ketiladze, D. M. Braginsky, A. P. Savinov and V. F. Poleschuk (1983). "Evidence for a virus in non-A, non-B hepatitis transmitted via the fecal-oral route." Intervirology **20**(1): 23-31.

Banerjee, D. and K. R. Reddy (2016). "Review article: safety and tolerability of direct-acting anti-viral agents in the new era of hepatitis C therapy." Aliment Pharmacol Ther **43**(6): 674-696.

Behm-Ansmant, I., J. Rehwinkel, T. Doerks, A. Stark, P. Bork and E. Izaurralde (2006). "mRNA degradation by miRNAs and GW182 requires both CCR4:NOT deadenylase and DCP1:DCP2 decapping complexes." Genes Dev **20**(14): 1885-1898.

Belsham, G. J. (2009). "Divergent picornavirus IRES elements." Virus Res **139**(2): 183-192.

Bernal, W. and J. Wendon (2013). "Acute liver failure." N Engl J Med **369**(26): 2525-2534.

Bleichert, F. and S. J. Baserga (2007). "The long unwinding road of RNA helicases." Mol Cell **27**(3): 339-352.

Blight, K. J., A. A. Kolykhalov and C. M. Rice (2000). "Efficient initiation of HCV RNA replication in cell culture." Science **290**(5498): 1972-1974.

Blight, K. J., J. A. McKeating and C. M. Rice (2002). "Highly permissive cell lines for subgenomic and genomic hepatitis C virus RNA replication." J Virol **76**(24): 13001-13014.

Blumberg, B. S., H. J. Alter and S. Visnich (1965). "A "New" Antigen in Leukemia Sera." JAMA **191**: 541-546.

Bordeleau, M. E., A. Mori, M. Oberer, L. Lindqvist, L. S. Chard, T. Higa, G. J. Belsham, G. Wagner, J. Tanaka and J. Pelletier (2006). "Functional characterization of IRESes by an inhibitor of the RNA helicase eIF4A." Nat Chem Biol **2**(4): 213-220.

Bordeleau, M. E., F. Robert, B. Gerard, L. Lindqvist, S. M. Chen, H. G. Wendel, B. Brem, H. Greger, S. W. Lowe, J. A. Porco, Jr. and J. Pelletier (2008). "Therapeutic

suppression of translation initiation modulates chemosensitivity in a mouse lymphoma model." J Clin Invest **118**(7): 2651-2660.
Boutz, D. R., P. J. Collins, U. Suresh, M. Lu, C. M. Ramirez, C. Fernandez-Hernando, Y. Huang, S. Abreu Rde, S. Y. Le, B. A. Shapiro, A. M. Liu, J. M. Luk, S. F. Aldred, N. D. Trinklein, E. M. Marcotte and L. O. Penalva (2011). "Two-tiered approach identifies a network of cancer and liver disease-related genes regulated by miR-122." J Biol Chem **286**(20): 18066-18078.
Bradley, D. W., K. Krawczynski, M. J. Beach and M. A. Purdy (1991). "Non-A, non-B hepatitis: toward the discovery of hepatitis C and E viruses." Semin Liver Dis **11**(2): 128-146.
Brass, V., D. Moradpour and H. E. Blum (2006). "Molecular virology of hepatitis C virus (HCV): 2006 update." Int J Med Sci **3**(2): 29-34.
Braun, J. E., E. Huntzinger and E. Izaurralde (2013). "The role of GW182 proteins in miRNA-mediated gene silencing." Adv Exp Med Biol **768**: 147-163.
Buchan, J. R. and R. Parker (2009). "Eukaryotic stress granules: the ins and outs of translation." Mol Cell **36**(6): 932-941.
Bush, M. S., N. Crowe, T. Zheng and J. H. Doonan (2015). "The RNA helicase, eIF4A-1, is required for ovule development and cell size homeostasis in Arabidopsis." Plant J **84**(5): 989-1004.
Caron, S., M. Charon, E. Cramer, N. Sonenberg and I. Dusanter-Fourt (2004). "Selective modification of eukaryotic initiation factor 4F (eIF4F) at the onset of cell differentiation: recruitment of eIF4GII and long-lasting phosphorylation of eIF4E." Mol Cell Biol **24**(11): 4920-4928.
Chambers, T. J., C. S. Hahn, R. Galler and C. M. Rice (1990). "Flavivirus genome organization, expression, and replication." Annu Rev Microbiol **44**: 649-688.
Chen, Y., C. Wang, Y. Liu, L. Tang, M. Zheng, C. Xu, J. Song and X. Meng (2013). "miR-122 targets NOD2 to decrease intestinal epithelial cell injury in Crohn's disease." Biochem Biophys Res Commun **438**(1): 133-139.
Choo, Q. L., G. Kuo, A. J. Weiner, L. R. Overby, D. W. Bradley and M. Houghton (1989). "Isolation of a cDNA clone derived from a blood-borne non-A, non-B viral hepatitis genome." Science **244**(4902): 359-362.
Choo, S. H., H. S. So, J. M. Cho and W. S. Ryu (1995). "Association of hepatitis C virus particles with immunoglobulin: a mechanism for persistent infection." J Gen Virol **76 (Pt 9)**: 2337-2341.
Chu, C. Y. and T. M. Rana (2006). "Translation repression in human cells by microRNA-induced gene silencing requires RCK/p54." PLoS Biol **4**(7): e210.
Coldwell, M. J., S. A. Mitchell, M. Stoneley, M. MacFarlane and A. E. Willis (2000). "Initiation of Apaf-1 translation by internal ribosome entry." Oncogene **19**(7): 899-905.
Cougot, N., S. Babajko and B. Seraphin (2004). "Cytoplasmic foci are sites of mRNA decay in human cells." J Cell Biol **165**(1): 31-40.
Denli, A. M., B. B. Tops, R. H. Plasterk, R. F. Ketting and G. J. Hannon (2004). "Processing of primary microRNAs by the Microprocessor complex." Nature **432**(7014): 231-235.
Dhir, A., S. Dhir, N. J. Proudfoot and C. L. Jopling (2015). "Microprocessor mediates transcriptional termination of long noncoding RNA transcripts hosting microRNAs." Nat Struct Mol Biol **22**(4): 319-327.
Douam, F., Q. Ding and A. Ploss (2016). "Recent advances in understanding hepatitis C." F1000Res **5**.
Dutkiewicz, M. and J. Ciesiolka (2005). "Structural characterization of the highly conserved 98-base sequence at the 3' end of HCV RNA genome and the

complementary sequence located at the 5' end of the replicative viral strand." Nucleic Acids Res **33**(2): 693-703.
Duvet, S., L. Cocquerel, A. Pillez, R. Cacan, A. Verbert, D. Moradpour, C. Wychowski and J. Dubuisson (1998). "Hepatitis C virus glycoprotein complex localization in the endoplasmic reticulum involves a determinant for retention and not retrieval." J Biol Chem **273**(48): 32088-32095.
Eltahla, A. A., C. Rodrigo, B. Betz-Stablein, J. Grebely, T. Applegate, F. Luciani, J. Schinkel, G. J. Dore, K. Page, J. Bruneau, M. D. Morris, A. L. Cox, A. Y. Kim, N. H. Shoukry, G. M. Lauer, L. Maher, M. Hellard, M. Prins, A. R. Lloyd, R. A. Bull and C. S. G. In (2016). "Analysis of resistance-associated substitutions in acute hepatitis C virus infection by deep sequencing across six genotypes and three continents." J Viral Hepat.
Evans, M. J., T. von Hahn, D. M. Tscherne, A. J. Syder, M. Panis, B. Wolk, T. Hatziioannou, J. A. McKeating, P. D. Bieniasz and C. M. Rice (2007). "Claudin-1 is a hepatitis C virus co-receptor required for a late step in entry." Nature **446**(7137): 801-805.
Fabian, M. R. and N. Sonenberg (2012). "The mechanics of miRNA-mediated gene silencing: a look under the hood of miRISC." Nat Struct Mol Biol **19**(6): 586-593.
Fabian, M. R., N. Sonenberg and W. Filipowicz (2010). "Regulation of mRNA translation and stability by microRNAs." Annu Rev Biochem **79**: 351-379.
Fairley, C. K. and T. R. Read (2012). "Vaccination against sexually transmitted infections." Curr Opin Infect Dis **25**(1): 66-72.
Feinstone, S. M., A. Z. Kapikian and R. H. Purceli (1973). "Hepatitis A: detection by immune electron microscopy of a viruslike antigen associated with acute illness." Science **182**(4116): 1026-1028.
Filbin, M. E., B. S. Vollmar, D. Shi, T. Gonen and J. S. Kieft (2013). "HCV IRES manipulates the ribosome to promote the switch from translation initiation to elongation." Nat Struct Mol Biol **20**(2): 150-158.
Friebe, P. and R. Bartenschlager (2009). "Role of RNA structures in genome terminal sequences of the hepatitis C virus for replication and assembly." J Virol **83**(22): 11989-11995.
Fried, M. W., M. L. Shiffman, K. R. Reddy, C. Smith, G. Marinos, F. L. Goncales, Jr., D. Haussinger, M. Diago, G. Carosi, D. Dhumeaux, A. Craxi, A. Lin, J. Hoffman and J. Yu (2002). "Peginterferon alfa-2a plus ribavirin for chronic hepatitis C virus infection." N Engl J Med **347**(13): 975-982.
Friedman, R. C., K. K. Farh, C. B. Burge and D. P. Bartel (2009). "Most mammalian mRNAs are conserved targets of microRNAs." Genome Res **19**(1): 92-105.
Fukao, A., Y. Mishima, N. Takizawa, S. Oka, H. Imataka, J. Pelletier, N. Sonenberg, C. Thoma and T. Fujiwara (2014). "MicroRNAs trigger dissociation of eIF4AI and eIF4AII from target mRNAs in humans." Mol Cell **56**(1): 79-89.
Fukaya, T., H. O. Iwakawa and Y. Tomari (2014). "MicroRNAs block assembly of eIF4F translation initiation complex in Drosophila." Mol Cell **56**(1): 67-78.
Galicia-Vazquez, G., R. Cencic, F. Robert, A. Q. Agenor and J. Pelletier (2012). "A cellular response linking eIF4AI activity to eIF4AII transcription." RNA **18**(7): 1373-1384.
Galicia-Vazquez, G., J. Chu and J. Pelletier (2015). "eIF4AII is dispensable for miRNA-mediated gene silencing." RNA **21**(10): 1826-1833.
Gebert, L. F., M. A. Rebhan, S. E. Crivelli, R. Denzler, M. Stoffel and J. Hall (2014). "Miravirsen (SPC3649) can inhibit the biogenesis of miR-122." Nucleic Acids Res **42**(1): 609-621.

Gingras, A. C., B. Raught and N. Sonenberg (1999). "eIF4 initiation factors: effectors of mRNA recruitment to ribosomes and regulators of translation." Annu Rev Biochem **68**: 913-963.
Gorbalenya, A. E. and E. V. Koonin (1993). "Helicases: amino acid sequence comparisons and structure-function relationships." Current opinion in structural biology **3**(3): 419-429.
Gower, E., C. Estes, S. Blach, K. Razavi-Shearer and H. Razavi (2014). "Global epidemiology and genotype distribution of the hepatitis C virus infection." J Hepatol **61**(1 Suppl): S45-57.
Gregory, R. I., K. P. Yan, G. Amuthan, T. Chendrimada, B. Doratotaj, N. Cooch and R. Shiekhattar (2004). "The Microprocessor complex mediates the genesis of microRNAs." Nature **432**(7014): 235-240.
Grobler, J. A., E. J. Markel, J. F. Fay, D. J. Graham, A. L. Simcoe, S. W. Ludmerer, E. M. Murray, G. Migliaccio and O. A. Flores (2003). "Identification of a key determinant of hepatitis C virus cell culture adaptation in domain II of NS3 helicase." J Biol Chem **278**(19): 16741-16746.
Guo, J. T., V. V. Bichko and C. Seeger (2001). "Effect of alpha interferon on the hepatitis C virus replicon." J Virol **75**(18): 8516-8523.
Hadziyannis, S. J., H. Sette, Jr., T. R. Morgan, V. Balan, M. Diago, P. Marcellin, G. Ramadori, H. Bodenheimer, Jr., D. Bernstein, M. Rizzetto, S. Zeuzem, P. J. Pockros, A. Lin, A. M. Ackrill and P. I. S. Group (2004). "Peginterferon-alpha2a and ribavirin combination therapy in chronic hepatitis C: a randomized study of treatment duration and ribavirin dose." Ann Intern Med **140**(5): 346-355.
Haid, S., T. Pietschmann and E. I. Pecheur (2009). "Low pH-dependent hepatitis C virus membrane fusion depends on E2 integrity, target lipid composition, and density of virus particles." J Biol Chem **284**(26): 17657-17667.
Han, J., Y. Lee, K. H. Yeom, Y. K. Kim, H. Jin and V. N. Kim (2004). "The Drosha-DGCR8 complex in primary microRNA processing." Genes Dev **18**(24): 3016-3027.
He, L. F., D. Alling, T. Popkin, M. Shapiro, H. J. Alter and R. H. Purcell (1987). "Determining the size of non-A, non-B hepatitis virus by filtration." J Infect Dis **156**(4): 636-640.
Heckel, J. L., E. P. Sandgren, J. L. Degen, R. D. Palmiter and R. L. Brinster (1990). "Neonatal bleeding in transgenic mice expressing urokinase-type plasminogen activator." Cell **62**(3): 447-456.
Hellen, C. U. (2009). "IRES-induced conformational changes in the ribosome and the mechanism of translation initiation by internal ribosomal entry." Biochim Biophys Acta **1789**(9-10): 558-570.
Henke, J. I., D. Goergen, J. Zheng, Y. Song, C. G. Schuttler, C. Fehr, C. Junemann and M. Niepmann (2008). "microRNA-122 stimulates translation of hepatitis C virus RNA." EMBO J **27**(24): 3300-3310.
Hilliard, A., B. Hilliard, S. J. Zheng, H. Sun, T. Miwa, W. Song, R. Goke and Y. H. Chen (2006). "Translational regulation of autoimmune inflammation and lymphoma genesis by programmed cell death 4." J Immunol **177**(11): 8095-8102.
Hinnebusch, A. G. (2011). "Molecular mechanism of scanning and start codon selection in eukaryotes." Microbiol Mol Biol Rev **75**(3): 434-467, first page of table of contents.
Horner, S. M. and M. Gale, Jr. (2009). "Intracellular innate immune cascades and interferon defenses that control hepatitis C virus." J Interferon Cytokine Res **29**(9): 489-498.

Huys, A., P. A. Thibault and J. A. Wilson (2013). "Modulation of hepatitis C virus RNA accumulation and translation by DDX6 and miR-122 are mediated by separate mechanisms." PLoS One **8**(6): e67437.
Ikeda, M., K. Abe, H. Dansako, T. Nakamura, K. Naka and N. Kato (2005). "Efficient replication of a full-length hepatitis C virus genome, strain O, in cell culture, and development of a luciferase reporter system." Biochem Biophys Res Commun **329**(4): 1350-1359.
Ikeda, M., M. Yi, K. Li and S. M. Lemon (2002). "Selectable subgenomic and genome-length dicistronic RNAs derived from an infectious molecular clone of the HCV-N strain of hepatitis C virus replicate efficiently in cultured Huh7 cells." J Virol **76**(6): 2997-3006.
Inada, T. and S. Makino (2014). "Novel roles of the multi-functional CCR4-NOT complex in post-transcriptional regulation." Front Genet **5**: 135.
Ito, T., S. M. Tahara and M. M. Lai (1998). "The 3'-untranslated region of hepatitis C virus RNA enhances translation from an internal ribosomal entry site." J Virol **72**(11): 8789-8796.
Jackson, A. L., J. Burchard, J. Schelter, B. N. Chau, M. Cleary, L. Lim and P. S. Linsley (2006). "Widespread siRNA "off-target" transcript silencing mediated by seed region sequence complementarity." RNA **12**(7): 1179-1187.
Jangra, R. K., M. Yi and S. M. Lemon (2010). "DDX6 (Rck/p54) is required for efficient hepatitis C virus replication but not for internal ribosome entry site-directed translation." J Virol **84**(13): 6810-6824.
Jangra, R. K., M. Yi and S. M. Lemon (2010). "Regulation of hepatitis C virus translation and infectious virus production by the microRNA miR-122." J Virol **84**(13): 6615-6625.
Jin, H., T. H. Kim, S. K. Hwang, S. H. Chang, H. W. Kim, H. K. Anderson, H. W. Lee, K. H. Lee, N. H. Colburn, H. S. Yang, M. H. Cho and C. S. Cho (2006). "Aerosol delivery of urocanic acid-modified chitosan/programmed cell death 4 complex regulated apoptosis, cell cycle, and angiogenesis in lungs of K-ras null mice." Mol Cancer Ther **5**(4): 1041-1049.
Jongjitwimol, J., R. A. Baldock, S. J. Morley and F. Z. Watts (2016). "Sumoylation of eIF4A2 affects stress granule formation." J Cell Sci **129**(12): 2407-2415.
Jopling, C. L. (2008). "Regulation of hepatitis C virus by microRNA-122." Biochem Soc Trans **36**(Pt 6): 1220-1223.
Jopling, C. L. (2010). "Targeting microRNA-122 to Treat Hepatitis C Virus Infection." Viruses **2**(7): 1382-1393.
Jopling, C. L., K. L. Norman and P. Sarnow (2006). "Positive and negative modulation of viral and cellular mRNAs by liver-specific microRNA miR-122." Cold Spring Harb Symp Quant Biol **71**: 369-376.
Jopling, C. L., S. Schutz and P. Sarnow (2008). "Position-dependent function for a tandem microRNA miR-122-binding site located in the hepatitis C virus RNA genome." Cell Host Microbe **4**(1): 77-85.
Jopling, C. L., M. Yi, A. M. Lancaster, S. M. Lemon and P. Sarnow (2005). "Modulation of hepatitis C virus RNA abundance by a liver-specific MicroRNA." Science **309**(5740): 1577-1581.
Kato, N. (2001). "Molecular virology of hepatitis C virus." Acta Med Okayama **55**(3): 133-159.
Kato, T., T. Date, M. Miyamoto, A. Furusaka, K. Tokushige, M. Mizokami and T. Wakita (2003). "Efficient replication of the genotype 2a hepatitis C virus subgenomic replicon." Gastroenterology **125**(6): 1808-1817.

Kawamura, T., A. Furusaka, M. J. Koziel, R. T. Chung, T. C. Wang, E. V. Schmidt and T. J. Liang (1997). "Transgenic expression of hepatitis C virus structural proteins in the mouse." Hepatology **25**(4): 1014-1021.
Kolykhalov, A. A., E. V. Agapov, K. J. Blight, K. Mihalik, S. M. Feinstone and C. M. Rice (1997). "Transmission of hepatitis C by intrahepatic inoculation with transcribed RNA." Science **277**(5325): 570-574.
Kolykhalov, A. A., S. M. Feinstone and C. M. Rice (1996). "Identification of a highly conserved sequence element at the 3' terminus of hepatitis C virus genome RNA." J Virol **70**(6): 3363-3371.
Kuroki, M., Y. Ariumi, M. Hijikata, M. Ikeda, H. Dansako, T. Wakita, K. Shimotohno and N. Kato (2013). "PML tumor suppressor protein is required for HCV production." Biochem Biophys Res Commun **430**(2): 592-597.
Kuzuoglu-Ozturk, D., D. Bhandari, E. Huntzinger, M. Fauser, S. Helms and E. Izaurralde (2016). "miRISC and the CCR4-NOT complex silence mRNA targets independently of 43S ribosomal scanning." EMBO J **35**(11): 1186-1203.
Kwong, A. D., B. G. Rao and K. T. Jeang (2005). "Viral and cellular RNA helicases as antiviral targets." Nat Rev Drug Discov **4**(10): 845-853.
Kyono, K., M. Miyashiro and I. Taguchi (2002). "Human eukaryotic initiation factor 4AII associates with hepatitis C virus NS5B protein in vitro." Biochem Biophys Res Commun **292**(3): 659-666.
Landgraf, P., M. Rusu, R. Sheridan, A. Sewer, N. Iovino, A. Aravin, S. Pfeffer, A. Rice, A. O. Kamphorst, M. Landthaler, C. Lin, N. D. Socci, L. Hermida, V. Fulci, S. Chiaretti, R. Foa, J. Schliwka, U. Fuchs, A. Novosel, R. U. Muller, B. Schermer, U. Bissels, J. Inman, Q. Phan, M. Chien, D. B. Weir, R. Choksi, G. De Vita, D. Frezzetti, H. I. Trompeter, V. Hornung, G. Teng, G. Hartmann, M. Palkovits, R. Di Lauro, P. Wernet, G. Macino, C. E. Rogler, J. W. Nagle, J. Ju, F. N. Papavasiliou, T. Benzing, P. Lichter, W. Tam, M. J. Brownstein, A. Bosio, A. Borkhardt, J. J. Russo, C. Sander, M. Zavolan and T. Tuschl (2007). "A mammalian microRNA expression atlas based on small RNA library sequencing." Cell **129**(7): 1401-1414.
Lauer, G. M. (2013). "Immune responses to hepatitis C virus (HCV) infection and the prospects for an effective HCV vaccine or immunotherapies." J Infect Dis **207 Suppl 1**: S7-S12.
Lavillette, D., E. I. Pecheur, P. Donot, J. Fresquet, J. Molle, R. Corbau, M. Dreux, F. Penin and F. L. Cosset (2007). "Characterization of fusion determinants points to the involvement of three discrete regions of both E1 and E2 glycoproteins in the membrane fusion process of hepatitis C virus." J Virol **81**(16): 8752-8765.
Le Hir, H., D. Gatfield, E. Izaurralde and M. J. Moore (2001). "The exon-exon junction complex provides a binding platform for factors involved in mRNA export and nonsense-mediated mRNA decay." EMBO J **20**(17): 4987-4997.
Lee, W. M. (2003). "Drug-induced hepatotoxicity." N Engl J Med **349**(5): 474-485.
Lewis, B. P., I. h. Shih, M. W. Jones-Rhoades, D. P. Bartel and C. B. Burge (2003). "Prediction of Mammalian MicroRNA Targets." Cell **115**(7): 787-798.
Li, K., E. Foy, J. C. Ferreon, M. Nakamura, A. C. Ferreon, M. Ikeda, S. C. Ray, M. Gale, Jr. and S. M. Lemon (2005). "Immune evasion by hepatitis C virus NS3/4A protease-mediated cleavage of the Toll-like receptor 3 adaptor protein TRIF." Proc Natl Acad Sci U S A **102**(8): 2992-2997.
Li, Q., H. Imataka, S. Morino, G. W. Rogers, Jr., N. J. Richter-Cook, W. C. Merrick and N. Sonenberg (1999). "Eukaryotic translation initiation factor 4AIII (eIF4AIII) is functionally distinct from eIF4AI and eIF4AII." Mol Cell Biol **19**(11): 7336-7346.
Li, X. D., L. Sun, R. B. Seth, G. Pineda and Z. J. Chen (2005). "Hepatitis C virus protease NS3/4A cleaves mitochondrial antiviral signaling protein off the

mitochondria to evade innate immunity." Proc Natl Acad Sci U S A **102**(49): 17717-17722.
Li, Y., T. Masaki, D. Yamane, D. R. McGivern and S. M. Lemon (2013). "Competing and noncompeting activities of miR-122 and the 5' exonuclease Xrn1 in regulation of hepatitis C virus replication." Proc Natl Acad Sci U S A **110**(5): 1881-1886.
Li, Z. Y., Y. Xi, W. N. Zhu, C. Zeng, Z. Q. Zhang, Z. C. Guo, D. L. Hao, G. Liu, L. Feng, H. Z. Chen, F. Chen, X. Lv, D. P. Liu and C. C. Liang (2011). "Positive regulation of hepatic miR-122 expression by HNF4alpha." J Hepatol **55**(3): 602-611.
Liang, C., E. Rieder, B. Hahm, S. K. Jang, A. Paul and E. Wimmer (2005). "Replication of a novel subgenomic HCV genotype 1a replicon expressing a puromycin resistance gene in Huh-7 cells." Virology **333**(1): 41-53.
Lindenbach, B. D. and C. M. Rice (2013). "The ins and outs of hepatitis C virus entry and assembly." Nat Rev Microbiol **11**(10): 688-700.
Linder, P. and E. Jankowsky (2011). "From unwinding to clamping - the DEAD box RNA helicase family." Nat Rev Mol Cell Biol **12**(8): 505-516.
Lindqvist, L., H. Imataka and J. Pelletier (2008). "Cap-dependent eukaryotic initiation factor-mRNA interactions probed by cross-linking." RNA **14**(5): 960-969.
Locarnini, S. (2004). "Molecular virology of hepatitis B virus." Semin Liver Dis **24 Suppl 1**: 3-10.
Logvinoff, C., M. E. Major, D. Oldach, S. Heyward, A. Talal, P. Balfe, S. M. Feinstone, H. Alter, C. M. Rice and J. A. McKeating (2004). "Neutralizing antibody response during acute and chronic hepatitis C virus infection." Proc Natl Acad Sci U S A **101**(27): 10149-10154.
Lohmann, V., F. Korner, J. Koch, U. Herian, L. Theilmann and R. Bartenschlager (1999). "Replication of subgenomic hepatitis C virus RNAs in a hepatoma cell line." Science **285**(5424): 110-113.
Lorsch, J. R. and D. Herschlag (1998). "The DEAD box protein eIF4A. 1. A minimal kinetic and thermodynamic framework reveals coupled binding of RNA and nucleotide." Biochemistry **37**(8): 2180-2193.
Lorsch, J. R. and D. Herschlag (1998). "The DEAD box protein eIF4A. 2. A cycle of nucleotide and RNA-dependent conformational changes." Biochemistry **37**(8): 2194-2206.
Low, W. K., Y. Dang, T. Schneider-Poetsch, Z. Shi, N. S. Choi, W. C. Merrick, D. Romo and J. O. Liu (2005). "Inhibition of eukaryotic translation initiation by the marine natural product pateamine A." Mol Cell **20**(5): 709-722.
Lukavsky, P. J. (2009). "Structure and function of HCV IRES domains." Virus Res **139**(2): 166-171.
Lukavsky, P. J., G. A. Otto, A. M. Lancaster, P. Sarnow and J. D. Puglisi (2000). "Structures of two RNA domains essential for hepatitis C virus internal ribosome entry site function." Nat Struct Biol **7**(12): 1105-1110.
Luna, J. M., T. K. Scheel, T. Danino, K. S. Shaw, A. Mele, J. J. Fak, E. Nishiuchi, C. N. Takacs, M. T. Catanese, Y. P. de Jong, I. M. Jacobson, C. M. Rice and R. B. Darnell (2015). "Hepatitis C virus RNA functionally sequesters miR-122." Cell **160**(6): 1099-1110.
Machlin, E. S., P. Sarnow and S. M. Sagan (2011). "Masking the 5' terminal nucleotides of the hepatitis C virus genome by an unconventional microRNA-target RNA complex." Proc Natl Acad Sci U S A **108**(8): 3193-3198.
Marascio, N., G. Pavia, A. Strazzulla, T. Dierckx, L. Cuypers, B. Vrancken, G. S. Barreca, T. Mirante, D. Malanga, D. M. Oliveira, A. M. Vandamme, C. Torti, M. C. Liberto, A. Foca and G. The Sinergie-Umg Study (2016). "Detection of Natural

Resistance-Associated Substitutions by Ion Semiconductor Technology in HCV1b Positive, Direct-Acting Antiviral Agents-Naive Patients." Int J Mol Sci **17**(9).
Marintchev, A. and G. Wagner (2004). "Translation initiation: structures, mechanisms and evolution." Q Rev Biophys **37**(3-4): 197-284.
Masciopinto, F., S. Campagnoli, S. Abrignani, Y. Uematsu and P. Pileri (2001). "The small extracellular loop of CD81 is necessary for optimal surface expression of the large loop, a putative HCV receptor." Virus Res **80**(1-2): 1-10.
Matheny, S. C. and J. E. Kingery (2012). "Hepatitis A." Am Fam Physician **86**(11): 1027-1034; quiz 1010-1022.
Mathys, H., J. Basquin, S. Ozgur, M. Czarnocki-Cieciura, F. Bonneau, A. Aartse, A. Dziembowski, M. Nowotny, E. Conti and W. Filipowicz (2014). "Structural and biochemical insights to the role of the CCR4-NOT complex and DDX6 ATPase in microRNA repression." Mol Cell **54**(5): 751-765.
Meijer, H. A., Y. W. Kong, W. T. Lu, A. Wilczynska, R. V. Spriggs, S. W. Robinson, J. D. Godfrey, A. E. Willis and M. Bushell (2013). "Translational repression and eIF4A2 activity are critical for microRNA-mediated gene regulation." Science **340**(6128): 82-85.
Mercer, D. F., D. E. Schiller, J. F. Elliott, D. N. Douglas, C. Hao, A. Rinfret, W. R. Addison, K. P. Fischer, T. A. Churchill, J. R. Lakey, D. L. Tyrrell and N. M. Kneteman (2001). "Hepatitis C virus replication in mice with chimeric human livers." Nat Med **7**(8): 927-933.
Messina, J. P., I. Humphreys, A. Flaxman, A. Brown, G. S. Cooke, O. G. Pybus and E. Barnes (2015). "Global distribution and prevalence of hepatitis C virus genotypes." Hepatology **61**(1): 77-87.
Modelska, A., E. Turro, R. Russell, J. Beaton, T. Sbarrato, K. Spriggs, J. Miller, S. Graf, E. Provenzano, F. Blows, P. Pharoah, C. Caldas and J. Le Quesne (2015). "The malignant phenotype in breast cancer is driven by eIF4A1-mediated changes in the translational landscape." Cell Death Dis **6**: e1603.
Mohd Hanafiah, K., J. Groeger, A. D. Flaxman and S. T. Wiersma (2013). "Global epidemiology of hepatitis C virus infection: new estimates of age-specific antibody to HCV seroprevalence." Hepatology **57**(4): 1333-1342.
Moriya, K., K. Nakagawa, T. Santa, Y. Shintani, H. Fujie, H. Miyoshi, T. Tsutsumi, T. Miyazawa, K. Ishibashi, T. Horie, K. Imai, T. Todoroki, S. Kimura and K. Koike (2001). "Oxidative stress in the absence of inflammation in a mouse model for hepatitis C virus-associated hepatocarcinogenesis." Cancer Res **61**(11): 4365-4370.
Nana-Sinkam, S. P. and C. M. Croce (2013). "Clinical applications for microRNAs in cancer." Clin Pharmacol Ther **93**(1): 98-104.
Nielsen, P. J. and H. Trachsel (1988). "The mouse protein synthesis initiation factor 4A gene family includes two related functional genes which are differentially expressed." EMBO J **7**(7): 2097-2105.
Nitschke, K., T. Flecken, J. Schmidt, E. Gostick, M. Marget, C. Neumann-Haefelin, H. E. Blum, D. A. Price and R. Thimme (2015). "Tetramer enrichment reveals the presence of phenotypically diverse hepatitis C virus-specific CD8+ T cells in chronic infection." J Virol **89**(1): 25-34.
Nothdurft, H. D. (2008). "Hepatitis A vaccines." Expert Rev Vaccines **7**(5): 535-545.
Nottrott, S., M. J. Simard and J. D. Richter (2006). "Human let-7a miRNA blocks protein production on actively translating polyribosomes." Nat Struct Mol Biol **13**(12): 1108-1114.
Nousch, M., V. Reed, R. J. Bryson-Richardson, P. D. Currie and T. Preiss (2007). "The eIF4G-homolog p97 can activate translation independent of caspase cleavage." RNA **13**(3): 374-384.

Ortega-Prieto, A. M. and M. Dorner (2016). "The expanding toolbox for hepatitis C virus research." J Viral Hepat **23**(5): 320-329.
Owttrim, G. W., S. Hofmann and C. Kuhlemeier (1991). "Divergent genes for translation initiation factor eIF-4A are coordinately expressed in tobacco." Nucleic Acids Res **19**(20): 5491-5496.
Pager, C. T., S. Schutz, T. M. Abraham, G. Luo and P. Sarnow (2013). "Modulation of hepatitis C virus RNA abundance and virus release by dispersion of processing bodies and enrichment of stress granules." Virology **435**(2): 472-484.
Palacios, I. M., D. Gatfield, D. St Johnston and E. Izaurralde (2004). "An eIF4AIII-containing complex required for mRNA localization and nonsense-mediated mRNA decay." Nature **427**(6976): 753-757.
Panel, A. I. H. G. (2015). "Hepatitis C guidance: AASLD-IDSA recommendations for testing, managing, and treating adults infected with hepatitis C virus." Hepatology **62**(3): 932-954.
Patel, S. S. and I. Donmez (2006). "Mechanisms of helicases." J Biol Chem **281**(27): 18265-18268.
Pause, A., G. Kukolj, M. Bailey, M. Brault, F. Do, T. Halmos, L. Lagace, R. Maurice, M. Marquis, G. McKercher, C. Pellerin, L. Pilote, D. Thibeault and D. Lamarre (2003). "An NS3 serine protease inhibitor abrogates replication of subgenomic hepatitis C virus RNA." J Biol Chem **278**(22): 20374-20380.
Pawlotsky, J. M. (2014). "What are the pros and cons of the use of host-targeted agents against hepatitis C?" Antiviral Res **105**: 22-25.
Penin, F., J. Dubuisson, F. A. Rey, D. Moradpour and J. M. Pawlotsky (2004). "Structural biology of hepatitis C virus." Hepatology **39**(1): 5-19.
Pestova, T. V., V. G. Kolupaeva, I. B. Lomakin, E. V. Pilipenko, I. N. Shatsky, V. I. Agol and C. U. Hellen (2001). "Molecular mechanisms of translation initiation in eukaryotes." Proc Natl Acad Sci U S A **98**(13): 7029-7036.
Pestova, T. V., I. N. Shatsky, S. P. Fletcher, R. J. Jackson and C. U. Hellen (1998). "A prokaryotic-like mode of cytoplasmic eukaryotic ribosome binding to the initiation codon during internal translation initiation of hepatitis C and classical swine fever virus RNAs." Genes Dev **12**(1): 67-83.
Petit, A. P., L. Wohlbold, P. Bawankar, E. Huntzinger, S. Schmidt, E. Izaurralde and O. Weichenrieder (2012). "The structural basis for the interaction between the CAF1 nuclease and the NOT1 scaffold of the human CCR4-NOT deadenylase complex." Nucleic Acids Res **40**(21): 11058-11072.
Pineiro, D. and E. Martinez-Salas (2012). "RNA structural elements of hepatitis C virus controlling viral RNA translation and the implications for viral pathogenesis." Viruses **4**(10): 2233-2250.
Ploss, A., M. J. Evans, V. A. Gaysinskaya, M. Panis, H. You, Y. P. de Jong and C. M. Rice (2009). "Human occludin is a hepatitis C virus entry factor required for infection of mouse cells." Nature **457**(7231): 882-886.
Popescu, C. I., L. Riva, O. Vlaicu, R. Farhat, Y. Rouille and J. Dubuisson (2014). "Hepatitis C virus life cycle and lipid metabolism." Biology (Basel) **3**(4): 892-921.
Purcell, R. (1997). "The hepatitis C virus: overview." Hepatology **26**(3 Suppl 1): 11S-14S.
Ranji, A. and K. Boris-Lawrie (2010). "RNA helicases: emerging roles in viral replication and the host innate response." RNA Biol **7**(6): 775-787.
Rho, H. W., B. C. Lee, E. S. Choi, I. J. Choi, Y. S. Lee and S. H. Goh (2010). "Identification of valid reference genes for gene expression studies of human stomach cancer by reverse transcription-qRT-QPCR." BMC Cancer **10**: 240.

Ribeiro, R. M., H. Li, S. Wang, M. B. Stoddard, G. H. Learn, B. T. Korber, T. Bhattacharya, J. Guedj, E. H. Parrish, B. H. Hahn, G. M. Shaw and A. S. Perelson (2012). "Quantifying the diversification of hepatitis C virus (HCV) during primary infection: estimates of the in vivo mutation rate." PLoS Pathog **8**(8): e1002881.
Rizzetto, M., M. G. Canese, S. Arico, O. Crivelli, C. Trepo, F. Bonino and G. Verme (1977). "Immunofluorescence detection of new antigen-antibody system (delta/anti-delta) associated to hepatitis B virus in liver and in serum of HBsAg carriers." Gut **18**(12): 997-1003.
Roberts, A. P., R. Doidge, A. W. Tarr and C. L. Jopling (2014). "The P body protein LSm1 contributes to stimulation of hepatitis C virus translation, but not replication, by microRNA-122." Nucleic Acids Res **42**(2): 1257-1269.
Roberts, A. P. and C. L. Jopling (2010). "Targeting viral infection by microRNA inhibition." Genome Biol **11**(1): 201.
Roberts, A. P., A. P. Lewis and C. L. Jopling (2011). "miR-122 activates hepatitis C virus translation by a specialized mechanism requiring particular RNA components." Nucleic Acids Res **39**(17): 7716-7729.
Rogers, G. W., Jr., A. A. Komar and W. C. Merrick (2002). "eIF4A: the godfather of the DEAD box helicases." Prog Nucleic Acid Res Mol Biol **72**: 307-331.
Rogers, G. W., Jr., W. F. Lima and W. C. Merrick (2001). "Further characterization of the helicase activity of eIF4A. Substrate specificity." J Biol Chem **276**(16): 12598-12608.
Rogers, G. W., Jr., N. J. Richter and W. C. Merrick (1999). "Biochemical and kinetic characterization of the RNA helicase activity of eukaryotic initiation factor 4A." J Biol Chem **274**(18): 12236-12244.
Romero-Lopez, C. and A. Berzal-Herranz (2009). "A long-range RNA-RNA interaction between the 5' and 3' ends of the HCV genome." RNA **15**(9): 1740-1752.
Rozen, F., I. Edery, K. Meerovitch, T. E. Dever, W. C. Merrick and N. Sonenberg (1990). "Bidirectional RNA helicase activity of eucaryotic translation initiation factors 4A and 4F." Mol Cell Biol **10**(3): 1134-1144.
Saldanha, J. A., H. C. Thomas and J. P. Monjardino (1990). "Cloning and sequencing of RNA of hepatitis delta virus isolated from human serum." J Gen Virol **71 (Pt 7)**: 1603-1606.
Scarselli, E., H. Ansuini, R. Cerino, R. M. Roccasecca, S. Acali, G. Filocamo, C. Traboni, A. Nicosia, R. Cortese and A. Vitelli (2002). "The human scavenger receptor class B type I is a novel candidate receptor for the hepatitis C virus." EMBO J **21**(19): 5017-5025.
Schmittgen, T. D. and B. A. Zakrajsek (2000). "Effect of experimental treatment on housekeeping gene expression: validation by real-time, quantitative RT-RT-QPCR." J Biochem Biophys Methods **46**(1-2): 69-81.
Schwarz, D. S., G. Hutvagner, T. Du, Z. Xu, N. Aronin and P. D. Zamore (2003). "Asymmetry in the assembly of the RNAi enzyme complex." Cell **115**(2): 199-208.
Shaoyan, X., Y. Juanjuan, T. Yalan, H. Ping, L. Jianzhong and W. Qinian (2013). "Downregulation of EIF4A2 in non-small-cell lung cancer associates with poor prognosis." Clin Lung Cancer **14**(6): 658-665.
Shibahara, K., M. Asano, Y. Ishida, T. Aoki, T. Koike and T. Honjo (1995). "Isolation of a novel mouse gene MA-3 that is induced upon programmed cell death." Gene **166**(2): 297-301.
Silberstein, S. and R. Gilmore (1996). "Biochemistry, molecular biology, and genetics of the oligosaccharyltransferase." FASEB J **10**(8): 849-858.
Simmonds, P. (1995). "Variability of hepatitis C virus." Hepatology **21**(2): 570-583.

Simmonds, P., J. Bukh, C. Combet, G. Deleage, N. Enomoto, S. Feinstone, P. Halfon, G. Inchauspe, C. Kuiken, G. Maertens, M. Mizokami, D. G. Murphy, H. Okamoto, J. M. Pawlotsky, F. Penin, E. Sablon, I. T. Shin, L. J. Stuyver, H. J. Thiel, S. Viazov, A. J. Weiner and A. Widell (2005). "Consensus proposals for a unified system of nomenclature of hepatitis C virus genotypes." Hepatology **42**(4): 962-973.

Simons, J. N., T. J. Pilot-Matias, T. P. Leary, G. J. Dawson, S. M. Desai, G. G. Schlauder, A. S. Muerhoff, J. C. Erker, S. L. Buijk, M. L. Chalmers and et al. (1995). "Identification of two flavivirus-like genomes in the GB hepatitis agent." Proc Natl Acad Sci U S A **92**(8): 3401-3405.

Spahn, C. M., J. S. Kieft, R. A. Grassucci, P. A. Penczek, K. Zhou, J. A. Doudna and J. Frank (2001). "Hepatitis C virus IRES RNA-induced changes in the conformation of the 40s ribosomal subunit." Science **291**(5510): 1959-1962.

Suzuki, T., K. Ishii, H. Aizaki and T. Wakita (2007). "Hepatitis C viral life cycle." Adv Drug Deliv Rev **59**(12): 1200-1212.

Teufel, A., P. R. Galle and S. Kanzler (2009). "Update on autoimmune hepatitis." World J Gastroenterol **15**(9): 1035-1041.

Thomas, D. L. (2013). "Global control of hepatitis C: where challenge meets opportunity." Nat Med **19**(7): 850-858.

Thompson, S. R. (2012). "So you want to know if your message has an IRES?" Wiley Interdiscip Rev RNA **3**(5): 697-705.

Thulasi Raman, S. N., G. Liu, H. M. Pyo, Y. C. Cui, F. Xu, L. E. Ayalew, S. K. Tikoo and Y. Zhou (2016). "DDX3 Interacts with Influenza A Virus NS1 and NP Proteins and Exerts Antiviral Function through Regulation of Stress Granule Formation." J Virol **90**(7): 3661-3675.

Tuplin, A., M. Struthers, J. Cook, K. Bentley and D. J. Evans (2015). "Inhibition of HCV translation by disrupting the structure and interactions of the viral CRE and 3' X-tail." Nucleic Acids Res **43**(5): 2914-2926.

Tuplin, A., J. Wood, D. J. Evans, A. H. Patel and P. Simmonds (2002). "Thermodynamic and phylogenetic prediction of RNA secondary structures in the coding region of hepatitis C virus." RNA **8**(6): 824-841.

Vivier, E., E. Tomasello, M. Baratin, T. Walzer and S. Ugolini (2008). "Functions of natural killer cells." Nat Immunol **9**(5): 503-510.

Wakita, T., A. Katsume, J. Kato, C. Taya, H. Yonekawa, Y. Kanegae, I. Saito, Y. Hayashi, M. Koike, M. Miyamoto, Y. Hiasa and M. Kohara (2000). "Possible role of cytotoxic T cells in acute liver injury in hepatitis C virus cDNA transgenic mice mediated by Cre/loxP system." J Med Virol **62**(3): 308-317.

Wakita, T., C. Taya, A. Katsume, J. Kato, H. Yonekawa, Y. Kanegae, I. Saito, Y. Hayashi, M. Koike and M. Kohara (1998). "Efficient conditional transgene expression in hepatitis C virus cDNA transgenic mice mediated by the Cre/loxP system." J Biol Chem **273**(15): 9001-9006.

Wang, B., H. Wang and Z. Yang (2012). "MiR-122 inhibits cell proliferation and tumorigenesis of breast cancer by targeting IGF1R." PLoS One **7**(10): e47053.

Wang, C., S. Y. Le, N. Ali and A. Siddiqui (1995). "An RNA pseudoknot is an essential structural element of the internal ribosome entry site located within the hepatitis C virus 5' noncoding region." RNA **1**(5): 526-537.

Williams-Hill, D. M., R. F. Duncan, P. J. Nielsen and S. M. Tahara (1997). "Differential expression of the murine eukaryotic translation initiation factor isogenes eIF4A(I) and eIF4A(II) is dependent upon cellular growth status." Arch Biochem Biophys **338**(1): 111-120.

Wilson, J. A., C. Zhang, A. Huys and C. D. Richardson (2011). "Human Ago2 is required for efficient microRNA 122 regulation of hepatitis C virus RNA accumulation and translation." J Virol **85**(5): 2342-2350.
Wree, A., L. Broderick, A. Canbay, H. M. Hoffman and A. E. Feldstein (2013). "From NAFLD to NASH to cirrhosis-new insights into disease mechanisms." Nat Rev Gastroenterol Hepatol **10**(11): 627-636.
Wu, S. Y., X. Yang, K. M. Gharpure, H. Hatakeyama, M. Egli, M. H. McGuire, A. S. Nagaraja, T. M. Miyake, R. Rupaimoole, C. V. Pecot, M. Taylor, S. Pradeep, M. Sierant, C. Rodriguez-Aguayo, H. J. Choi, R. A. Previs, G. N. Armaiz-Pena, L. Huang, C. Martinez, T. Hassell, C. Ivan, V. Sehgal, R. Singhania, H. D. Han, C. Su, J. H. Kim, H. J. Dalton, C. Kovvali, K. Keyomarsi, N. A. McMillan, W. W. Overwijk, J. Liu, J. S. Lee, K. A. Baggerly, G. Lopez-Berestein, P. T. Ram, B. Nawrot and A. K. Sood (2014). "2'-OMe-phosphorodithioate-modified siRNAs show increased loading into the RISC complex and enhanced anti-tumour activity." Nat Commun **5**: 3459.
Yang, Y., K. U. Jooss, Q. Su, H. C. Ertl and J. M. Wilson (1996). "Immune responses to viral antigens versus transgene product in the elimination of recombinant adenovirus-infected hepatocytes in vivo." Gene Ther **3**(2): 137-144.
Yoder-Hill, J., A. Pause, N. Sonenberg and W. C. Merrick (1993). "The p46 subunit of eukaryotic initiation factor (eIF)-4F exchanges with eIF-4A." J Biol Chem **268**(8): 5566-5573.
Zeisel, M. B., J. Lupberger, I. Fofana and T. F. Baumert (2013). "Host-targeting agents for prevention and treatment of chronic hepatitis C - perspectives and challenges." J Hepatol **58**(2): 375-384.
Zekri, L., E. Huntzinger, S. Heimstadt and E. Izaurralde (2009). "The silencing domain of GW182 interacts with PABPC1 to promote translational repression and degradation of microRNA targets and is required for target release." Mol Cell Biol **29**(23): 6220-6231.
Zhang, C., A. Huys, P. A. Thibault and J. A. Wilson (2012). "Requirements for human Dicer and TRBP in microRNA-122 regulation of HCV translation and RNA abundance." Virology **433**(2): 479-488.
Zhang, T., Y. Li, J. P. Lai, S. D. Douglas, D. S. Metzger, C. P. O'Brien and W. Z. Ho (2003). "Alcohol potentiates hepatitis C virus replicon expression." Hepatology **38**(1): 57-65.
Zhou, X., R. A. de Man, R. J. de Knegt, H. J. Metselaar, M. P. Peppelenbosch and Q. Pan (2013). "Epidemiology and management of chronic hepatitis E infection in solid organ transplantation: a comprehensive literature review." Rev Med Virol **23**(5): 295-304.
Zhou, X., J. Luo, L. Mills, S. Wu, T. Pan, G. Geng, J. Zhang, H. Luo, C. Liu and H. Zhang (2013). "DDX5 facilitates HIV-1 replication as a cellular co-factor of Rev." PLoS One **8**(5): e65040.
Zuck, P., E. M. Murray, E. Stec, J. A. Grobler, A. J. Simon, B. Strulovici, J. Inglese, O. A. Flores and M. Ferrer (2004). "A cell-based beta-lactamase reporter gene assay for the identification of inhibitors of hepatitis C virus replication." Anal Biochem **334**(2): 344-355.